NOVEL MOLECULAR STRATEGIES FOR THE DETECTION AND CHARACTERIZATION OF TICK-BORNE PATHOGENS IN DOMESTIC DOGS

A Dissertation

by

JOSEPH JAMES MODARELLI II

Submitted to the Office of Graduate and Professional Studies of
Texas A&M University
in partial fulfillment of the requirements for the degree of

DOCTOR OF PHILOSOPHY

Chair of Committee,	Maria D. Esteve-Gasent
Co-Chair of Committee,	James N. Derr
Committee Members,	Pamela J. Ferro
	John M. Tomeček
Head of Department,	David Threadgill

December 2018

Major Subject: Genetics

ABSTRACT

Tick-borne diseases (TBD) are common across the United States and can result in critical and chronic disease states in a variety of veterinary patients, specifically domesticated dogs. Borreliosis, anaplasmosis, rickettsiosis, ehrlichiosis, and babesiosis have been cited as the most common TBDs. Despite recent reports revealing past exposure of TBD, there are no molecular epidemiological reports for dogs in Texas. Therefore, data to support the level of actively infected dogs in the population is inadequate. Limited molecular data for TBDs is due, in part, to the lack of consolidated molecular tools available to researchers. Real-time PCR (qPCR) assays are a commonly utilized tool for molecular detection of TBDs, and achieve species specificity by assigning each pathogen a unique fluorogenic label. However, current limitations of qPCR instruments include restricting the number of fluorogenic labels that can be differentiated by the instrument per a given reaction. As such, this dissertation explored the development of a qPCR methodology, termed layerplexing, that would allow for the simultaneous detection and characterization of 11 pathogens responsible for causing common TBDs in domestic dogs. Additionally, an endogenous internal positive control was designed and integrated into the assay for quality assurance of attained molecular results. Analysis revealed that the layerplex assay format was comparable in terms of target sensitivity and specificity to other qPCR assays utilized in the field. The layerplex assay was then applied to conducting a molecular prevalence investigation of TBDs affecting dogs across Texas ecoregions. By conducting molecular prevalence studies for TBDs, updated rates of active exposure and specific regions that may contain sentinels of disease could be identified. Results obtained

indicated molecular prevalence of borrelial, rickettsial, and babesial pathogens varied across the Texas study area and indicated specific regions where susceptible hosts may be at higher risk for infection with TBD. Furthermore, the layerplex assay lead to the first reported molecular detection of *Anaplasma platys* in Texas and coinfection with *Ehrlichia canis* and *A. platys* in Texas dogs. Overall, findings from this dissertation provided substantial evidence that the layerplex technique can be utilized for grouping multiple targets under a single fluorogenic label without impeding diagnostic efficacy. The layerplex technique also demonstrated utility in facilitating large scale molecular analyses of animals in Texas. Surveillance data obtained from this study may aid public health agencies in updating maps depicting high-risk areas of disease and provide baseline data for future research aiming to characterize TBDs in additional animal models.

DEDICATION

To my family, for always supporting my endeavors.

To my friends, for humoring my passions.

To the Interdisciplinary Graduate Program in Genetics, College of Veterinary Medicine, and the TVMDL, for providing me the opportunity to apply my research to the field of diagnostics.

Most of all, to my wife, Rachel, who has never stopped encouraging or inspiring me.

ACKNOWLEDGEMENTS

I would like to thank my committee chair Dr. Esteve-Gasent for all her patience, guidance, and support; my co-chair Dr. Derr for introducing me to the field of genetics; and my committee members, Dr. Ferro for teaching me how to apply a pursuit in genetics to the field of veterinary diagnostics, Dr. Tomeček for introducing me to the importance of wildlife surveillance, and Dr. Walt Cook for his willingness to assist in my defense. Special thanks to the TVMDL for providing me the opportunity to pursue a graduate degree and equipping me with a wealth of knowledge from on-site subject matter experts. I want to extend additional thanks to Dr. Ferro for not only supporting my desire to pursue a career in research, but also for pushing me out of my comfort zone so that I can attain the full graduate student experience.

Special thanks to Interdisciplinary Graduate Program in Genetics Chair Dr. Threadgill, Veterinary Pathobiology Department Head Dr. Vemulapalli, as well as the faculty and staff of the departments for their support. Thanks also to our laboratory's former students Dr. Christina Brock and Dr. Amer Fadhl Alhaboubi, and all of my current laboratory colleagues Dr. Wisam Hassan, Dr. Reem Elkalouby, Bonnie Gulas-Wroblewski, Rachel Cook, Wojciech Futoma, Roukaya Mabizari; as well colleagues and collaborators from numerous Departments for making my time at Texas A&M University a great experience.

It also goes without saying how thankful and appreciative I am for my wife, Dr. Rachel Modarelli. She has been a shining example of excellence in academia, and a constant source of motivation as I pursued this degree.

CONTRIBUTORS AND FUNDING SOURCES

Contributors

This work was supervised by a dissertation committee consisting of Dr. Maria D. Esteve-Gasent (chair), Dr. James N. Derr (co-chair), and Dr. Pamela J. Ferro of the Department of Veterinary Pathobiology and Dr. John M. Tomeček of the Department of Wildlife and Fisheries Sciences (members).

All work for this dissertation was completed independently under the supervision of Dr. Esteve-Gasent. Contributors include TVMDL, College Station, TX; Rocky Mountain Laboratories, Hamilton, Montana; UC Davis School of Veterinary Medicine, Davis, California; and USDA-ARS, Kerrville, TX.

Funding Sources

Graduate study was supported by Texas A&M AgriLife and Texas A&M Veterinary Medical Diagnostic Laboratory (TVMDL) seed grant Molecular Diagnosis of Zoonotic Tick-Borne Diseases.

NOMENCLATURE

CDC	Centers for Disease Control and Prevention
CGE	Canine granulocytic ehrlichiosis
CME	Canine monocytic ehrlichiosis
cnPCR	Conventional polymerase chain reaction
Cq	Quantification cycle
DIVA	Differentiating infected and vaccinated animals
DNA	Deoxyribonucleic acid
EIPC	Endogenous internal positive control
ELISA	Enzyme-linked immunosorbent assay
GCE	Genome copy equivalents
GG	Genomic groups
HME	Human monocytic ehrlichiosis
IFA	Immunofluorescence assay
LD	Lyme Disease
PCR	Polymerase chain reaction
qPCR	Quantitative real-time polymerase chain reaction
RMSF	Rocky Mountain spotted Fever
SFGR	Spotted fever group rickettsioses
SNP	Single nucleotide polymorphism
TBD	Tick-borne disease
TBRF	Tick-borne relapsing Fever

TVMDL	Texas A&M Veterinary Medical Diagnostic Laboratory
Tm	Melting temperature
µl	Microliter
U.S.	United States

TABLE OF CONTENTS

Page

LIST OF FIGURES

Page

LIST OF TABLES

Page

CHAPTER I

INTRODUCTION AND LITERATURE REVIEW[*]

Tick-borne diseases affecting dogs

Tick-borne diseases (TBD) are responsible for significant illnesses in susceptible hosts across the United States. Encompassing five major disease groups in the U.S., including borreliosis, anaplasmosis, rickettsiosis, ehrlichiosis, and babesiosis, these diseases have been reported to the Centers for Disease Control and Prevention (CDC) to affect a conservative 48,000 humans every year (Centers for Disease, 2017). At this time, however, there are limited epidemiological reports for domestic dogs. Therefore, data to support the severity of these diseases within the canine population is inadequate. The most prevalent causative agents for the respective canine diseases consist of 11 pathogens of bacterial and parasitic origin, as depicted in Table 1-1 and further described below.

Borrelial pathogens

Borrelial pathogens afflicting dogs are comprised of two groups; those responsible for causing Lyme disease (LD) and those residing within the tick-borne relapsing fever (TBRF) group. Both groups of spiral-shaped bacteria are responsible for causing borreliosis with varying levels of severity. While morphological similarities exist between

[*] Reprinted with permission from "Novel real-time PCR assays for genomic group identification of tick-borne relapsing fever species *Borrelia hermsii*" by Joseph J. Modarelli, Julie Piccione, Pamela J. Ferro, and Maria Esteve-Gasent, 2018. *Diagnostic Microbiology and Infectious Disease*, in press, Copyright 2018 Elsevier Publications. DOI: 10.1016/j.diagmicrobio.2018.08.001.

[*] Reprinted with permission from "Molecular identification of *Ehrlichia ewingii* in a polyarthritic Texas dog" by Joseph J. Modarelli, Mindy M. Borst, Julie Piccione, Pamela J. Ferro, and Maria Esteve-Gasent, 2018. *Veterinary Clinical Pathology*, in press, Copyright 2018 Sage Publications.

LD and TBRF, the pathogenesis of disease between the two varies due to phases of spirochetemia and bouts of cyclic fever in the latter (Lopez et al., 2016).

Table 1-1. Tick-borne diseases of dogs targeted by this study.

Disease group	Disease agent	Tick vectors	Geographical distribution†
Borrelial	*Borrelia burgdorferi*	*Ixodes scapularis, I. pacificus*	Northeast, Midwest
	B. turicatae	*Ornithodoros turicata*	South, southeast
	B. hermsii	*O. hermsii*	Western
	B. parkeri	*O. parkeri*	Midwestern
Rickettsial	*Ehrlichia canis*	*Rhipicephalus sanguineus*	Complete
		Dermacentor variabilis	South
	E. chaffeensis	*Amblyomma americanum*	Southeast, southcentral
	E. ewingii	*A. americanum*	Southeast, southcentral
	Anaplasma phagocytophilum	*I. scapularis, I. pacificus*	Northeast, Midwest
	Rickettsia rickettsii	*D. variabilis, D. andersoni*	Southeast, southcentral
		R. sanguineus, A. cajennense	Southeast, southcentral
Babesial	*Babesia gibsoni*	*R. sanguineus*	Complete
	B. canis vogeli	*R. sanguineus*	Complete

† Geographical distribution within the United States.

Borreliosis

Lyme disease is caused by *Borrelia burgdorferi* and is transmitted to the canine host by the bite of an infected tick. In the U.S., LD is credited with being the most prevalent human tick-borne illness with more than 30,000 annual cases reported to the CDC (Centers for Disease, 2017). However, recent studies propose that the true number of infections is 10-fold greater than what has been reported in the U.S. alone (Kuehn, 2013). While national surveillance data does not currently exist for dog cases, the prevalence of LD within the human population alone can be appreciated.

The most common competent tick vectors for LD in the U.S. include *Ixodes scapularis* and *Ixodes pacificus*, also known as the deer/blacklegged tick or the western-blacklegged tick, respectively. Small mammals (e.g. mice and rabbits) and larger mammals

(e.g. raccoons and deer) are common hosts for *I. scapularis*. Other animals, including humans and dogs, can act as incidental hosts for the ticks, and may subsequently contract the disease if adequately exposed (Littman et al., 2018). Lyme disease is comprised of a large system of species, also known as the *Borrelia burgdorferi sensu lato* (sl) complex. At this time, there are approximately 20 species known to cause LD, many of which circulate within the U.S.; although it is not fully understood if all species within this group are known to establish an infection in dogs (Becker et al., 2016).

In dogs, clinical signs for LD may be associated with stiffness, lameness, swollen joints, inappetence, pyrexia, and fatigue, and are generally considered nonspecific due to resembling other tick-borne infections (e.g. flu-like presentation); though the complete lack of signs in dogs indicating serological exposure is also common (Littman et al., 2018). If an infection occurs, a dog may not show signs until several months after initial infection. If left unmanaged, LD may progress to the chronic stage which may result in permanently affected skin, joints and nervous system (Littman et al., 2018). Though a characteristic rash, known as an erythema migrans, is commonly associated with LD, the ability to reliably detect the rash on a non-human animal (e.g. domestic dog) is limited and can result in misdiagnosis if the presence of a rash is used as the sole means for differential diagnosis (Skotarczak, 2014).

Reliable diagnostic detection of LD in an affected host is complicated and controversial. Though there have been numerous diagnostic assays developed for a variety of platforms (e.g. an indirect immunofluorescence assay [IFA], western blots, IDEXX SNAP® 4Dx® Plus, polymerase chain reaction [PCR], culture, etc.), few are endorsed for confirming diagnoses. The CDC currently recommends a two-tier testing process for

diagnosing LD in humans; consisting of first round testing with either an enzyme immunoassay (EIA) or an IFA, followed by a Western blot test if a positive was revealed in the first round. Similar recommendations exist for dogs (Littman et al., 2018), however, veterinary practitioners are not required to follow these guidelines before administering treatment. Another diagnostic procedure for detecting LD include bacterial culturing, but is not regularly utilized due to being time consuming and expensive (Babady et al., 2008).

Molecular testing with real-time polymerase chain reaction (qPCR) assays are common within the literature, consisting of both singleplex and multiplex assays (Primus et al., 2018). Popular gene targets, for example, include *23S rRNA* (Courtney et al., 2004), flagellar filament cap (*filD*) (Hojgaard et al., 2014), outer surface protein A (*ospA*) (Ivacic et al., 2007), *hbb* (encodes a member of histone-like proteins) (Portnoi et al., 2006), and flagellin (*flaB*) (Scott et al., 2016). All genes have proven to be highly specific and sensitive as targets for qPCR detection, though the conservation of *flaB* across the *Borrelia* genus has resulted in increased difficulties when ascertaining a specific species (Wodecka, 2011). Due to increased importance of LD in human health, few assays have been specifically designed for use in a dog model. However, most aforementioned qPCR assays can be adapted for use with dogs if properly validated.

It is important to note that the main limitation of molecular diagnostics for LD is the limited spirochetemic stage of pathogenesis. During the acute phase of infection low numbers of LD related spirochetes circulate in the blood, and quickly penetrate endothelial cells as the infection persists (Coburn et al., 2013). Molecular tools, such as qPCR, may only be valuable in detecting infection during the acute stages, therefore reducing the usefulness of utilizing blood as a sample type for screening. Although the consensus is that

molecular detection of LD in blood is considered rare and generally inadvisable, recent studies have documented a low percentage of detection of the spirochete in blood samples (Primus et al., 2018). As the practicality of molecular methodologies in diagnosing LD reliably in noninvasive sample types (e.g. blood vs. tissue biopsies) is restricted, serological assays remain the "gold standard" to achieve diagnosis. However, screening ticks collected from a potentially infected patient, in contrast to a blood sample, may prove efficacious when utilizing molecular assays.

The other group of species responsible for borreliosis in the U.S. are identified as TBRF species, and have been noted as an emerging infectious disease to both animals and humans (Lopez et al., 2016). TBRF is a zoonotic blood-borne disease endemic throughout many regions of the world (Lopez et al., 2016, Talagrand-Reboul et al., 2018). Species responsible for causing TBRF in North America include *B. hermsii, B. turicatae,* and *B. parkeri,* though the later has not been found to play a major role in reported infections (Dworkin et al., 2008). Each of these three species of *Borrelia* are transmitted through a soft tick vector including *Ornithodoros hermsi, O. turicata,* and *O. parkeri,* respectively. Human infections with TBRF are caused by *B. hermsii* and *B. turicatae,* with the majority of cases reported in the western United States and associated with *B. hermsii*. Although there is limited documentation of TBRF in dogs, most reports indicate infection with *B. turicatae* (Esteve-Gasent et al., 2017, Piccione et al., 2016, Whitney et al., 2007), with a more recent case study identifying *B. hermsii* (Kelly et al., 2014).

TBRF infections are hypothesized to be underreported for several reasons, one of which is current diagnostics are confounded by genetically similar organisms such as *Borrelia burgdorferi sensu lato,* the causative agent of LD (Esteve-Gasent et al., 2017,

Kelly et al., 2014, Piccione et al., 2016). Furthermore, signs and symptoms associated with TBRF during febrile states can be similar to LD and most other tick-borne diseases during initial stages of infection (i.e. flu-like illness) or when a readily identifiable rash is overlooked (Dworkin et al., 2008, Little et al., 2010a, Stanek et al., 2012). However, TBRF is only detectable during limited stages, denoted as "relapses", which may further complicate an accurate diagnosis by limiting the window in which a presentation can be evaluated (Talagrand-Reboul et al., 2018). Currently, the most reliable method of TBRF diagnosis is the observation of spirochetemia through blood smear examination (Esteve-Gasent et al., 2017). While this diagnostic method is highly specific to TBRF *Borrelia* species, there is currently limited documentation to support microscopic detection during non-spirochetemic phases of infection (Piccione et al., 2016).

Borrelia species responsible for TBRF in susceptible hosts generally display a cyclic form of clinical manifestation, hence the name relapsing fever (Dworkin et al., 2008). In humans, the febrile stage of TBRF persists for roughly three to four days and is associated with spirochetemia (Lopez et al., 2016). The bacteria are then systematically targeted for elimination by the host immune system, and the host becomes asymptomatic for an afebrile stage that lasts roughly seven to ten days (Lopez et al., 2016). Similar to LD, TBRF spirochetes utilize antigenic variation during this stage to alter outer surface proteins, allowing a population minority to escape from immune system detection and a subsequent relapse to occur within the host (Dworkin et al., 2008).

Interestingly, the TBRF species *B. hermsii* has been noted to diverge into two genetically distinct genomic groups (GG), denoted as GGI and GGII (Schwan et al., 2007). This sub-speciation-like divergence has not yet been found to affect their subsequent

human/animal host uniquely, but a recent study has suggested potentially distinctive modes of virulence associated with the two genomic groups in a pine squirrel model (Johnson et al., 2016). Further characterization of these genomic groups within affected hosts will provide insight into the plausibility of genomic group-dependent virulence and pathogenicity. The two genomic groups of *B. hermsii* have also indicated a potentially unique geographic distribution in a study limited to infected humans, chipmunks, and *Ornithodoros hermsi* ticks, sampled in the Western United States (Schwan et al., 2007). While preliminary, the isolates belonging to GGII were found to mostly cluster in northwestern regions while GGI isolates depicted a grouping pattern in both northwestern and southwestern regions. It is hypothesized that infected migratory birds may be responsible, at least in part, for the geographic distribution of *B. hermsii* genomic groups (Schwan et al., 2007). Further, *B. hermsii* is predicted to continue migrating, and may reach as far south as Texas (Sage et al., 2017).

Because of the genetic similarities between *B. hermsii* GGI and GGII, molecular detection in research laboratories has been primarily limited to multiple gene specific conventional PCR assays with GG identification *via* sequencing (Policastro et al., 2013). While this approach has proven to be mostly effective, it is time consuming, expensive, and heavily dependent on sample availability. Reliance on the multilocus sequence typing (MLST) method to identify GGs may inhibit future studies aiming to rapidly screen a collection of samples, or perform further downstream applications. As TBRF causing species are closely related to agents of LD borreliosis, PCR assays that target conserved genes, such as the *Borrelia flaB* gene, may cross amplify between the species in a similar

fashion to the cross-reactivity seen on serologic platforms (Esteve-Gasent et al., 2017, Piccione et al., 2016).

While alternative genes limited to TBRF species, such as the *Borrelia* immunogenic protein A (*bipA*) (Lopez et al., 2010) and the glycerophosphodiester phosphodiesterase gene (*glpQ*) (Schwan et al., 1996), might be more apt targets for qPCR development, TBRF species discrimination may prove unsuccessful due to genetic conservation between closely related species. Recently limited analysis of a hypothetical protein within the *bh0260* open reading frame conducted in a previous study has shown potential (Policastro et al., 2013).

Furthermore, studies have not reached a consensus on whether TBRF spirochetes can be regularly detected by qPCR methodology through all stages of disease (Lopez et al., 2014). Due to a cyclic form of clinical manifestation that result in limited spirochetemic phases that correlate with febrile states, further studies are needed to determine if molecular tools are sufficient in accurately and reliably detecting TBRF species infections.

Rickettsial pathogens

Rickettsial pathogens of zoonotic importance are represented by three closely related genera within the order Rickettsiales: *Anaplasma, Ehrlichia,* and *Rickettsia* (Renvoise et al., 2011). These genera are responsible for causing rickettsiosis, and ehrlichiosis/anaplasmosis, and reside within the families of Rickettsiaceae and Anaplasmataceae, respectively. The bacterial species within the rickettsial group are generally morulae forming pathogens that parasitize various host sample types.

Anaplasmosis

Anaplasmosis in dogs is primarily caused by the species *Anaplasma phagocytophilum* and *A. platys,* while the latter has limited documentation in dogs of Texas (Little, 2010). Both pathogens are gram-negative cocci bacteria known for forming cellular inclusions, or morulae, in an infected host. Infection with *A. phagocytophilum* causes canine or human granulocytic anaplasmosis (CGA or HGA) by parasitizing circulating monocytes (Carrade et al., 2009). In contrast, *A. platys* targets circulating platelets of dogs, and is commonly referred to as infectious canine cyclic thrombocytopenia (ICCT) (De Tommasi et al., 2014). Traditionally, *A. phagocytophilum* was considered the only zoonotic cause of anaplasmosis; however, a recent study has highlighted the potential for *A. platys* to emerge as a potential threat to human health (Maggi et al., 2013).

The blacklegged tick and the western-blacklegged tick, as with LD, are also responsible for transmitting *A. phagocytophilum* to susceptible hosts (Woldehiwet, 2010). Potential reservoir species in North America include a variety of mammals, including rodents, deer, and some birds (Little, 2010). Dog and human exposure to *A. phagocytophilum* is generally highest in the northeast and the west coast of the U.S., and correlates with regions featuring the highest activity of the tick vectors. In respect to *A. platys,* the role of a specific tick vector is currently not fully understood. Recent reports have reported amplifying *A. platys* from *R. sanguineus sensu lato* ticks, however, the vector competency of this tick still needs to be further verified (Inokuma et al., 2000, Sanogo et al., 2003). It is important to note that neither study conducted by Inokuma et al.

nor Sanogo et al. have detected *A. platys* in U.S. ticks, and therefore, remains vector elusive within the U.S.

Anaplasmosis in dogs due to *A. phagocytophilum* regularly presents with pyrexia, lethargy, and anorexia. Interestingly, it is reported that roughly 60% of dogs that indicate exposure to *A. phagocytophilum* serologically remain asymptomatic (Little, 2010). If left untreated, severe disease may arise from increased susceptibility to secondary opportunistic infections for the patient (Chan et al., 2013). It is important to note that both *B. burgdorferi* and *A. phagocytophilum* are transmitted by the same tick species, and therefore, coinfections in endemic areas of the country are possible.

Infection with *A. platys* is generally considered less severe, and presents with recurrent thrombocytopenia that typically resolves without treatment (Little, 2010). However, coinfections with *A. platys* in dogs may complicate disease progression and alter prognosis. Studies have documented infection with *Ehrlichia canis*, alongside *A. platys*, to be a typical coinfection found in dogs (Ybanez et al., 2012). Further, these pathogens may circulate together in nature due to a shared tick vector, the brown dog tick. Interestingly, despite containing the appropriate tick vectors, competent reservoir hosts, and a naïve population of susceptible dogs, neither *A. phagocytophilum* nor *A. platys* have been detected in Texas dogs outside of seroprevalence indicators.

Diagnosis of anaplasmosis in infected dogs generally begins with a clinical evaluation for a febrile state, or a noted history of tick exposure. A complete blood count (CBC) work up on the dog with anaplasmosis may reveal thrombocytopenia and other abnormalities, but can resemble other tick-borne infections at this stage of infection (Little, 2010). Diagnostic methodologies, consisting of blood smear review and point-of-care

testing (e.g. IDEXX SNAP® 4Dx® Plus Test), or serological (e.g. IFA) and molecular assays (e.g. PCR) are more specific, and therefore recommended. It should be noted that diagnosis may be achieved more efficiently if both molecular and serological tools are utilized concurrently (Little, 2010). However, limitations in sensitivity and specificity featured across diagnostic modalities may result in inaccurate diagnosis or incomplete prevalence studies. Of note, limitations consist of cross-reactions and cross-amplifications across serological and molecular assays, respectively (Little, 2010). In these instances, if another closely related species is reported in place of anaplasmosis, treatment times may be altered and current disease prevalence maps may accumulate inconsistencies. Further, the IDEXX SNAP® 4Dx® Plus Test reports findings at the *Anaplasma* genus level, and therefore cannot be utilized for determining a species-specific differential diagnosis (IDEXX, 2016).

In respect to molecular diagnostics, PCR assays are generally designed to amplify conserved genes within the respective species' genomes. The major surface protein 2 (*msp2*) of *A. phagocytophilum* has been shown to be relatively species specific, though orthologs have been discovered in closely related *Anaplasma* spp. (Lin et al., 2004, Sarkar et al., 2008). Few molecular diagnostic assays have been developed in respect to *A. platys* and are generally limited to detecting the *23S rRNA* gene (Dahmani et al., 2015). A popular gene for molecular targeting both *Anaplasma* spp. is the *16S rRNA* gene (Huber et al., 2017). However, careful consideration must be applied when designing an assay for detecting this target due to the close genetic similarity of the *16S rRNA* gene shared across species within the Rickettsiales order.

Rickettsiosis

Within the rickettsiosis disease group, Rocky Mountain spotted fever (RMSF) has been reported to be of most concern to canine health (Chomel, 2011). RMSF is caused by the gram-negative intracellular pleomorphic bacterial pathogen *Rickettsia rickettsii*, and is transmitted by several tick vectors. Vectors include the American dog tick (*Dermacentor variabilis*), the Rocky Mountain wood tick (*D. andersoni*), the brown dog tick (*Rhipicephalus sanguineus*), and the cayenne tick (*Amblyomma cajennense*), all of which are found in the U.S. and the transboundary regions with Mexico (Labruna et al., 2011). Of note, within transboundary U.S. and Mexican states, prevalence rates of RMSF closely correlate with the presence of brown dog ticks on dogs, and therefore potentially represent the primary vector in the regions (Alvarez-Hernandez, 2010, Tinoco-Gracia et al., 2018).

Dogs are highly susceptible to RMSF, and present with similar signs as with ehrlichiosis, though in a more advanced form. In addition to typical CBC abnormalities, dogs will also present with petechial hemorrhaging due to the bacterium invading endothelial cells, as well as advanced neurological signs (Allison and Little, 2013). A rash has been known to develop in conjunction with infection, but is not reliable in all cases as the rash is short lived and even absent for many canine, and human, patients (Chapman et al., 2006).

It is important to note that *R. rickettsii* is one species within a larger complex of *Rickettsia* species known as spotted fever group rickettsioses (SFGR). Within the U.S., three additional diseases caused by SFGR species have been identified, including *Rickettsia parkeri* rickettsiosis, Pacific Coast tick fever caused by *R. philipii* (formerly *Rickettsia* sp. 364D), and rickettsialpox caused by *R. akari* (Eremeeva et al., 2018, Trout

Fryxell et al., 2015). Tick vectors for each SFGR species varies slightly, ranging from the Gulf Coast tick (*Amblyomma maculatum*) for *R. parkeri* (Trout Fryxell et al., 2015), and the Pacific Coast tick (*Dermacentor occidentalis*) for *R. philipii* (Eremeeva et al., 2018). Interestingly, *R. akari* is not tick-borne but instead spreads through infected mouse-mites (*Liponyssoides sanguineus*) (Zavala-Castro et al., 2009). Of note, all species represented within the SFGR in the U.S. have demonstrated zoonotic potential by causing disease in humans and dogs (Dall'Agnol et al., 2018, Tomassone et al., 2018).

In addition, there are also numerous non-pathogenic forms of *Rickettsia, R. montanensis* for example (Uchiyama et al., 2012). These species can persist in canine species without causing adverse effects unlike the closely related RMSF causing *R. rickettsii*. Furthermore, these species are genetically similar across numerous genes commonly targeted by qPCR assays, and thus potentially result in false positive results during general epidemiological screenings of ticks or dogs (Raoult and Parola, 2008). In respect to qPCR assay development for differentiating *R. rickettsii*, popular targets consist of the genes encoding the citrate synthase (*gltA*), rickettsial outer-membrane protein A and B (*rOmpA, rOmpB*), and the 17 kD antigen protein (Kato et al., 2013, Trout Fryxell et al., 2015). However, these genes are not limited to *R. rickettsii* and depict high conservation in respect to other pathogenic and non-pathogenic rickettsial species. Recently, a gene encoding a hypothetical protein (A1G_04230) called *rrhyp* has revealed high specificity to *R. rickettsii* alone, and may be an apt target for qPCR development (Kato et al., 2013). As is the case with *B. burgdorferi, R. rickettsii* circulates within the blood stream in low numbers during the acute phase of infection, and invades endothelial cells as the infection

persists (Kidd et al., 2008). Therefore, molecular techniques may be restricted in detecting *R. rickettsii* during all phases of infection.

Ehrlichiosis

Ehrlichiosis in dogs is caused by three species within the genus *Ehrlichia: E. canis*, *E. chaffeensis*, and *E. ewingii*; and can present with a variety of clinical signs, such as lethargy, anorexia, evidence of bleeding, and polyarthritis (Neer et al., 2002). A recent species addition to the *Ehrlichia* genus, known as *E. minasensis*, has also been suggested to cause canine ehrlichiosis, though, its pathogenesis is currently not fully understood (Thomson et al., 2018). While treatment is similar, clinical pathology findings can vary dramatically between dogs with ehrlichiosis; though, thrombocytopenia and mild anemia are common findings, but not definitive (Gieg et al., 2009, Neer et al., 2002). Additional recognized species within the *Ehrlichia* genus, including *E. muris* and *E. ruminantium*, are currently only of major concern to humans and agriculture animals, respectively (Snowden and Simonsen, 2018). However, a recent report has proposed that *E. muris* may be emerging as a threat to canine health (Hegarty et al., 2012).

The brown dog tick, *Rhipicephalus sanguineus*, has also been documented as a competent vector for transmitting *Ehrlichia canis* to canine hosts, and in some instances to humans (Maeda et al., 1987, Perez et al., 2006). Though the brown dog tick is understood to be the most common vector of *E. canis*, the American wood tick (*Dermacentor variabilis*) has also been reported to competently transmit the pathogen (Chomel, 2011). The urban cycle of *E. canis* is dependent on maintenance within the brown dog tick and its predominant blood meal source, the domestic dog (Little, 2010). Due to the brown dog

ticks' ability to thrive in domestic home and kennel habitats, along with its ability to reservoir *E. canis* through transovarial and transstadial passages, a tick infested environment is sufficient in maintaining a competent infection source of *E. canis* within the environment (Dantas-Torres, 2008).

Infection with *E. canis* causes canine monocytic ehrlichiosis (CME) or human monocytic ehrlichiosis (HME) by parasitizing circulating monocytes (Harrus et al., 1999). CME is an important veterinary pathogen due to its worldwide distribution and severe clinical outcomes (Harrus and Waner, 2011). Generally, CME progresses through three phases of disease, acute, subclinical, and chronic. Within the acute phase, a majority of signs associated with infection closely resemble those seen in anaplasmosis, including pyrexia, anemia, dysthymia, lethargy, and inappetence (Harrus and Waner, 2011). Additional signs including nasal or ocular discharge may also be noted, as well as a range of neurological manifestations (Komnenou et al., 2007). The disease may also enter the subclinical phase where, as the name suggests, signs of infection may not be apparent (Waner et al., 1997). If an established infection with CME remains undiagnosed, or its treatment mismanaged, the disease may reach the chronic phase, where prognosis is poor (Mylonakis et al., 2004). As with *B. burgdorferi* and *A. phagocytophilum,* coinfections are common since the same tick vector can transmit both RMSF and CME/HME pathogens (Kordick et al., 1999). Further, *E. canis* has been documented to circulate alongside other tick-borne pathogens such as *Hepatozoon canis*, and *Babesia canis vogeli,* again due to a shared vector (Gal et al., 2007). In the case of coinfections, disease prognosis becomes unpredictable, but typically more severe.

Ehrlichia chaffeensis, a close relative to *E. canis* both in family relation and clinical presentation, is credited with being one of the main causes of HME in humans (Rikihisa, 2015). However, recent studies have revealed the ability of *E. chaffeensis* to colonize dogs in addition to humans and depict the seroprevalence of *E. chaffeensis* in North American dogs (Beall et al., 2012, Nair et al., 2016). Therefore, *E. chaffeensis* should not be omitted when determining a differential diagnosis for a dog presenting with signs resembling ehrlichiosis. *E. chaffeensis* is primarily transmitted to a dog/human host by the bite of an infected lone star tick (*Amblyomma americanum*) in the U.S. (Heitman, 2016). *E. chaffeensis*, in contrast to *E. canis*, is maintained in nature by a sylvatic cycle involving lone star ticks and the primary reservoir host, white-tailed deer (Yabsley, 2010). In addition, while *Rhipicephalus sanguineus* is the primary vector for *E. canis*, studies have suggested that this tick can also be a vector for *E. chaffeensis* (Koh et al., 2016).

E. ewingii is responsible for causing canine or human granulocytic ehrlichiosis (CGE or CHE, respectively) by forming characteristic morulae within circulating granulocytes. Like *E. chaffeensis*, *E. ewingii* is generally transmitted by the lone star tick (*Amblyomma americanum*), which currently remains the only proven competent vector (Gieg et al., 2009, Heitman, 2016). Recently, the tick species *A. inornatum* has also been identified as infected with *E. ewingii*, though further studies would need to be conducted to definitively prove the vector competency of the tick species (Medlin et al., 2015). In Texas, both species of opportunistic feeding ticks have been identified harboring *E. ewingii* (Long et al., 2004, Medlin et al., 2015). It has been accepted that *E. ewingii* is a zoonotic pathogen initially recognized as a distinct etiological agent of dogs in 1992 and later of humans in 1999. The Centers for Disease Control and Prevention began monitoring *E.*

ewingii infections in humans in 2008; however, the majority of ehrlichiosis cases are reported as *E. chaffeensis* despite the potential that a proportion of cases currently reported may be miscategorized (Harris et al., 2016). Furthermore, a recent study indicated *E. ewingii* infections may have been underreported in humans in the United States by as much as 7.0% due to limited molecular testing, nonspecific serological tests, and disease treatment prior to etiologic diagnosis (Harris et al., 2016). Clinical presentations of CGE are similar to other *Ehrlichia* species but are noted as generally less severe in comparison. However, *E. ewingii* infections in dogs are more likely to be associated with polyarthritis than other species of *Ehrlichia* (Gieg et al., 2009, Neer et al., 2002). Therefore, *E. ewingii* should be considered in the differential diagnosis of dogs suspected of having polyarthropathy.

In Texas, ehrlichiosis is primarily associated with *E. chaffeensis* in humans and *E. canis* in dogs with seroprevalence rates of 3.8% and 2.0%, respectively (Beall et al., 2012, Harris et al., 2016). Although *E. ewingii* has not been detected in Texas in recent reviews of human ehrlichiosis prevalence, this organism has been reported serologically in Texas dogs, which have been implicated as effective sentinels (Beall et al., 2012, Harris et al., 2016, Heitman, 2016). Further, all three *Ehrlichia* spp. have an established serological and molecular presence in dogs as shown in prevalence studies of states neighboring Texas, such as Oklahoma and Arkansas (Beall et al., 2012, Little et al., 2010b). A concern remains, however, regarding the detection specificity of serologic assays between other species of *Ehrlichia,* which may lead to pathogen misclassification (Harris et al., 2016). Therefore, there is a need for the continued implementation of species specific serological

tools when conducting *Ehrlichia* species seroprevalence studies on canines (Qurollo et al., 2014).

Difficulties in diagnosing specific *Ehrlichia* species are due in part to limitations of current screening methods. The popular IDEXX SNAP® 4Dx® Plus test utilized by veterinarians advertises detection of antibodies for *E. canis* in addition to other unrelated vector-borne infections (*Dirofilaria immitis*, *Borrelia burgdorferi*, and *Anaplasma* spp.). However, as stated in a peer reviewed IDEXX publication, this test will also detect antibodies recognizing *E. ewingii* and *E. chaffeensis* antigens, thus true *Ehrlichia* species identification through this system may not be achievable (IDEXX, 2016). Additionally, in serologic techniques utilized by diagnostic laboratories, antibodies against *E. ewingii* may cross-react with targets intended for *E. canis*, *E. chaffeensis*, and *A. phagocytophilum*, thus leading to further misclassifications of ehrlichiosis (Harris et al., 2016, Modarelli et al., In press, Rodgers et al., 1989).

While the morulae formed by *E. canis* and *E. chaffeensis* are generally found within monocytes, those formed by *E. ewingii* are most commonly observed within neutrophils. In addition, the morulae of *E. ewingii* appear identical morphologically to *A. phagocytophilum*, thus confounding microscopic discrimination between the two agents. It was not until the advent of molecular diagnostics that it became conceivable to definitively identify between the *Ehrlichia* species, and to provide an accurate prevalence study of the organism within host populations (Buller et al., 1999). Currently, molecular analysis through PCR techniques are considered the most sensitive and specific method in identifying *Ehrlichia* species (Heitman, 2016).

These three species of *Ehrlichia* are of specific interest to the public health field due to potential zoonotic implications, but remain diagnostically problematic due to the conservation observed within the genomes featured across the genus. This lack of differentiation between species has resulted in current published qPCR assays unable to discriminate specific species at the molecular level, due to targeting the conserved *16S rRNA* gene (Peleg et al., 2010), or more recently, the citrate synthase (*gltA*) and heat-shock operon (*groEL*) genes (Ybanez et al., 2012). The scientific importance of differentiating these particular species is two-fold, diagnostic applications as well as species level surveillance. By monitoring the progression of *E. canis*, *E. chaffeensis,* and *E. ewingii* infections within canine hosts, researchers can begin to predict the spillover of the diseases into other species' niches. Although colonization of *E. canis* in humans and *E. chaffeensis* in canines is generally considered rare, an increased occurrence of these events should alert practitioners as the diseases may be adapting new phenotypic traits that could negatively affect a broader range of hosts.

Babesial pathogens

Canine babesiosis is caused by piroplasmic pathogens characterized by intraerythrocytic inclusions and a parasitic life cycle that induces hemolytic anemia within infected dogs. Within the U.S., four species of *Babesia*: *B. gibsoni, B. canis vogeli, B. conradae*, and *Babesia spp.* coco (also known as NC *Babesia*), are responsible for the majority of babesiosis infections in domesticated dogs (Shock et al., 2014). Morphologically, these organisms are often referred to as large (*B. canis vogeli*, NC *Babesia*) and small (*B. gibsoni, B. conradae*) *Babesia* in a clinical hematology setting.

While all aforementioned species can cause severe infection is dogs, currently only *B. gibsoni* and *B. canis vogeli* are of most concern in the veterinary field (Sudhakara Reddy et al., 2016).

Clinically, canine babesiosis can be significant, but are especially variable (Sudhakara Reddy et al., 2016). Generally, infected dogs present as pyrexic and anemic, though, advanced forms of disease can also result in organ failure. In most cases, pear-shaped piroplasms can be viewed within the erythrocytes, though it is unclear if the parasite can be viewed microscopically through all phases of pathogenesis within a host (Homer et al., 2000).

While current studies have not confirmed a tick vector for all four pathogens causing canine babesiosis within the U.S., several tick species have been strongly suspected to play a role in their transmission to canines, such as Ixodid ticks. The ticks *Haemaphysalis longicornis* and *Haemaphysalis bispinosa* are potential vectors of babesiosis as shown in other countries, but have not been identified in the U.S. (Birkenheuer et al., 2005). Studies have reported *R. sanguineus* to be a competent vector for *B. gibsoni* and *B. canis vogeli* within the U.S.; however, this mode of transmission has not been definitively proven (Chomel, 2011, Jongejan et al., 2018). In addition, NC *Babesia* has been detected within *A. americanum* in several U.S. states, and *D. variabilis* is also a strongly suspected vector of the pathogen (Shock et al., 2014). Further, a competent tick vector for *B. conradae* has not yet been identified, though a recent study reported isolating the pathogen from *R. sanguineus* and *Ornithodoros* species ticks (Di Cicco et al., 2012).

In addition to transmission by ticks, an alternate route of babesiosis transmission to canines by direct contact (e.g. fighting) has been proposed (Jefferies et al., 2007), and evidence supporting the hypothesis has been documented (Cannon et al., 2016). Studies have identified *B. gibsoni* as a prominent pathogen found in dogs associated with dogfighting operations, but other pathogens responsible for causing babesiosis should not be ruled out (Cannon et al., 2016, Yeagley et al., 2009). Of note, pit bull-type dogs rescued from various dogfighting operations have revealed the presence of *B. gibsoni* at 33.8% (Yeagley et al., 2009), and 39.0% (Cannon et al., 2016) within the dogs, and later suggested that further infection transmissions are possible as these fighting dogs are reintegrated into the general canine population. Interestingly, Yeagley et al. also reported that dogs with indications of fighting, such as scars on the body, were 5.5 times more likely to be infected with *B. gibsoni* than dogs presenting without scars. It should be made clear, however, that *Babesia* species responsible for causing canine babesiosis are not of zoonotic concern by either tick or direct blood transmission routes.

Diagnostic detection of babesiosis is relatively straight forward, and can consist of a variety of assay types (e.g. serological, culturing, molecular, blood smear evaluation, etc.) (Kubelova et al., 2013). Like many other tick-borne diseases, cross-reactivity can occur between species when utilizing serological techniques, limiting species specific identification in some cases (Kubelova et al., 2013). Culturing *Babesia* species from a potentially infected host can be achieved but is generally not utilized in veterinary diagnostic laboratories due to the extensive training and length of time required to successfully propagate the organism (Schuster, 2002). Microscopic detection of the parasite by blood smear evaluation is a common method for identifying the parasite, and is

routinely performed during clinical presentations or CBCs. However, morphological similarities within respective large (*B. canis vogeli*, NC *Babesia*) and small (*B. gibsoni, B. conradae*) *Babesia* groups may render species specific identification impossible. Molecular methodologies for detecting the parasite within an infected dog has proven to be very successful, even when the organism is not present on blood smear review (Teal et al., 2012). Frequently utilized targets for qPCR assays consist of the following genes: heat shock protein 70 (*hsp70*), beta-tubulin, two internal transcribed spacers (ITS1 and ITS2), and thrombospondin related adhesive protein (*P18*); though the *18S rRN*A gene is by far the most documented target (Rozej-Bielicka et al., 2017).

Prevalence of tick-borne pathogens within Texas dogs

Few molecular prevalence studies concerning TBDs have been conducted in the U.S., including limited surveillance of dogs residing in Minnesota (Beall et al., 2008) and Oklahoma (Little et al., 2010b), but none within Texas. Instead, the majority of TBD prevalence studies in the U.S. have been limited to molecular detection in humans (Harris et al., 2016, Heitman, 2016), or serological analyses in dogs (Beall et al., 2012, Bowman et al., 2009, Esteve-Gasent et al., 2017, Little et al., 2014, Little et al., 2010b, Qurollo et al., 2014). Thus, the majority of surveillance investigations for the aforementioned tick-borne pathogens that affect Texas dogs are currently limited to brief seroprevalence studies and summary reports generated by IDEXX Laboratories.

Seroprevalence studies in dogs are generally conducted with species or genus specific IFA assays, and therefore, indicate past or recent exposure to pathogen(s) by detecting antibodies that are generated by the host in response to an infection. While

generally target specific, there are documented concerns with specificity when applying the tools to characterizing infections by tick-borne pathogens (Harrus and Waner, 2011, Kamani et al., 2013, Piccione et al., 2016). Therefore, seroprevalence studies should be interpreted as baseline for findings and used alongside additional surveillance tools in order to determine true prevalence of a specific pathogen(s) in an area of interest.

The consensus from these reports indicated an approximate tick-borne pathogen seroprevalence ranging from 0.2 - 2.0% across Texas (Table 1-2) (Beall et al., 2012, Esteve-Gasent et al., 2017, Qurollo et al., 2014). In addition, over the last 5 years IDEXX laboratories has documented 11,406 cases of ehrlichiosis, 5,040 of anaplasmosis, and 2,705 of Lyme disease in dogs from the state of Texas (http://www.dogsandticks.com, accessed July 2018). It is important to note, however, that prevalence data for many species within each genera (i.e. *Borrelia hermsii, B. parkeri, Rickettsia rickettsii, Babesia gibsoni, B. canis vogeli*) is not currently available due to lack of appropriate screening for the respective pathogens. Furthermore, IDEXX data reports are limited to indicating exposure at the genus level (*Ehrlichia*, *Anaplasma*), and for Lyme disease (*Borrelia burgdorferi sensu lato*) infections, and therefore, are not fully representative of exposure to specific species. While the available seroprevalence information is beneficial in providing preliminary analysis of dog exposure to various TBDs, the data also brings attention to the gaps in knowledge concerning the prevalence of other species also responsible for causing disease.

Although there is seroprevalence documentation of TBDs in Texas dogs, little is known about the prevalence of actively infected dogs. Molecular prevalence studies, in contrast to seroprevalence studies, detect the DNA presence of a pathogen within an

animal, and therefore, may reveal active infections. Documenting active tick-borne infections by molecular analysis may provide updated rates of active exposure within an area and indicate specific regions that may contain sentinels of disease. However, it should be noted that molecular analysis of an area should be used in conjunction with seroprevalence studies to fully characterize the true prevalence, as discussed in more detail below. In that respect, serological tools highlight areas that have experienced infection in the past, while molecular tools indicate areas currently, or potentially, infected. Together, disease maps may be modeled to predict how a disease will spread or where new infections may emerge.

Table 1-2. Documented prevalence of common tick-borne pathogens of dogs in Texas.

Disease group	Disease agent	Serological prevalence	Molecular prevalence	Reference
Borrelial	*Borrelia burgdorferi*	1.7%*	NA	(Esteve-Gasent et al., 2017, Qurollo et al., 2014)
	B. turicatae	2.0%	NA	(Esteve-Gasent et al., 2017)
	B. hermsii	NA	NA	NA
	B. parkeri	NA	NA	NA
Rickettsial	*Ehrlichia canis*	2.6%*	NA	(Beall et al., 2012, Qurollo et al., 2014)
	E. chaffeensis	0.6%*	NA	(Beall et al., 2012, Qurollo et al., 2014)
	E. ewingii	0.2%*	NA	(Beall et al., 2012, Qurollo et al., 2014)
	Anaplasma phagocytophilum	2.2%	NA	(Qurollo et al., 2014)
	Rickettsia rickettsii	NA	NA	NA
Babesial	*Babesia gibsoni*	NA	NA	NA
	B. canis vogeli	NA	NA	NA

*Average prevalence calculated from referenced studies.

For example, specific species of concern to canine health, such as *Ehrlichia ewingii* or *Anaplasma phagocytophilum*, have been documented serologically in Texas dogs, but have not yet been molecularly detected (Qurollo et al., 2014). While seroprevalence of a

pathogen in an area may indicate true prevalence, concurrent molecular detection of the same pathogen will provide more confidence in the findings due to potential cross-reactivity of the former. Further, species such as *Borrelia hermsii* and *B. parkeri* have not been detected either serologically or molecularly in Texas dogs. However, recent studies have predicted that the tick vectors for the respective pathogens are migrating south and may eventually reach Texas (Sage et al., 2017). Therefore, consistent surveillance of these pathogens, both serologically and molecularly, will allow public health agencies to better prepare for introductions of non-domestic diseases in naïve Texas dog populations. It should also be concluded, however, that insufficient screening for the aforementioned pathogens in Texas may also be indicative of current lack of prevalence data for the organisms in Texas.

It is also important to note that a majority of available TBD prevalence data is based on the analyses of relatively small sample sets of dogs which were collected from Texas with no indication of region of origin, and were instead generalized to the state level. Ecologists commonly delineate Texas into 10 natural ecological regions, primarily based on unique plant communities as a result of differing climate, soil, and weather conditions (Figure 1-1). As depicted by the Gould ecoregions of Texas map, each ecoregion of Texas offers unique ecological perspectives in respect to habitat and climate (Gould et al., 1960). Ranging from west arid deserts, eastern swamps, southern subtropical, and a temperate north; in addition to 91mountain peaks contrasted by vast cave systems and canyons, the state of Texas is home to a unique geography. Conducting prevalence studies with an emphasis on distribution within each ecoregion may indicate specific

ecoregions that contain sentinels of disease, and therefore, regions of high disease risk to susceptible species.

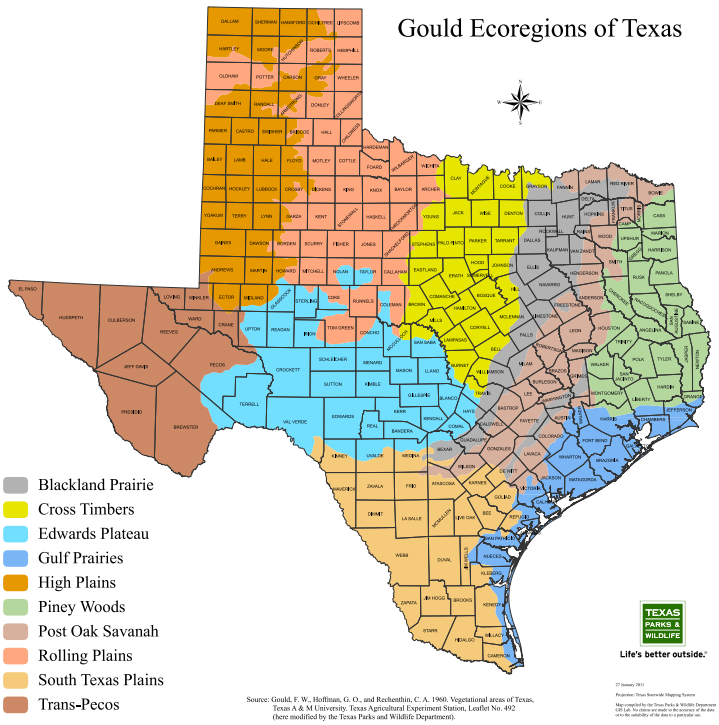

Figure 1-1: Gould Ecoregions of Texas. Texas counties divided into ten natural ecological regions. Map reprinted with permission courtesy Texas Parks and Wildlife Department © 2011 (Wildlife, 2011).

Furthermore, among all U.S. states Texas shares the most significant amount of land bordering Mexico. This transboundary region consists of 1,254 miles of common border per the Texas Department of Transportation (https://www.txdot.gov/inside-txdot.html, accessed July 2018). These regions within Mexico, like Texas, provide unique ecological niches for many TBDs and their respective tick vectors to thrive. Of most concern, the transboundary region has a long history of exchanging pathogens and vectors

that can be detrimental for foreign environments. For example, the highly-invasive tick species *Rhipicephalus microplus* and *R. annulatus* currently residing within Mexico transmit the causative agents for Texas cattle fever (i.e. *Babesia bovis* and *B. bigemina*), which is potentially threatening Texas cattle (Abdullah et al., 2018, Lohmeyer et al., 2018). Although this example details a transboundary risk to cattle, it should be noted that many zoonotic canine tick-borne pathogens are circulating unchecked within Mexico, and may spillover to Texas dogs (Esteve-Gassent et al., 2014). Therefore, investigations aiming to characterize tick-borne prevalence within Texas should also focus on the prevalence of the same organisms within Mexico.

Significance to public health

A majority of tick vectors responsible for transmitting the aforementioned tick-borne pathogens generally seek blood meals from wildlife, whom consequently serve as primary reservoirs for the pathogens through a sylvatic cycle. However, both dogs and humans can act as incidental hosts and may potentially manifest disease if exposed (Dantas-Torres, 2008, Lopez et al., 2016). Therefore, dogs may be considered effective sentinels for human TBDs and might indicate geographical areas of increased zoonotic risk (Abdullah et al., 2018, Esteve-Gasent et al., 2017, Mead et al., 2011). The modern symbiotic relationship humans and companion animals share presents an extended pathway for TBDs to migrate between both species. Pets may bring ticks directly into the yard and home setting, where incidences of ticks feasting from pet to owner may inadvertently occur.

In addition, increased interaction between companion animals and wildlife may also fuel these diseases' inadvertent migration to pets, and subsequently their owners, through the introduction of infected ticks or direct transfer (e.g. fighting) of specific agents. One such wildlife-to-domestic migration route may potentially be facilitated through feral canids such as coyotes (*Canis latrans*), especially among southern U.S. states and transboundary regions with Mexico. Studies have long suspected coyotes as natural reservoirs of TBDs, and their ability to colonize both rural and semi urban areas allow them to consistently live amongst both domestic animals and humans (Bischof and Rogers, 2005, Brzeski et al., 2015, Dworkin et al., 2008, Paras et al., 2012, Starkey et al., 2013).

Surveillance investigations of TBDs in the coyote population should be conducted in order to characterize their role as prospective reservoirs of disease; though to current date none have been conducted in Texas. It is important to note, that Texas supports a thriving coyote population, contains competent tick vectors for a majority of zoonotic TBDs, and resides along the transboundary region with Mexico where reservoirs, vectors, and pathogens can freely migrate unburdened. Therefore, Texas represents an ideal region to characterize TBD prevalence in order to reveal which geographic areas, if any, are at the most risk for wildlife-to-domestic disease transfer, and consequently impacting human health.

Limitations in detecting tick-borne pathogens

Thrombocytopenia is a common and clinically significant finding in veterinary patients, most specifically in dogs. Severely decreased platelets (less than 50,000 K/µL) are most commonly associated with TBD, idiopathic/primary immune-mediated

destruction, or occasionally with disseminated intravascular coagulation (DIC) or bone marrow failure. Thus, significant thrombocytopenia is considered a common clinicopathologic finding in TBDs (Carrade et al., 2009, Neer et al., 2002, Piccione et al., 2016). Clinical signs, pertinent history, and full CBC data are imperative for interpretation of thrombocytopenia, but are not ideal tools for determining the specific tick-borne species responsible for infection due to similar presentations between species.

When a TBD is suspected, it is common to review blood smears for potential inclusions or circulating organisms. However, as discussed prior, it may not be feasible to detect the pathogens responsible for infection during all stages of pathogenesis. Further, many tick-borne pathogens are indistinguishable morphologically (i.e. TBRF species, *Ehrlichia* species, *Babesia* species, etc.), restricting the use of blood smear review for determining a species-specific diagnosis.

Culturing tick-borne pathogens is another potential diagnostic tool for determining causative agents of disease. However, many species have demonstrated difficulties in obtaining viable cultures, and some have yet to be successfully cultured (Michelet et al., 2014). Reduced sensitivity, coupled with being labor intensive and time constraining, have severely restricted the application of culturing as a practical means of TBD diagnosis. Therefore, in a clinical setting small serological panels, or in-house tick-screen assays, are often used to rule-out TBDs and determine the causative agent of said disease.

Gold standard tests are not clearly defined for all TBDs, yet diagnosis primarily relies on several serological assays (ELISA, immunofluorescence, and immunoblot) which rely on detecting antibody levels generated by the host's immune response to a pathogen (Maggi et al., 2014). Although clinical signs can be detected within days of infection,

antibody production can take up to 28 days (Neer et al., 2002). In some cases, dogs do not generate an antibody response of a large enough magnitude to be detectable by the currently available serological assays, even when early clinical signs are present (e.g. thrombocytopenia) (Maggi et al., 2014). In dogs, clinical signs are similar among several TBDs, thus deducing a diagnosis would require multiple serological panels and result in a delay in effective treatment. Additionally, high antibody titers may persist for months to years following clinical resolution of some tick-borne pathogens, limiting the value of monitoring titers during treatment and confounding the detection of repeat or concurrent infections (Fritz, 2009, Maggi et al., 2014). Finally, as more vaccinations for TBDs enter the market, current serological assays may experience inconclusive results or end in misdiagnoses if not DIVA (Differentiating Infected from Vaccinated Animals) strategy compatible (Small et al., 2014).

Occasional cross-reactivity is also a common issue in some serological panels. For example, species responsible for causing TBRF can cross react with *Borrelia burgdorferi* serologic tests, resulting in the inaccurate diagnosis of Lyme disease (Piccione et al., 2016). Further, the popular pen side SNAP® 4Dx® Plus test by IDEXX detects antibodies recognizing *Ehrlichia* (i.e. *E. canis, E. chaffeensis, E. ewingii*) and *Anaplasma* (i.e. *A. phagocytophilum, A. platys*) species without discrimination. Thus, true species identification through this system may not be achievable (IDEXX, 2016).

While serologic assays for diagnosing TBDs in veterinary patients are highly utilized and provide valuable information, molecular diagnostic tools (e.g. PCR), in contrast, are often used for detecting acute infections and monitoring responses to treatment due to detecting the presence of the pathogen's DNA. However, some TBD

pathogens only circulate in blood in low numbers during the acute phase of infection, as is the case for *B. burgdorferi* and *R. rickettsii* (Kidd et al., 2008, Primus et al., 2018). PCR may be valuable in detecting an infection prior to seroconversion but may lose its effectiveness as the infection persists. Moreover, current qPCR assays are limited in the number of pathogens that can be detected simultaneously. As discussed prior, many pathogen species can be responsible for a single TBD in a susceptible dog. Due to the limitations in detecting unique pathogen targets imposed by current qPCR technology, this diagnostic modality may be restricted in its overall effectiveness as a TBD screening tool, as discussed further in the following section. Therefore, the limitations of molecular and serological diagnostic tools should be recognized, and may be most effective in determining a differential diagnosis when utilized in parallel (Maggi et al., 2014).

Effective parallel diagnosis has been documented extensively in a human model, and can be extrapolated to an animal model. For example, an infected host that produces a positive enzyme-linked immunosorbent assay (ELISA) and is detected by qPCR may be indicative of an ongoing infection that the immune system has now recognized and mounted a response to, with an estimated infection time of three weeks (Chapman et al., 2006, Wormser et al., 2006). A positive qPCR but negative ELISA may represent an early infection in which the immune system has not been able to establish itself against the pathogen, with an estimated time of less than three weeks since infection (Johnson, 2011). Lastly, a positive ELISA but negative qPCR in asymptomatic animals could represent an infection that has reduced bacteremia below detectable levels, due to the immune system response or antibiotics treatment, and thus further treatment might not be needed (Chan et al., 2013). These examples provide a practitioner a complete window of treatment options

for the affected animal, allowing tailored treatments and providing a specific time frame of pathogen clearing from the host.

A brief history of molecular diagnostic tools

The history of PCR to become a fundamental tool for molecular analysis is ripe with significant innovation and scientific advances. With humble beginnings that can be traced back to a simple tool for facilitating traditional gel-based Sanger sequencing, it was not until the idea catalyst from Dr. Kary Mullis that this simple technique accelerated into the indispensable laboratory tool it is today.

Sanger sequencing

DNA sequencing was developed as a way to visualize the nucleotide composition of a specific sequence. The development of such a system was not immediate, and the methodology was tweaked and built upon by various researchers. In 1965 Dr. Fred Sanger published an article describing the detection of radiolabeled partial-digested fragments, the precursor to traditional first-generation sequencing; or more commonly, Sanger sequencing (Sanger et al., 1965). After undergoing various modifications over the next few years, the Sanger sequencing method lead to the complete sequencing of the first DNA genome (Sanger et al., 1977a, Sanger et al., 1977b). Briefly, the Sanger sequencing method of that time encompassed a single short primer binding onto a region of interest and the implementation of the dideoxy technique, also known as the “chain-termination” reaction (Heather and Chain, 2016). The reaction is then driven by a DNA polymerase enzyme that incorporates chemical analogs of deoxynucleotides (i.e. dideoxyribonucleotides

[ddNTPs]). Four parallel reactions are then performed containing each ddNTP on a polyacrylamide gel, which allows the DNA sequence to be visualized and pieced together. Further iterations of the technique included implementing uniquely radio-labeled deoxynucleotides into the reaction, allowing the DNA sequence to be viewed by a computer reading the reaction (Heather and Chain, 2016). In recent years, more sequencing options have been developed and are widely used (e.g. next-generation sequencing [NGS]), though few rely on the Sanger sequencing method to obtain nucleotide data.

Next generation diagnostic tool

Initially, NGS platforms (e.g. Ion Torrent, HiSeq/MiSeq, GeneReader, etc.) were developed for gathering and analyzing long stretches of DNA and RNA that were previously unachievable by Sanger sequencing methods. The various NGS systems utilize numerous approaches to achieve results, each with their own strengths and limitations (Glenn, 2011). Typically, NGS methods have been utilized for full genome sequencing, identification of potential genetic diseases, and studying pharmacogenomics of drug response (Pareek et al., 2011). These methods have been widely successful, and over the years have become increasingly more cost efficient. Due to the rising popularity of the technology, an additional branch of NGS has formed concerning diagnostic applications in regards to identifying infectious diseases within host samples (Radford et al., 2012).

Briefly, a sample is collected and DNA/RNA purified from a potentially infected host and screened, using NGS methodology, for all present DNA/RNA sequences. The obtained nucleic acid sequences are then analyzed for the presence of sequences matching those of infectious agents. (Frey and Bishop-Lilly, 2015). This technology can

theoretically detect all agents circulating in a host sample despite prior knowledge of specific pathogens in which to target, as is the case with PCR-based diagnostics discussed in the following sections.

This method, however, is currently experiencing technology restrictions involving the analyses of raw data generated by each reaction. Each NGS run collects an immense amount of sequence data of varying depth and coverage which has led to bioinformatic barriers in efficiently analyzing the information in a timely manner (Finotello et al., 2012). This flood of sequence data has become especially debilitating in the analyses of samples containing viruses. NGS indiscriminately gathers all available nucleotide sequences, resulting in a complex mix of various genetically similar viral pathogens, colloquially referred to as quasispecies (Lauring and Andino, 2010). Further, some microbial genomes with large mobile elements and highly variable regions can regularly complicate genome assembly (Tritt et al., 2012). NGS systems have also been noted as generally less cost effective than other diagnostic platforms, with each reaction costing roughly $1000 and requiring an estimated 24 hours to generate raw data; limiting regular usage as a tool in veterinary diagnostic laboratories seeking to conduct rapid and cost efficient differential diagnoses (Frey and Bishop-Lilly, 2015). Though, the overall consensus is that cost and time per reaction will continue to decrease over time.

Therefore, while this technology has demonstrated potential as a versatile molecular diagnostic tool, current limitations in cost, time, and general data analyses have restricted its use to mainly research endeavors. However, with continued innovations of the technology, NGS will become a more beneficial tool in both veterinary and human diagnostic laboratories.

Conventional PCR

Dr. Kary Mullis described the notion for what is now known as conventional polymerase chain reaction (cnPCR) in 1983 (Mullis, 1990), but was not reported until 1985 where cnPCR was sparingly utilized in an experiment involving sickle cell anemia mutations (Saiki et al., 1985). Briefly, the cnPCR process encompasses the amplification of a specific sequence of genomic DNA from any organism of interest by utilizing short oligonucleotide primers that match the DNA sequence and drive the reaction. While resembling the general protocol for conducting Sanger sequencing with a single primer, cnPCR instead incorporates two unique forward and reverse primers into the same reaction, representing 5' and 3' directionality, respectively. The cnPCR process is then subjected to multiple rounds of cycling temperatures which involve denaturing the genomic DNA and permitting the annealing of the primers, mimicking *in vivo* DNA replication. The cnPCR method was more thoroughly described in later publications released in 1986 (Mullis et al., 1986) and 1987 (Mullis and Faloona, 1987).

The first iteration of cnPCR utilized DNA polymerase enzymes purified from the *Escherichia coli* bacterium. However, this process severely limited cnPCR methodology as the enzyme was heat labile and required additions every subsequent temperature cycle. Here, the first significant innovation of the PCR process occurred when a more thermostable DNA polymerase enzyme purified from the *Thermus aquaticus* bacterium was incorporated into the reaction and replaced any use of enzymes derived from *E. coli* (Saiki et al., 1988). The enzyme was later cloned and manufactured in a way where the cnPCR process could be confined to a single tube with no need to consistently open the tube to add extra reagents (Lawyer et al., 1993). Over the following years, the PCR process

was made more efficient and utilized throughout a multitude of experiments and publications. In 1993 Dr. Kary Mullis's discovery of PCR lead to his recognition with a Nobel Prize in chemistry. Though Dr. Mullis's contributions to the development of PCR is substantial, later advances to the process by other scientific teams have allowed the system to evolve into a more versatile tool.

cnPCR has been implemented in numerous experimental studies, including characterizing mutations, gene cloning, molecular diagnostic of pathogens, etc. The first use of the cnPCR process as a tool for conducting molecular diagnostics occurred shortly after Dr. Mullis published his findings (Drake et al., 1987, Lewis et al., 1993, Musial et al., 1988). While mostly effective, limitations regarding assay specificity, time efficiency, and inability to quantify data influenced the conception of a "real-time" PCR system.

Intercalating molecule PCR

The first description of a PCR reaction analyzed in "real-time" was in 1993 as described in Higuchi et al. (Higuchi et al., 1993). Here, the first iteration of a real-time PCR system utilized ethidium bromide that intercalated double stranded DNA during each amplification reaction, and then irradiated the samples to view the subsequent fluorescence during each amplification cycle at an excitation wavelength of 520 nm (Navarro et al., 2015). This methodology allowed the starting DNA concentration of a sample to be determined, as opposed to the reliance on agarose gel band intensity with cnPCR. Furthermore, potential contamination events were significantly reduced by containing the DNA amplification and analysis within a single tube. The most common form of intercalating molecule PCR is the SYBR® Green reaction (Navarro et al., 2015). The

SYBR® Green reaction utilizes a forward and reverse primer similar to cnPCR, but can display results quantitatively or through the analysis of dissociation curves. Dissociation curves represent the fluorescence signal dissociating from amplified double stranded DNA. The generated dissociation curve is dependent on the length and nucleotide composition of the amplified sequence. Reports have indicated that as each target sequence is different in length and composition in comparison to one another, sequence multiplexing (i.e. detecting and distinguishing multiple pathogens simultaneously) may be accomplished, though the current consensus is that specificity is not always maintained (Navarro et al., 2015). Limitations regarding the SYBR® Green PCR reaction include the lack of true multiplex capabilities, where more than one pathogen can be targeted concurrently without relying on generated dissociation curves. Therefore, while SYBR® Green based PCR reactions were heavily utilized within the field of molecular diagnostics, limitations involving multiplex capabilities reduced the systems usefulness in screening for multiple pathogens and determining a differential diagnosis.

Fluorescent molecule PCR

TaqMan probes were first described in 1996, and depict the addition of fluorogenic labeled probes to the PCR process, which allowed for reliable singleplex (i.e. single target) or multiplex (i.e. multiple target) detection in a diagnostic setting (Gibson et al., 1996). Probes are similar to traditional oligonucleotide (primer) sequences but feature a fluorescent moiety on the 5’ end, and an acceptor moiety on the 3’ end that acts as a fluorescent quencher when in close proximity to the 5’ end. Probes are designed to anneal in front of either the 5’ forward or 3’ reverse primer on a specific sequence of interest. The

real-time PCR (qPCR) reaction is then driven by temperature cycles and DNA polymerase, similar to cnPCR, but as the new amplicon is generated the probe is sheared from the sequence and allowed to emit a fluorescence signal that the qPCR instrument reads and interprets in real-time (Navarro et al., 2015).

Though additional versions of the primer-probe system exist (e.g. Scorpions, LUX™, Angler®, etc.), currently TaqMan probes are considered the most popular tool for conducting molecular diagnostics in the veterinary field. It is important to note that a majority of U.S. veterinary diagnostic laboratories operate as state reference laboratories, and therefore, are required to adhere to guidelines enforced by accreditation agencies (e.g. American Association of Veterinary Laboratory Diagnosticians [AAVLD]) and national programs (e.g. National Animal Health Laboratory Network [NAHLN]). Laboratories are required to maintain NAHLN proficiency testing certifications to participate in state surveillance programs, such as screening for high consequence diseases (e.g. avian influenza, foot and mouth disease, etc.). NAHLN approved validation analysis has currently only been conducted on TaqMan qPCR-based instruments, such as the ABI® 7500 Fast real-time PCR and the BioRad CFX96 Touch™ Real-Time PCR Detection System. As such, the ABI system, for example, has become a common qPCR instrument in many veterinary diagnostic laboratories, including the 59 state veterinary diagnostic laboratories within the U.S. Therefore, future molecular assays aiming to be implemented into veterinary diagnostic laboratories should be developed and validated on the aforementioned qPCR systems in order to more efficiently be adapted into current laboratory workflow.

Multiplex real-time PCR

The qPCR system is generally considered more sensitive than cnPCR, though some studies have suggested otherwise (Bastien et al., 2008). Regardless, the qPCR system allows for the facilitation of multiplex reactions that can detect a variety of pathogens simultaneously. Currently, there are a wide assortment of probe fluorophores that emit at a specific wavelength typically ranging from 520 nm to 705 nm (Figure 1-2). However, current qPCR platforms limit the number of probes that can be detected by a given instrument which subsequently limits the number of pathogens that can be screened by a single test. For example, the ABI® 7500 Fast Real-Time PCR System offers the ability to detect any four compatible fluorogenic probes per qPCR assay. Recently, the detection flexibility for the ABI system has been increased to five dyes with the advent of the 7500 Fast Dx Real-Time PCR System. Another common qPCR instrument includes the BioRad CFX96 Touch™ Real-Time PCR Detection System. However, this system is also currently limited to detecting five dyes per assay.

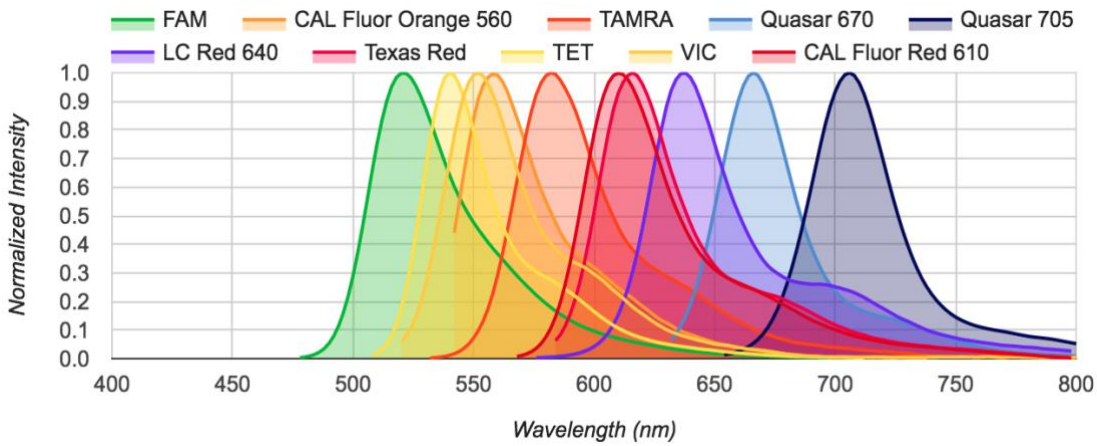

Figure 1-2: Spectral overlay analysis of common real-time PCR fluorophores. Wavelengths (nm) of fluorophores range from 520 to 705**.** Data generated utilizing the Spectral Overlay Tool for Multiplexed qPCR reprinted with permissions from LGC Biosearch Technologies, Inc. (Technologies, 2018).

In respect to the ABI® 7500 Fast system, recommendations for achieving efficacious multiplex testing for four targets (i.e. quadruplex) of interest include utilizing the FAM, CFO560, Q670, and TAMRA probes (Figure 1-3). Here, the wavelength (nm) distance between each probe represents the minimum distance required in order to reduce potential fluorescent interference when analyzed by the instrument. Therefore, although current qPCR instruments can detect numerous probe labels over a broad spectrum of wavelengths, the limiting factor for the instrument's diagnostic capability is the inability to differentiate between the probes when wavelengths are similar. As such, current approaches to molecular screening for more than four to five targets at a time require testing to be conducted by more than one multiplex panel. Consequently, comprehensive molecular testing of a single sample increases associated costs by requiring more reagents and additional time to reach diagnoses.

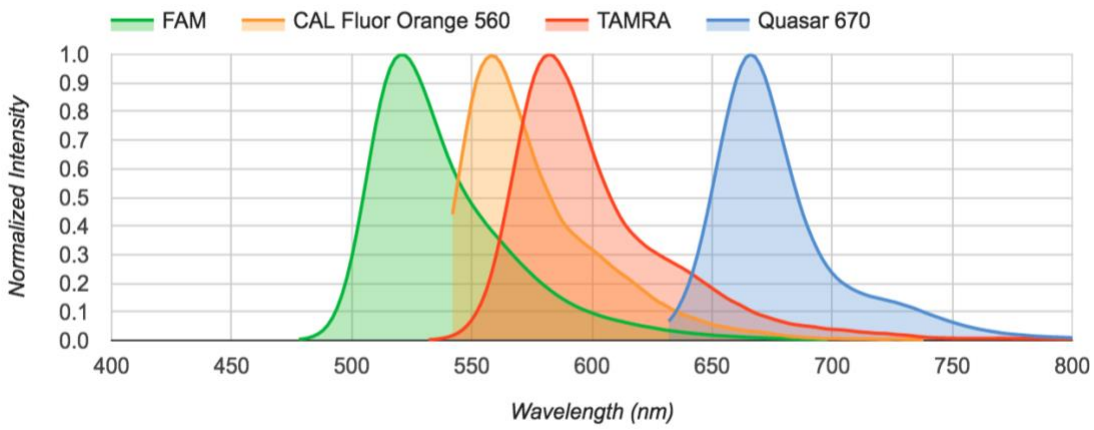

Figure 1-3: Spectral overlay analysis of fluorophores for real-time PCR quadruplex format. Representative fluorophores include FAM, CFO560, TAMRA, and Q670, and emit fluorescence (nm) at 520, 559, 583, and 670, respectively. Data generated utilizing the Spectral Overlay Tool for Multiplexed qPCR reprinted with permissions from LGC Biosearch Technologies, Inc. (Technologies, 2018).

Target/probe restrictions can also have an effect on the quality assurance of a qPCR assay. There exists the potential, when utilizing qPCR assays for molecular diagnostics, for the generation of false negative or false positive results due to assay inhibition during nucleic acid extraction and/or qPCR reaction process. The use of an internal control, either endogenous or exogenous, to mitigate this issue has become more commonplace but requires the use of a separate probe label. Therefore, although qPCR instruments are commonly utilized in the field of veterinary diagnostics and multiplex techniques allow for the analysis of more than one target concurrently, there is a need for a novel technique that can facilitate the detection of more than four to five targets while remaining compatible with currently utilized qPCR instruments. It is interesting to note, that while adding more targets within the fluorescent spectrum is currently not possible due to the inability of qPCR instruments to differentiate between probes emitting similar wavelengths, there may

be potential in modifying the current multiplex qPCR technique to allow for increased detection.

Luminex platform

Another innovation of the general PCR process is represented by a prospective molecular diagnostic tool offered by Luminex® Corporations. The Luminex® platform is a highly multiplexable microsphere-based system that currently allows for more than 100 independent fluorescent channels, analogous to TaqMan probes, to be characterized concurrently (Dunbar, 2006). Briefly, the Luminex® process consists of coupling cnPCR generated products with specific capture probes labeled with fluorescent microspheres, and analyzing the products utilizing their instrument (e.g. xMAP™). This system is exceedingly customizable for detecting any target of interest, and eliminates the fluorescent probe detection limitation featured by traditional qPCR instruments. Recently, this system has been used to simultaneously detect 10 insect-borne pathogens in a host sample (Wang et al., 2018). However, the Luminex™ platform requires a minimum of three steps to reach usable data, consisting of conducting the cnPCR process, followed by coupling the microspheres with the cnPCR products, then transferring the reaction to a Luminex® instrument for final analysis.

Although this methodology has the potential for complete automation of the process, there still exists many possible avenues to introduce contaminates into the reactions. Further, the Luminex® methodology, in current iteration, requires multiple instruments and extended personal attentiveness to generate data. It is also important to note, that the Luminex® platform is not an approved NAHLN testing procedure for the

surveillance of high-impact pathogens. As such, the system is not currently readily equipped nor utilized in a majority of veterinary diagnostic laboratories. In contrast, multiplex qPCR systems allow for a prepared reaction to be placed into a single instrument where results are then provided roughly one to two hours later. Therefore, though the Luminex® system will inevitably improve through new versions, current molecular diagnostic needs may be best satisfied through modifying current multiplex qPCR methodologies.

Modified multiplex real-time PCR

Within the literature, there is an indicated need for a consolidated molecular tool that can screen for a wide variety of pathogens simultaneously for detecting and characterizing TBDs of interest. A molecular tool of such kind would be useful not only as a potential diagnostic tool, but would also facilitate the construction of disease maps within Texas and other underserved areas. Taken together, the main topic of this dissertation is to produce a highly multiplexable molecular tool that can screen for numerous tick-borne pathogens of interest to canine health, be readily utilizable with current technology, and be applicable to conducting molecular prevalence studies within regions containing gaps in knowledge. To accomplish these goals, the ideal result of this work would be the discovery of a novel technique that modifies the qPCR reaction process while maintaining compatibility with commonly utilized probe labels and qPCR instruments.

A potential avenue to achieve these goals may be through a typically underutilized, yet perhaps familiar, technique that may allow numerous pathogens to be detected in a single qPCR reaction. This process involves the of assigning of more than one target

pathogen to a single fluorogenic label, as briefly described previously (Wernike et al., 2013). While Wernike et al. documents the use of a single fluorogenic probe (i.e. Texas Red) to label four pathogens responsible for transboundary animal diseases, the technique may also be adapted to employ multiple probes within a single assay, and for targeting a different group of diseases caused by tick-borne pathogens. Therefore, increased target detection may be achieved by layering the targets within each established probes' emitted wavelength (Figure 1-4).

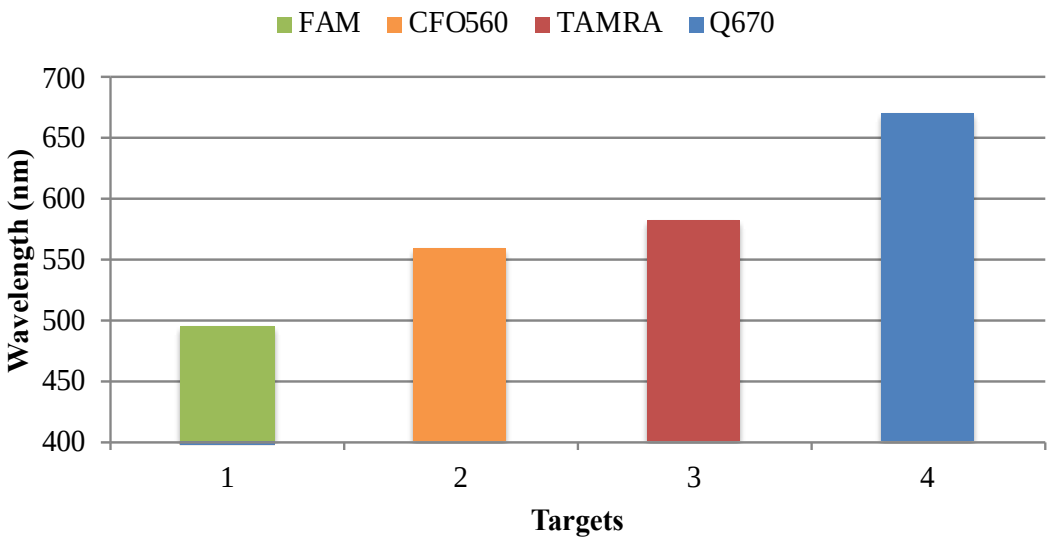

Figure 1-4: Wavelength analysis of fluorophores for quadruplex real-time PCR detection. Targets 1-4 represent potential pathogens labeled with fluorophores FAM, CFO560, TAMRA, and Q670, respectively.

As depicted in Figure 1-4, when the wavelengths (nm) of each fluorophore is displayed along the y-axis, the potential to layer multiple pathogens within the same probe layer can be observed. As this study aims to simultaneously detect and characterize more than four pathogens of interest to canine health, along with an endogenous internal positive control (EIPC), the herein termed "layerplex" technique may be a viable solution (Figure 1-5).

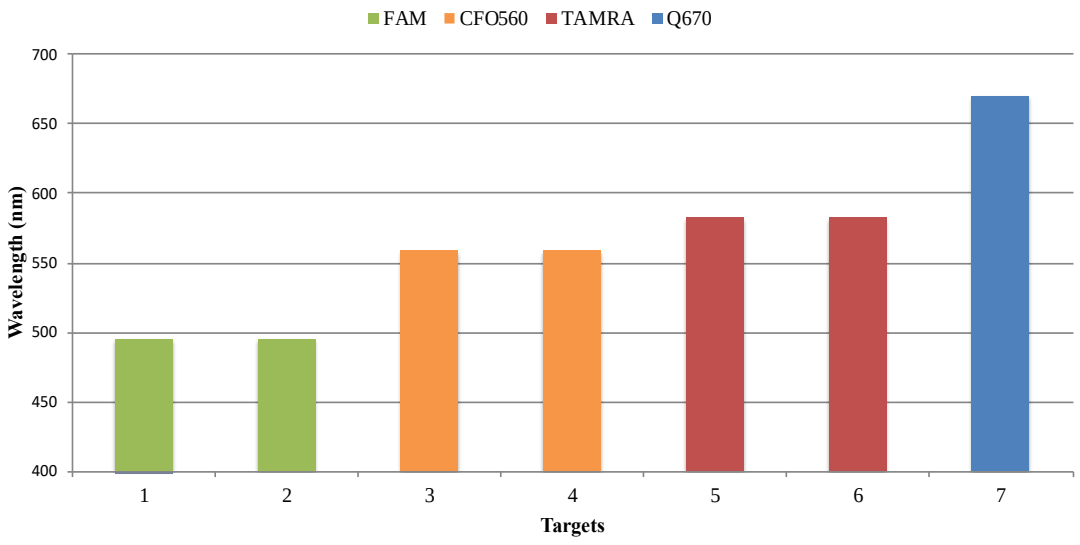

Figure 1-5: Wavelength analysis of fluorophores for layerplex real-time PCR detection. Targets 1-6 represent potential pathogens and are grouped, based on genetic similarity, into three groups labeled with FAM, CFO560, and TAMRA, respectively. Target 7 represents an endogenous internal positive control mechanism for assay quality control, and is labeled with Q670.

As detailed in Figure 1-5, six targeted hypothetical pathogens (1-6) were organized into three groups, or layers, based on species similarity and labeled with the same fluorogenic probes: 1-2 with FAM (520 nm); 3-4 with CFO560 (559 nm); and 5-6 with TAMRA (583 nm). A fourth probe was also needed in order to label a target representing an EIPC for diagnostic quality assurance of DNA extractions using Q670 (670 nm). While this technique will require extensive sensitivity and specificity validation analysis in order to provide evidence of efficacy for use in molecular diagnostics, the technique adheres to the detection requirements of commonly utilized by qPCR instruments.

Thus, within this study, the layerplex qPCR technique will be further investigated to determine its potential for use as a consolidated molecular tool that can detect and characterize numerous tick-borne pathogens concurrently in both diagnostic and surveillance settings.

Central hypothesis and specific aims

Based on the literature review presented, my central hypothesis is that by utilizing a novel multiplexing technique for qPCR assays, termed layerplexing, detection limitations set by traditional qPCR instruments can be bypassed, subsequently allowing the detection of a multitude of pathogens in one reaction.

To evaluate this hypothesis experimentally, the following specific aims will be carried out using *in silico*, analytical, and diagnostic validation methodologies;

Aim I: Establish a canine specific endogenous internal positive control (EIPC-K9) that will mitigate potential false-negative results when screening samples originating from domestic dogs.

Aim II: Develop a layerplex qPCR platform for detecting the most prevalent pathogens responsible for common tick-borne diseases of dogs in a single consolidated molecular assay.

Aim III: Evaluate the combined EIPC-K9 and layerplex qPCR assay in a molecular surveillance investigation of tick-borne diseases in dogs across Texas.

The main objective of this work was to design and develop a novel consolidated molecular assay that can detect the most common tick-borne pathogens of interest to canine health concurrently. This work is significant because current molecular assays have

focused on detecting pathogens in multiple assay formats, therefore limiting their usefulness in large scale molecular prevalence studies. As such, a consolidated layerplex assay may provide efficacious, rapid, and cost-effective means of screening for tick-borne pathogens. Further, the development of a layerplex assay may aid public health agencies in updating maps depicting high-risk areas of disease and developing preventative measures for the affected areas.

CHAPTER II

DEVELOPMENT AND APPLICATION OF A CANINE ENDOGENOUS INTERNAL POSITIVE CONTROL FOR USE IN REAL-TIME PCR ASSAYS[*]

Introduction

To ensure proper performance of real-time PCR (qPCR) assays, diagnostic laboratories utilize internal positive controls (IPC) to monitor nucleic acid extraction and subsequent test results (Goncalves-de-Albuquerque Sda et al., 2014, Huhn et al., 2010). Traditional IPC methodologies utilize exogenous controls (XIPC) for monitoring qPCR assays but feature limitations that may not fully mitigate false-negative results. There are many types of XIPCs, such as plasmids and phages. In general, XIPCs are utilized by spiking a known quantity of control material along with the biological sample undergoing DNA and/or RNA purification (purNA) (Mikel et al., 2015, Schroeder et al., 2013).

Both control types have subsequent primers/probe sequences designed for detection of the XIPC material prepared within multiplex mixtures alongside additional primers/probes pertaining to specific pathogens of interest for a respective assay. The plasmid approach involves the addition of purNA in the form of a plasmid (containing the XIPC specific nucleotide sequence) directly to the biological sample being processed, or to the lysis solution, as previously described (Schroeder et al., 2013). This process focuses on plasmid presence throughout the qPCR testing process and viability of the utilized master

[*] Reprinted with permission from "Development and application of a canine endogenous internal positive control for use in real-time PCR assays" by Joseph J. Modarelli, Pamela J. Ferro, and Maria Esteve-Gasent, 2018. *Journal of Veterinary Diagnostic Investigation*, in press, Copyright 2018 Sage Publications. DOI: 10.1177/1040638718795206.

mix reagents. The presence of a plasmid in a reaction does not necessarily represent either host purNA presence or the occurrence of host cell lysis. The second type of XIPC features the addition of a specific phage to the sample or lysis solution, allowing the verification of cell lysis, in that the phage purNA will only be amplified under true lysis conditions (Mikel et al., 2015). However, this method does not verify the lysis of either the host cell or the lysis of any potentially present pathogens, and therefore may not completely monitor the efficacy of the purNA extraction process. Thus, uses of EIPCs are subject to potential false negative results as these methods are not necessarily fully representative of true sample lysis conditions. Therefore, although utilizing an XIPC is generally sufficient, cases exist in which an endogenous IPC (EIPC) is necessary.

The aim of our study was to identify a genetic marker that could be standardized to specifically amplify a conserved gene region located within canine mitochondrial DNA (mtDNA) for use as an endogenous internal control. The methodology of an EIPC mitigates the need to spike a specific amount of an XIPC into an extracted sample, and alleviates the necessity to rely on the lysis of a phage for monitoring the purNA extraction process. The proposed canine specific EIPC (EIPC-K9) control could potentially work as an internally regulated genetic marker that removes the need for additional external control reagents to the purNA extraction process. The control would theoretically amplify within a qPCR reaction only if the host (*Canis* sp.) cell has fully lysed. A standardized endogenous internal control could benefit future research studies by limiting the time and reagents necessary for developing such a control for experiments, as well as provide a means for uniform qPCR testing across studies. Although alternative endogenous internal housekeeping genes have been utilized (e.g., GAPDH), the emphasis has been placed on

targeting these genes as a reference for gene expression analysis (van Rijn et al., 2014). Our study focused on targeting a region of mtDNA for identifying the species regardless of the sample type being extracted in a veterinary laboratory environment.

Material and methods

Oligonucleotide design

All available domestic dog (*Canis lupus familiaris*) mtDNA nucleotide sequences available in GenBank (*n* = 1,129; query Nov 2016) were sorted and independently aligned (CLC Main Workbench v.7.7, Qiagen Aarhus, Aarhus, Denmark) for gene sequence alignments and nucleotide conservation identification. Subsequent analysis identified the most conserved sequence regions in the canine mtDNA complete genomes that featured nucleotide mismatches with respect to heterologous species mtDNA complete genomes commonly screened in veterinary laboratories (e.g., horse, cat, goat, sheep, white-tailed deer, skunk, cow, pig, chicken, raccoon, and red fox; represented by *n* = 441, 176, 184, 102, 13, 2, 290, 196, 103, 14, and 6, respectively) for primers-probe selection (data not shown). Sequence analysis also included region homology to closely related *Canis* species to ensure adaptive usage of the internal control for future studies aimed at utilizing wildlife samples such as gray wolf (*Canis lupus*, *n* = 112) and coyote (*Canis latrans*, *n* = 8) (data not shown).

Oligonucleotide evaluation

Primers and probes were positioned over aforementioned sequence regions and further analyzed (Primer Express v.3.0, Applied Biosystems, Carlsbad, CA). Sequences were then evaluated on the basis of the following criteria: predicted cross-reactivity with closely related organisms, internal primer binding properties for hairpin and primer-dimer (cross dimerization) potential, physical attributes of primers for extended base-pair repeats and runs, length of the desired amplicon, GC-content, melting temperatures (Tm) of primers and probes, and desired distance between 3'-end of primer and 5'-end of the probe. Oligonucleotide sequences were then searched using BLAST and the *C. lupus familiaris* genome to confirm specificity.

Real-time PCR amplification

Sequence analysis revealed a 96-bp region targeting the NADH:ubiquinone oxidoreductase core subunit 5 (*MT-ND5*) gene within canine mtDNA as the ideal and specific internal control location. Amplifying the selected region with the qPCR assay proved efficacious by performing the reaction using primers EIPC.K9mt.12942F and EIPC.K9mt.13018R, and dual-labeled probe (BioSearch, Novato, CA) EIPC.K9mt.12980P (Table 2-1). The qPCR assay was evaluated in both singleplex and multiplex formats with a final reaction volume of 25.0 µL, by following optimal reaction conditions consisting of 12.5 µL of 2x qPCR Path-ID buffer (Thermo Fisher Scientific, Waltham, MA), 1.0 µL of 25x primer-probe mix (singleplex: working 25x concentration of primers EIPC.K9mt.12942F, EIPC.K9mt.13018R, and probe EIPC.K9mt.12980P-TAMRA at 31.25 nM each; multiplex: the aforementioned EIPC-K9 oligonucleotides at the same

concentration and up to 3 additional unique pathogen primer sets and probe labels), 8.0 µL template DNA, and 3.5 µL of RNase-free water (Applied Biosystems® 7500 Fast Real-Time PCR System, Thermo Fisher Scientific). Recommended cycling conditions include an initial activation of the DNA polymerase at 95°C for 10 min, 40 cycles of a 1 s denaturation at 95°C, followed by a 30 sec annealing-extension step at 60°C.

Table 2-1. Primers and probe used for the detection of *Canis lupus familiaris*.

Oligo ID	Sequence (5'–3')	Amplicon
EIPC.K9mt.12942F	GGATTCTACTCCAAAGACCTGATCA	
EIPC.K9mt.13018R	GGTTAGGGATGTGGCAACGA	96 bp
EIPC.K9mt.12980P	TAM-CACGTCGAATACCAACGCCTGAGCC-BHQ2	

BHQ = black hole quencher; TAM = TAMRA (N,N,N′,N′-tetramethyl-6-carboxyrhodamine).

A positive amplification control (PAC) and standard for the quantitation of the qPCR assay was developed by cloning a 96-bp segment of the *MT-ND5* region that spans the coordinates 12942 and 13037 of the complete mtDNA genome (GenBank® accession EU408254.1). This segment was amplified with the designed primers (Table 1) from a template of genomic DNA extracted and purified from *C. lupus familiaris* blood (MagMax Total Nucleic Acid Extraction Kit, KingFisher Flex Purification System, Thermo Fisher Scientific), as described previously (Schroeder et al., 2013). The PCR products were then cloned in *Escherichia coli* following manufacturer's recommendations (TOPO TA Cloning Kit, Invitrogen, Carlsbad, CA).

Results

qPCR linear dynamic range, efficiency, and analytical sensitivity

To evaluate the analytical sensitivity of the assay, a 10-fold dilution series was conducted with the constructed plasmid PAC to determine a quantification cycle (Cq) cutoff for the qPCR assay, as well as provide the limit of detection (LOD) of gene copies. An efficiency of 92% and an R^2 value of 0.999 was calculated based on the 10-fold dilution series (D'Haene et al., 2010). A LOD of 2 plasmid copies at a Cq cutoff of 38.0 was determined based on the data collected from the generated standard curve.

Analytical and in silico specificity analysis

The diagnostic specificity of the EIPC-K9 control was assessed by demonstrating in duplicate the failure to amplify DNA extracted from opportunistically collected blood samples originating from species routinely tested at the Texas A&M Veterinary Medical Diagnostic Laboratory (TVMDL; College Station, TX). The species tested included: gray wolf, coyote, horse, cat, goat, sheep, white-tailed deer, skunk, cow, pig, chicken, raccoon, and red fox (Figure 2-1). Specificity analysis revealed that a positive EIPC-K9 result indicates that the tested specimen originates from 1 of 3 *Canis* species (*C. lupus familiaris*, *C. lupus*, and *C. latrans*).

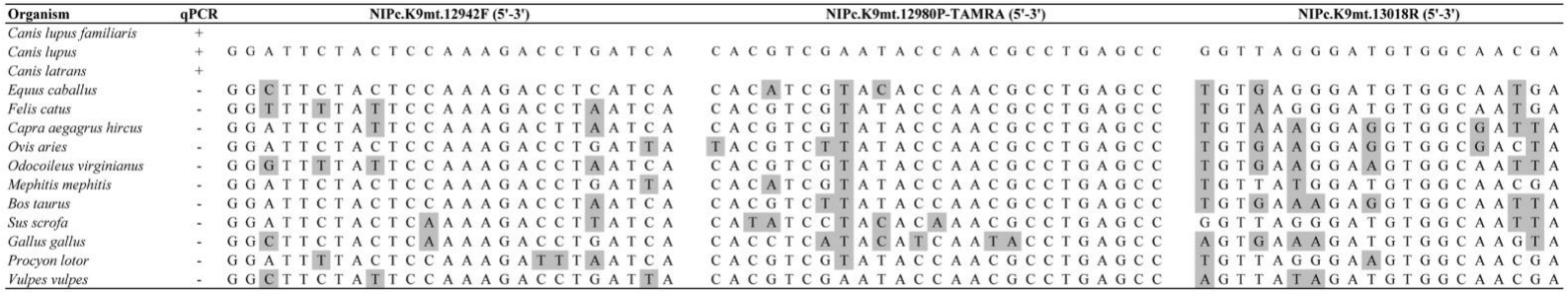

Organism	qPCR	NIPc.K9mt.12942F (5'-3')	NIPc.K9mt.12980P-TAMRA (5'-3')	NIPc.K9mt.13018R (5'-3')
Canis lupus familiaris	+			
Canis lupus	+	GGATTCTACTCCAAAGACCTGATCA	CACGTCGAATACCAACGCCTGAGCC	GGTTAGGGATGTGGCAACGA
Canis latrans	+			
Equus caballus	-	GGCTTCTACTCCAAAGACCTCATCA	CACATCGTACACCAACGCCTGAGCC	TGTGAGGGATGTGGCAATGA
Felis catus	-	GGTTTTATTCCAAAGACCTAATCA	CACGTCGTATACCAACGCCTGAGCC	TGTAAGGGATGTGGCAATGA
Capra aegagrus hircus	-	GGATTCTATTCCAAAGACTTAATCA	CACGTCGTATACCAACGCCTGAGCC	TGTAAAGGAGGTGGCGATTA
Ovis aries	-	GGATTCTACTCCAAAGACCTGATTA	TACGTCTTATACCAACGCCTGAGCC	TGTGAAGGAGGTGGCGACTA
Odocoileus virginianus	-	GGGTTTATTCCAAAGACCTAATCA	CACGTCGTATACCAACGCCTGAGCC	TGTGAAGGAAGTGGCAATTA
Mephitis mephitis	-	GGATTCTACTCCAAAGACCTGATTA	CACATCGTATACCAACGCCTGAGCC	TGTTATGGATGTGGCAACGA
Bos taurus	-	GGATTCTACTCCAAAGACCTAATCA	CACGTCTTATACCAACGCCTGAGCC	TGTGAAAGAGGTGGCAATTA
Sus scrofa	-	GGATTCTACTCAAAAGACCTTATCA	CATATCCTACACAAACGCCTGAGCC	GGTTAGGGATGTGGCAATTA
Gallus gallus	-	GGCTTCTACTCAAAAGACCTGATCA	CACCTCATACATCAATACCTGAGCC	AGTGAAAGATGTGGCAAGTA
Procyon lotor	-	GGATTTTACTCCAAAGATTTAATCA	CACGTCGTATACCAACGCCTGAGCC	TGTTAGGGAAGTGGCAACGA
Vulpes vulpes	-	GGCTTCTATTCCAAAGACCTGATTA	CACGTCGAATACCAACGCCTGAGCC	AGTTATAGATGTGGCAACGA

Figure 2-1: Oligonucleotide analysis of the EIPC-K9 assay in respect to homologous and heterologous species' mitochondrial DNA target sequences. The second column indicates qualitative results (positive or negative) in respect to EIPC-K9 specificity to 2 independent blood samples from homologous and heterologous species (dog, gray wolf, coyote, horse, cat, goat, sheep, white-tailed deer, skunk, cow, pig, chicken, raccoon, and red fox). Mismatch analysis of base-pair positions that are not conserved against EIPC-K9 primers and probe are highlighted in gray.

Analysis of diagnostic specificity

To test the detection and sample specificity utility of the EIPC-K9 assay in canine samples, DNA was screened from 240 (123 from blood, 71 from urine, 21 from nasal swabs, and 25 from tissues biopsies) domestic canine samples, collected opportunistically at TVMDL. EIPC-K9 results of the specimens yielded a detection rate of 100%, and their mean Cq values were noted (Figure 2-2). One-way ANOVA statistical analysis revealed that each specimen type's mean Cq value was significantly different from every other specimen (*p* - values of <0.0001 for blood-urine, <0.01 for blood-nasal swab, <0.0001 for blood-tissue, <0.001 for urine-nasal swab, <0.0001 for urine-tissue, and <0.0001 for nasal swab-tissue). This utility may be extrapolated to act as a quality control method, in which quality of DNA extracted from a canine sample can be monitored by its subsequent EIPC-K9 Cq value. EIPC-K9 was not tested against other sample types derived from dogs, given that we focused on the evaluation of the internal control in respect to commonly tested laboratory specimens. Further studies to determine the efficacy of EIPC-K9 as a standard with other sample types, and to evaluate the control under various inhibitory effects, will be needed for complete analysis.

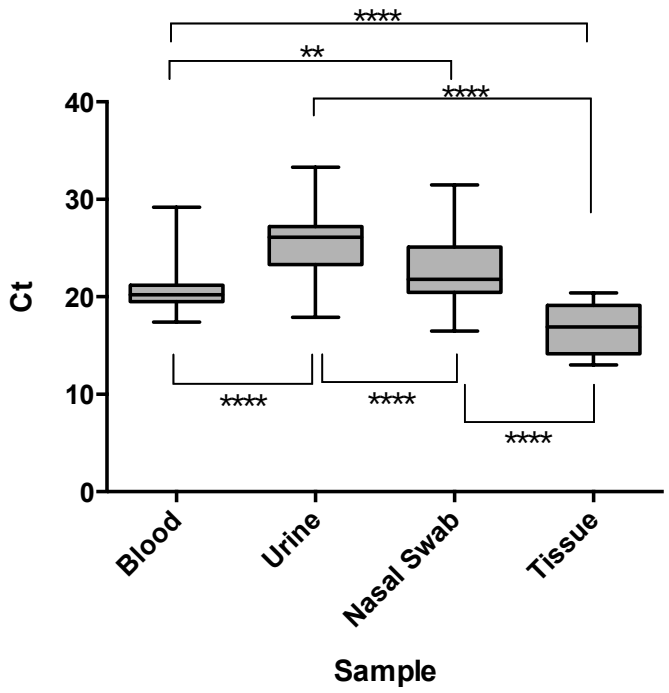

Figure 2-2: Canine biological sample analysis with the EIPC-K9. Mean Cq values ± standard deviation for sample types screened with the EIPC-K9: 16.8, 20.5, 22.5, 25.5, respectively. Samples originated from archived TVMDL cases. "Tissue" denotes variety of tissue samples used for testing (e.g., lung, kidney, cerebrum, brain). One-way ANOVA statistical analysis of sample types in respect to other sample types is represented by asterisks (** = $p < 0.01$, **** = $p < 0.0001$).

Multiplex qPCR compatibility analysis

The utility of EIPC-K9 for use in a multiplex format was also tested and proved useful (Figure 2-3). The qPCR results revealed no significant inhibition regardless of multiplex reaction format in respect to Cq value production by one-way ANOVA analysis for EIPC-K9 and the 3 select pathogen assays (*Borrelia* sp., *Ehrlichia* sp., and *Babesia* sp.). Although initial analysis using the listed pathogens revealed no significant difference for pathogen Cq values, it is important that future use of the control with other targets

include verifying that no inhibition is observed in a multiplex format with the intended assays.

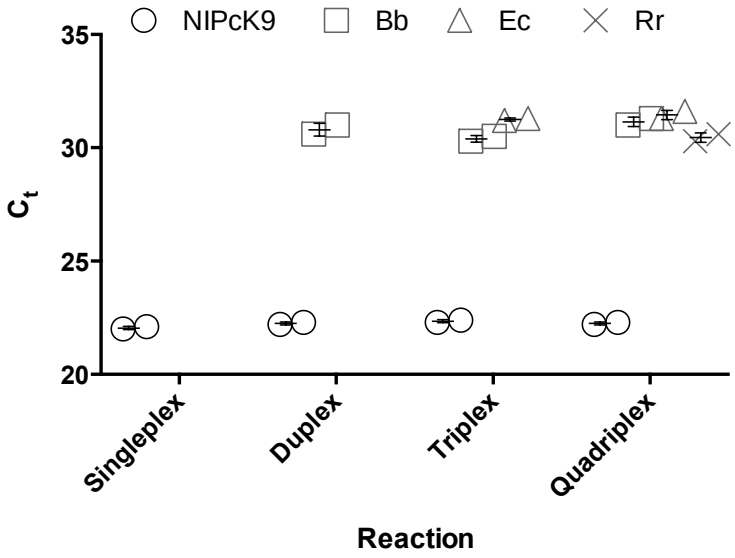

Figure 2-3: Real-time PCR plex reaction analysis with the EIPC-K9. Mean Cq values ± standard deviation from performing duplicate real-time PCR runs using the EIPC-K9 assay and various pathogen-specific assays (*Borrelia burgdorferi* [Bb], *Ehrlichia canis* [Ec], and *Rickettsia rickettsii* [Rr]) under various plex reaction formats. Multiplex assays consisted of duplex (EIPC-K9, Bb), triplex (EIPC-K9, Bb, Ec), and quadruplex (EIPC-K9, Bb, Ec, Rr). EIPC-K9 Cq of ~22.0 represents genomic DNA (gDNA) purified from canine blood and spiked with each pathogen (gDNA at Cq of ~31.0). Concentration of EIPC-K9 and each pathogen is estimated to be 150,000 and 2,000 gene copies per plasmid serial-dilution calculations, respectively.

Discussion

Limitations of the assay include Cq value irregularity within sample types that may be influenced by the nature in which specimens are collected. For example, DNA samples derived from blood featured the least variability in respect to produced Cq values, whereas

urine and nasal swabs experienced higher variability. Blood collection may feature the least inconsistency from animal to animal, whereas a urine or nasal swab sample may be collected from animals experiencing various health conditions (hematuria or epistaxis) and subsequently influence the cellularity of the sample, resulting in a higher or lower Cq value. In addition, sample collection methodology among veterinarians may differ, resulting in further irregularities. Additional limitations include potential inhibition by EIPC-K9 on low levels of target pathogens in a tested sample, and the lack of true analytical specificity evaluations for the control. However, the specificity of the control for only amplifying canine targets should be concluded based on the extensive diagnostic specificity analysis, including the use of homologous and heterologous species, conducted on the control. Finally, as the EIPC-K9 control is limited to detecting genomic DNA, it cannot verify the fidelity of the reverse transcription process in assays intended for RNA targets.

The EIPC proved efficacious when supplemented into qPCR assays that screen canine samples for pathogens of interest. The control may be incorporated into similar assays that feature a melting temperature of 60°C, and may be utilized in multiplex qPCR panels of up to 4 detectors. Although limited, obtained data indicate the potential use of this assay to monitor cellularity of a sample type, verify cell lysis and DNA extraction, as well as species verification.

CHAPTER III

A REAL-TIME PCR LAYERPLEX METHODOLOGY FOR THE DETECTION AND MOLECULAR SURVEILLANCE OF TICK-BORNE PATHOGENS IN DOMESTIC DOGS

Introduction

Tick-borne diseases (TBD) affecting domestic dogs are prevalent throughout the United States and are considered an emerging infectious threat (Chomel, 2011). Tick-borne pathogens, including *Borrelia hermsii* (Bh), *B. turicatae* (Bt), *B. parkeri* (Bp), *B. burgdorferi* (Bb), *Ehrlichia canis* (Ec), *E. chaffeensis* (Ech), *E. ewingii* (Ee), *Anaplasma phagocytophilum* (Ap), and *Rickettsia rickettsii* (Rr), have been documented to infect both dogs and humans, resulting in increased zoonotic threats (Chomel, 2011, Dantas-Torres et al., 2012, Lopez et al., 2016). Though there is limited documentation of infection with pathogens such as Ec in humans, or Bp in both dogs and humans, the risk potential should be recognized (Bouza-Mora et al., 2017, Lopez et al., 2016). Further, protozoan parasites such as species of *Babesia* (Bab), have a worldwide distribution and can result in various levels of clinical severity (Sudhakara Reddy et al., 2016). Of most concern within U.S. dog hosts are *B. gibsoni* and *B. canis vogeli*, though *B. conradae* has also recently been implicated in canine babesiosis (Di Cicco et al., 2012, Solano-Gallego and Baneth, 2011).

Tick vectors responsible for transmitting TBDs vary across disease groups and even at the pathogens' genus level. Currently, proven primary vectors for the assortment of pathogens discussed here include various species within the family of Ixodidae (hard ticks) and Argasidae (soft ticks) (Dantas-Torres et al., 2012). Wildlife are generally considered

appropriate hosts for the majority of these ticks, though dogs and humans can also act as incidental hosts for the majority of these tick species (Dantas-Torres et al., 2012, Lopez et al., 2016). Given domestic dogs and humans frequently share environments, dogs could be considered sentinels for the risk of human exposure to infected tick vectors and may indicate geographical areas of increased zoonotic risk (Abdullah et al., 2018, Esteve-Gasent et al., 2017).

Gold standard tests are not clearly defined for all TBDs affecting dogs, yet diagnosis primarily relies on several serological assays (ELISA, immunofluorescence, and immunoblot) and blood smear examination (Esteve-Gasent et al., 2017, Harrus and Waner, 2011, Otranto et al., 2010). Although clinical signs can be observed within days of infection, detectable antibody production can take up to 28 days (Neer et al., 2002). In some cases, dogs do not generate an antibody response of a large enough magnitude to be detectable by the currently available serological assays, even when clinical signs are present (Maggi et al., 2014). In dogs, clinical signs are similar among several tick-borne diseases, thus deducing a diagnosis would require multiple serological panels and result in a delay in effective treatment. Additionally, high antibody titers may persist for months to years following clinical resolution of some tick-borne pathogens, limiting the value of monitoring titers during treatment and confounding the detection of repeat or concurrent infections (Fritz, 2009, Maggi et al., 2014). As more vaccinations for TBDs enter the market, current serological assays may experience inconclusive results or end in misdiagnoses if not DIVA (Differentiating Infected from Vaccinated Animals) strategy compatible (Small et al., 2014). While serologic assays for diagnosing TBDs in veterinary patients are highly utilized and provide valuable information, molecular diagnostic tools

(e.g. PCR), in contrast, are often used for detecting acute infections and monitoring responses to treatment due to detecting the presence of the pathogen's DNA. However, some TBD pathogens only circulate in blood in low numbers during the acute phase of infection, as is the case for Bb and Rr (Kidd et al., 2008, Primus et al., 2018). PCR may be valuable in detecting an infection prior to seroconversion but may lose its effectiveness as the infection persists. Therefore, the limitations of molecular and serological diagnostic tools should be recognized and may be considered most effective in determining a differential diagnosis when utilized in parallel (Maggi et al., 2014).

Newer molecular assays permit the addition of fluorogenic probes (e.g. quantitative real-time PCR, or qPCR) that allows for a technique known as multiplexing, which has proven to be a useful tool in screening an animal sample for more than one TBD pathogen at a time (Hojgaard et al., 2014, Peleg et al., 2010). Since many TBDs can present with similar clinical signs or as coinfections, panels detecting multiple pathogens would be ideal for comprehensive pathogen identification. However, current qPCR platforms limit the number of probes that can be detected by a given instrument, which subsequently limits the number of pathogens that can be screened in a single test. Most of the widely-utilized qPCR platforms are limited to multiplexing 4-5 fluorophores in a single reaction without interfering with pathogen detection. Current approaches to molecular screening for more than four to five targets at a time require the testing to be conducted in more than one multiplex panel. Consequently, comprehensive molecular testing of a single sample increases associated costs by requiring more reagents and possibly, depending on the number of instruments available, additional time to reach diagnoses.

For these reasons, the development of an affordable molecular screening test for a broad array of pathogens is desirable. Many of the molecular assays currently employed for detecting these TBDs in dogs include various conventional PCR (gel based), singleplex qPCR (single target), or multiplex qPCR assays (multiple targets dependent on instrument capabilities) (Annoscia et al., 2017, Courtney et al., 2004, Hojgaard et al., 2014, Kledmanee et al., 2009, Peleg et al., 2010, Rodriguez et al., 2015, Sirigireddy and Ganta, 2005). However, a typically unutilized, yet perhaps familiar, technique that allows numerous pathogens to be detected in a single qPCR reaction is the process of assigning more than one target pathogen to a single fluorogenic label, as briefly demonstrated in a previous study (Wernike et al., 2013). While colloquially referred to as typical qPCR multiplexing, this study proposes a terminology distinction to differentiate this qPCR technique, herein referred to as layerplexing. Layerplexing represents utilizing any probe to label more than one target assay in a given reaction. In contrast, general qPCR multiplexing would represent utilizing the same probe but for only labeling a single target assay in a reaction. Layerplexing would allow for a large number of unique target assays to be grouped under each probe label, up to the qPCR instruments fluorogenic limit (e.g. 11 targets under 4 probe labels). Once a sample has been screened using the layerplex technique (initial layer), subsequent testing using singleplex or multiplexing versions of each target assay would then be necessary to identify the specific pathogen(s) responsible for infection depending on which initial probe indicated amplification. While additional testing is required after the initial layer to characterize positive species, a negative layerplex result would indicate that the sample was negative for all pathogens screened. This increased screening capability enhances not only animal diagnostics, but also

surveillance studies. Further, the layerplex technique achieves high-throughput testing for all targets by utilizing a single DNA extraction and one qPCR reaction, effectively circumventing current qPCR platform's unique-probe limitations while maintaining compatibility with commonly utilized qPCR instruments.

This study aimed to design a molecular diagnostic tool, using the qPCR layerplex technique, that would screen for the most common TBDs affecting domestic dogs by simultaneously targeting a broad spectrum of pathogens responsible for causing the TBDs. To this end, the pathogenic species that are of most concern to domesticated dogs within five TBD groups (i.e. borreliosis, anaplasmosis, rickettsiosis, ehrlichiosis, and babesiosis) were determined based on past prevalence studies and subsequently targeted for qPCR assay development (Beall et al., 2012, Bowman et al., 2009, Esteve-Gasent et al., 2017, Little et al., 2014, Little et al., 2010b, Piccione et al., 2016). In order to consolidate testing into a single layerplex format, 10 targeted pathogens were organized into three groups, or layers, based on species similarity and labeled with the same fluorogenic probe: borrelial: Bh, Bt, Bp, Bb; rickettsial: Ec, Ech, Ee, Ap, Rr; and pan-*Babesia* species babesial: Bab. A fourth probe was also utilized in order to label an 11th target, represented as an endogenous internal positive control for diagnostic quality control of DNA extractions (Modarelli et al., 2018a). Overall, this study details the design and validation of 10 singleplex assays for each of the targeted pathogens, and the subsequent validation of integrating 11 assays into a single layerplex qPCR assay.

Material and methods

Reference controls

Bacteria and protozoa strains used for the analytical sensitivity and specificity analysis were as follows. Culture from wildlife isolates: *Borrelia hermsii* GGI DAH, *B. hermsii* GGII MTW-4, *B. turicatae* TCBP2, *B. parkeri* SLO, *B. miyamotoi* FR64b, *B. coriaceae* Co53, *B. anserina* BA-2, *B. crocidurae* DOS-56, and *B. recurrentis* 132 were provided by Dr. Tom Schwann at the Laboratory of Zoonotic Pathogens Rocky Mountain Laboratory NIAID Facility. Laboratory isolates: *Borrelia burgdorferi* B31 MSK5, *B. burgdorferi* B31 A3, *B. garinii* (ATCC® 5183™), and *B. afzelii* (ATCC® 51567) were cultured by Dr. Maria Esteve-Gasent at the Texas A&M College of Veterinary Medicine. Laboratory isolates: *Babesia conradae* Wideload, *B. microti* CMNI, and *B. duncani* COA3 were cultured and provided by Dr. Patricia Conrad at UC Davis School of Veterinary Medicine. Laboratory isolates: *Babesia canis vogeli* Buster, *Babesia gibsoni* Ruby, *Babesia duncani* WA3, *B. bovis* Mexico, *B. bovis* TAMU, *B. caballi* Mexico, *B. cabalii* USDA, *B. divergens* Purnell, *B. microti* Ruebush, *B. odocoilei* Wisconsin, *B. bigemina*, *Theileria equi* USDA, and *Cytauxzoon felis* Tyson were cultured and provided by Dr. Patricia Holman at the Texas A&M College of Veterinary Medicine. Genomic DNA isolated from FA substrate slides (VMRD, Pullman, WA; Focus Diagnostics, Cypress, CA; Protatek, St. Paul, MN): *Ehrlichia canis* (SLD-IFA-EC), *E. chaffeensis* (IF1003), *Anaplasma phagocytophilum* (AG-112), *Rickettsia rickettsii* (SLD-IFA-RMSF), *R. typhi* (SLD-IFA-RMSF), *Babesia canis* (AG-119), *B. gibsoni* (AG-123), and *Borrelia burgdorferi* (SLD-IFA-LD). Substrate slides were prepared for DNA extraction by

rehydration with 10.0 µL Phosphate-buffered saline (PBS) onto a single slide well and then suspended in 90.0 µL PBS. The 100.0 µL solution was then purified using the MagMAX™ Nucleic Acid Isolation Kit AMB1836 (Thermo Fisher Scientific, Waltham, MA) following manufacturers recommendations adopted from a previous publication (Schroeder et al., 2013). *16S rRNA* gene gBlocks (IDT, San Jose CA) consisting of: *Ehrlichia ewingii* Stillwater (NR_044747, 1435 base pairs), *E. ruminantium* Welgevonden (NR_074513, 1507 base pairs), *E. muris* AS145 (NR_025962, 1428 base pairs). gBlocks were utilized for validation purposes due to the inability to obtain genomic DNA for the aforementioned isolates. The artificially synthesized gBlocks were constructed based on respective pathogen type-strain *16S rRNA* sequences found in the National Center for Biotechnology Information (NCBI) database. Genomic DNA reference strains provided by the Texas A&M Veterinary Medical Diagnostic Laboratory (TVMDL): *Ehrlichia canis, Anaplasma phagocytophilum, A. marginale, A. centrale,* and *A. ovis*.

Clinical and diagnostic sample collection

In addition to tick vectors, the ideal pre-mortem biological sample type for screening the aforementioned tick-borne pathogens in dogs is whole blood (Bilgic et al., 2013, Elbir et al., 2013, Rosenberg et al., 2018, Vojdani et al., 2009). DNA detection of Bb within blood is considered rare and generally inadvisable, though studies have documented a low percentage of detection of the spirochete in blood samples (Babady et al., 2008, Primus et al., 2018). Therefore, the majority of validation analysis for the assay detailed in this study focused on utilizing ticks and whole blood samples. However, due to the limited blood borne circulation nature of the Bb spirochete, laboratory infected mice were utilized

to simulate infection. 9 infected skin biopsies and 9 joints were harvested for analysis. This study also collected 1,171 archived blood samples originating from dogs that were submitted to two full-service Texas A&M Veterinary Service Laboratory (TVMDL) facilities (i.e. College Station, TX and Amarillo, TX). All samples were archived after the 15-day hold period in which TVMDL has analyzed the samples and provided results to veterinarians, but prior to their destruction and disposal. Further, a total of 211 *Rhipicephalus sanguineus* (brown dog ticks), and 35 *Ixodes scapularis* (black-legged ticks) were utilized for this study.

Oligonucleotide design

Pathogens were separated into three groups (layers) based on species classification: borrelial (*Borrelia* species: Bb, Bh, Bt, Bp); rickettsial (Rickettsiales pathogens: Rr, Ap, Ec, Ech, Ee); and babesial (*Babesia* species: Bab). Assays were designed to target specific gene targets (i.e. *16S rRNA* for *Ehrlichia* spp., *msp2* for *Anaplasma phagocytophilum*, *18S rRNA* for *Babesia* spp., *flaB* and *bipA* for *Borrelia* spp., and *rrhyp* for *Rickettsia rickettsii*) based on previous studies (Babady et al., 2008, Courtney et al., 2004, Kato et al., 2013, Lopez et al., 2013, Modarelli et al., 2018b, Peleg et al., 2010, Rozej-Bielicka et al., 2017). Up to 100 individual nucleotide sequences available in GenBank® greater than 500 bp for each target pathogen were acquired, aligned, and evaluated along with homologous and heterologous gene sequences from closely related species for each respective layer as detailed in the supplementary information (n = 610, 70, 564, 268, 86, and 12 for *16S rRNA*, *msp2*, *18S rRNA*, *flaB*, *bipA*, and *rrhyp*, respectively; Appendix A 1-5). Due to the conservation of the *msp2* and *rrhyp* genes within the respective pathogens, available

sequences were limited to only target pathogens for evaluation. CLC Main Workbench 7.7 (CLCbio, Aarhus, Denmark) was utilized for gene sequence alignments and nucleotide mismatch identification. Additional analysis was performed with Primer Express 3.0 software (Thermo Fisher Scientific, Waltham, MA) to verify primer/probe conformance to an annealing temperature of 60ºC and thermoprofile protocol developed for this project. Sequences were then evaluated on the basis of previously established criteria, and mismatch locations in respect to heterologous pathogens were identified (Modarelli et al., 2018a). Oligonucleotide sequences were then BLAST® searched against the NCBI database and respective pathogen genomes to confirm specificity (Altschul et al., 1990). Sequence information and the final reaction concentrations for oligonucleotides utilized in the qPCR assay are provided in Table 3-1. All primers and Dual-Labeled BHQ® Probes were purchased from a commercial source (LGC Biosearch Technologies, Petaluma, CA). Primer and probe sequences for detection of Bb, Bh, Bt, Bp, Ec, Ech, Ee, Ap, Rr, and Bab were developed in house, EIPC-K9 was taken from a previous publication, and optimal oligonucleotide concentrations were determined through empirical testing (Modarelli et al., 2018a).

Plasmid positive amplification control DNA

A single plasmid control featuring the Bb, Bh, Bt, Bp, Ec, Ech, Ee, Ap, Rr, and Bab target regions was utilized as a positive amplification control (PAC), and for determination of analytical sensitivity and limit of detection (LOD). The plasmid PAC was synthetically generated commercially by inserting the select gene fragments into pUC57 plasmid DNA (GenScript, Piscataway, NJ) and cloned into TOP10 competent *Escherichia coli* cells

(Thermo Fisher Scientific, Waltham, MA). The plasmid was quantified using a NanoDrop™ 8000 Spectrophotometer (Thermo Fisher Scientific, Waltham, MA). An endogenous internal positive control (EIPC-K9) was prepared as described previously (Modarelli et al., 2018a). The final PAC was prepared by combining the target pathogen plasmid DNA with EIPC-K9 target plasmid DNA at 1,000 and 150,000 copies/µL, respectively. The PAC was used for each qPCR run to ensure functionality of the qPCR conditions.

Nucleic acid purification

Nucleic acid purification performed on all samples used in this study for assay validation utilized the MagMAX™ Nucleic Acid Isolation Kit AMB1836 (Thermo Fisher Scientific, Waltham, MA) following manufacturers recommendations adopted from a previous publication (Schroeder et al., 2013).

Layerplex real-time PCR

In order to facilitate the simultaneous screening off all pathogens in a single multiplex format, multiple pathogens were grouped together under specific "layers" and labeled with the same Dual-Labeled BHQ® Probe. Termed here as "layerplexing", four unique probes were utilized to accommodate all 10 assays and the endogenous internal positive control (EIPC-K9) in a single qPCR reaction. The layerplex qPCR was performed with Bb, Bh, Bt, Bp, Ec, Ech, Ee, Ap, Rr, Bab, and EIPC-K9 specific primers and probes (Table 3-1) using qPCR Path-ID™ buffer (Thermo Fisher Scientific, Waltham, MA) according to manufacturer's instructions. Each 25 µL of qPCR contained 12.5 µL of 2x

qPCR buffer, 2 µL of 12.5x primer-probe mix consisting of all oligonucleotides in Table 2-1, 2.5 µL of nuclease-free water, and 8 µL of nucleic acid template. Layerplex qPCR was performed using an Applied Biosystems® 7500 Fast Real-Time PCR System (Thermo Fisher Scientific). Cycling conditions (thermal profile) consisted of activation and denaturation at 95°C for 10 min (1 cycle), and 40 cycles of amplification at 95°C for 1 sec and 60°C for 30 sec, for a total run time of 59 min. Samples with a quantification cycle (Cq) ≤ 38 were considered positive.

Singleplex and conventional multiplex real-time PCR

Singleplex analyses for the detection of individual pathogens were conducted by following the same qPCR reaction template with modifications to the primer-probe mixes. For specific species detection, the associated primer-probe mix was added in place of the layerplex primer-probe mix and was dependent upon intended species detection as detailed further in Appendix B. Conventional multiplex qPCR analysis where each probe labels only one species assay is feasible for a combination of most pathogens, including *Borrelia* spp. and Rickettsiales pathogens. However, as the *Ehrlichia* spp. share a probe label, singleplex analysis would be required if an *Ehrlichia* spp. infection is suspected. Future studies should be conducted in order to further validate individual use of the multiplex capabilities.

Confirmatory conventional PCR analysis

All positive and suspect results from layerplex qPCR analysis were compared with those obtained by conventional PCR. Conventional PCR protocols for the detection of the

16S rRNA gene of *Ehrlichia* and *Anaplasma* species (Wen et al., 1997), the *ompA* gene of *Rickettsia* species, the intergenic spacer sequence (*16S rRNA-23S rRNA*) of *Borrelia* species (Bunikis et al., 2004), and the *18S rRNA* of *Babesia* species were utilized as described previously (Davitkov et al., 2015). Positive (genomic) controls and negative controls (water) were included in all PCR assays. All attained DNA amplicons were then Sanger sequenced in both directions to obtain a consensus sequence (Eurofins Scientific, Louisville, KY).

Data analysis

Polymerase chain reaction efficiency was calculated using the following formula: $E = 10^{(-1/\text{slope})} - 1 \times 100$, and R^2 was calculated using the method described previously (D'Haene et al., 2010). To determine the LOD in terms of copy number, linear regression analysis and serial dilutions of the PAC (working stock: 7.59×10^{-5} ng/µL or 1.27×10^5 copies/µL) were used as template. The LOD was expressed as copy number of the plasmid per assay where each copy of the plasmid represents 1 copy of the pathogen's genome, or genome copy equivalents per microliter (GCE/µL). The copy number of the plasmid was calculated using the formula: copy number = [mass (g) × 6.022×10^{23}] / [length (bp) × 650 Da]. Diagnostic test evaluation for determining sensitivity and specificity, with 95% confidence intervals, was determined by following previously established formulas (Glas et al., 2003).

Table 3-1. Tick-borne pathogen assays organized by layers and EIPC-K9 PCR primers and probes sequences, amplicon sizes, and oligonucleotide concentrations.

Oligonucleotide	Sequence (5′–3′) and reporter dye*	Amplicon (bp)	Concentration (nM)	Target	Reference
Borrelial					
Bb.flaB.161F	AAGAGGGTGTTCAACAGGAAGG		450		
Bb.flaB.213R	GAGAATTAACTCCGCCTTGAGAA	75	450	*flaB*	This study
Bb.flaB.186P	FAM-TCAACAGCCAGCACCTGCTACAGCA-BHQ1		125		
Bh.flaB.531F-1	GGGCGCAAATCAGGATGAG		450		
Bh.flaB.529F-2	GTGGGAGCAAATCAGGATGAG	119, 117	450	*flaB*	This study
Bh.flaB.647R	TCCTCTTGCTGTCCTATCTCTTGC		450		
Bh.flaB.615P	FAM-AGCCTGAGCRCCTTCACCTGCAAAAAGA-BHQ1		125		
Bt.bipA.728F-1	AGACCGGTACACAGGATTCTAAAGC		450		
Bt.bipA.731F-2	CCGGCACACAGGATTCTAAAAC	139, 142	450	*bipA*	This study
Bt.bipA.869R	GTTCCTGCTCCCTGAATAACATTATC		450		
Bt.bipA.818P	FAM-AGTTTTGGGAAGTGTTGTTGGTGGCGT-BHQ1		125		
Bp.flaB.406F	TTGTCCAATAAGTCAGCTGCTCAG		450		
Bp.flaB.522R	TCTTAATGTCCATGAAGCTTGTGC	117	450	*flaB*	This study
Bp.flaB.443P	FAM-CTGAAGAGCTTGGAATGCAACCTGCA-BHQ1		125		
Rickettsial					
Rr.hyp.724702F	AGAGTAAATCAACGGAAGAGCAAAAC		450		
Rr.hyp.724860R	CCCCTCCACTACCTGCATCAT	159	450	*rrhyp*	This study
Rr.hyp.724788P	CFO560-TCCTCTCCAATCAGCGATTCAGGCA-BHQ1		125		
Ap.msp2.420F	GACTTTCCTAGCATGGAGTTGGTT		450		
Ap.msp2.514R	GCGTGCCCTTTTGTAATACCTATAA	95	450	*msp2*	This study
Ap.msp2.452P	CFO560-CATTTCACCTTACACATGCGCCGGA-BHQ1		125		
Ech.16S.64F	GAACGGACAATTGCTTATAACCTTTT	111	450		
Ech-Ee.16S.174R	CCATCATTTCTAATGGCTATTCCATACT		450		
Ee.16S.40F	CGAACGAACAATTCCTAAATAGTCTCT	114	450	*16S rRNA*	This study
Ec.16S.61F	GCCTCTGGCTATAGGAAATTGTTAGT		450		
Ec.16S.148R	CTCGGGGATTATACAGTATTACCCAC	113	450		
Ehrl-spp.16S.83P	CFO560-AGATTCCTACGCATTACTCACCCGTCTGC-BHQ1		125		
Babesial					
Babsp.18S.65F-1	CGCATTTAGCGATGGACCA		450		
Babsp.18S.67F-2	GCTTTTAGCGATGGACCATTCA	94, 93	450	*18S rRNA*	This study
Babsp.18S.289R	CCTAATTCCCCGTTACCCGTT		450		
Babsp.18S.228P	Q670-CATCAGCTTGACGGTAGGGTATTGGCC-BHQ2		125		
EIPC-K9					
EIPC.K9mt.12942F	GGATTCTACTCCAAAGACCTGATCA		31.25		
EIPC.K9mt.13018R	GGTTAGGGATGTGGCAACGA	96	31.25	*MT-ND5*	(Modarelli et al., 2018a)
EIPC.K9mt.12980P	TAM-CACGTCGAATACCAACGCCTGAGCC-BHQ1		31.25		

* FAM= 6-carboxyfluorescein; CFO560= CAL Fluor Orange 560; Q670= Quasar670; TAM= N,N,N′,N′-tetramethyl-6-carboxyrhodamine; BHQ1&2= black hole quencher 1&2.

Results

Layerplex and singleplex detection of target DNA

The layerplex assay was designed for the detection of Bh, Bt, Bp, Bb, Ec, Ech, Ee, Ap, Rr, and pan-Bab species in domesticated dog diagnostic specimens. Each pathogen specific set of oligonucleotides was optimized individually, and then layered together based on species similarity into a single-reaction assay. A canine specific endogenous internal positive control (EIPC-K9) was utilized in the consolidated layerplex assay (Modarelli et al., 2018a). The sequences of all oligonucleotides, their reaction concentrations, and their respective target genes are detailed in Table 3-1.

qPCR linear dynamic range, efficiency, and analytical sensitivity

The linear dynamic range and efficiency of the layerplex qPCR assay, using the listed primers and probes (Table 3-1), was determined using serial dilutions of the plasmid positive amplification control (PAC). Analytical sensitivity for each pathogen in the layerplex assay was assessed in comparison to the respective single pathogen assays. This comparison approach was performed to evaluate the multiple oligonucleotides' combinatory effects on performance. Analytical sensitivities of the layerplex and singleplex assays were comparable for the detection of all pathogens as indicated by linear regression plots (Figure 3-1 A-D). Results were obtained in duplicate experiments to verify the results provided in Figure 3-1.

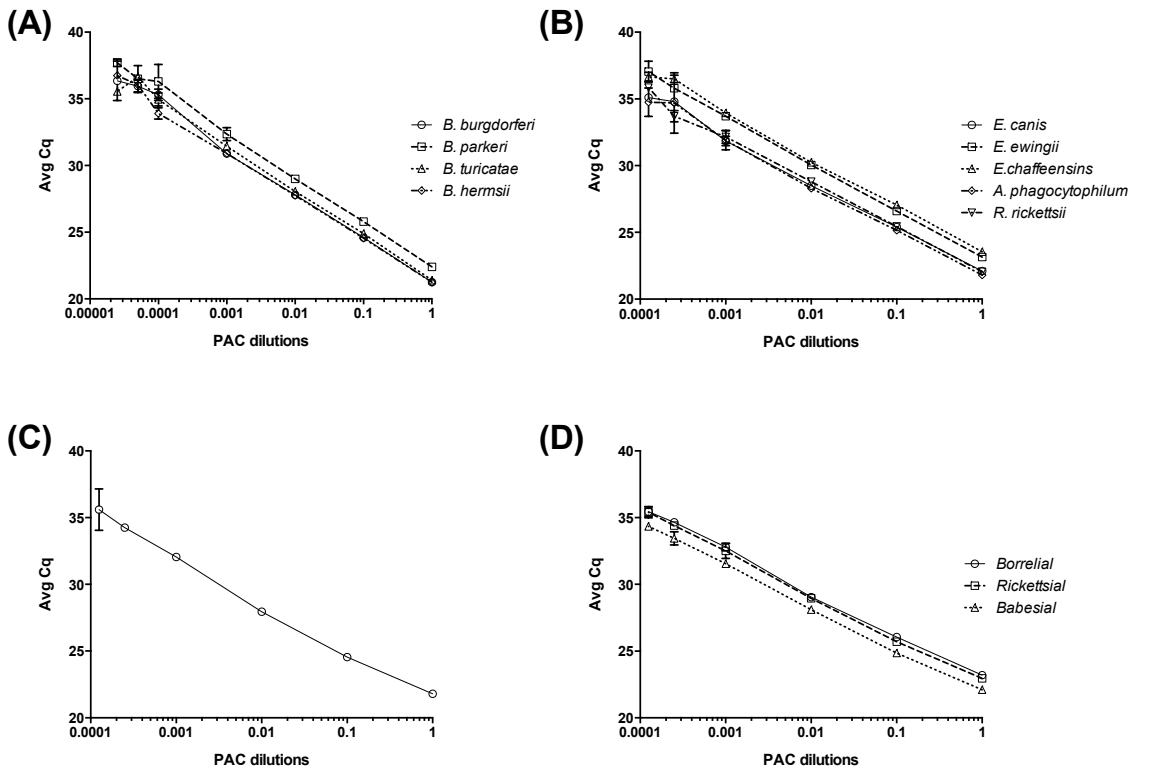

Figure 3-1. Analytical sensitivity of singleplex and layerplex real-time PCR assays. Assays consist of (A) *Borrelia* species (*B. burgdorferi*, *B. parkeri*, *B. turicatae*, *B. hermsii*), (B) Rickettsiales (*Ehrlichia canis*, *E. ewingii*, *E. chaffeensis*, *Anaplasma phagocytophilum*, *Rickettsia rickettsii*), (C) *Babesia* species, and (D) combined pathogen layers (borrelial, rickettsial, and babesial) detection. Plasmid positive amplification control (PAC) was serial diluted and analyzed by qPCR for each singleplex and combined layerplex assays. Each dilution was tested in duplicate.

The singleplex and layerplex assays exhibited 91-105% efficiency ($R^2 > 0.99$) for the detection of serial dilutions of each target (Table 3-2). Copy number calculations for limit of detection (LOD) of the qPCR were estimated to be roughly 16 genome copy equivalents per microliter (GCE/μL) of each target using linear regression analysis and serial dilutions of the plasmid PAC; evaluated independently by singleplex and combined by layerplex (Appendix C).

Table 3-2. Assay efficiencies and R^2 values for singleplex and layerplex assays.

Plex	Assays	Efficiency (%)	R^2
Layerplex	Borrelial layer	105%	0.998
	Rickettsial layer	104%	0.999
	Babesial layer	105%	0.999
Singleplex	Bh	99%	0.996
	Bt	101%	0.990
	Bp	99%	0.998
	Bb	97%	0.996
	Ap	95%	0.996
	Rr	97%	0.995
	Ec	97%	0.996
	Ech	94%	0.997
	Ee	91%	1.000
	Bab	91%	0.995

Analytical and in silico specificity analysis

Analytical specificity was assessed by demonstrating failure to amplify representative species reference controls (i.e. genomic DNA and gBlocks) in duplicate testing from each species other than the intended targets. All homologous and heterologous reference controls used for analytical specificity analysis are detailed in Table 3-3. Further, through *in silico* analysis of respective gene sequences available through GenBank®, each assay was aligned with homologous and heterologous species to verify oligonucleotide mismatch analysis against all available strains and isolates gene sequences (Appendix B). There was no off-target amplification observed through analytical or *in silico* analysis from any borrelial or rickettsial assay in both layerplex and singleplex formats, thus revealing the high specificity of the assays. The babesial layer was designed with the intention to act as a pan-*Babesia* assay for canine, equine, bovine and cervine specific species. In that respect, the assay detected the desired canine pathogens and also detected a number of

equine, bovine, and human *Babesia* pathogens as well (i.e. *B. canis*, *B. gibsoni*, *B. caballi*, *B. odocoilei*, *B. divergens*, and *B. bigemina*) (Table 3-3).

Table 3-3. Analytical specificities of each layer in the real-time PCR assay.

Panel	No. of samples tested	Layer Result		
		Borrelial	**Rickettsial**	**Babesial**
Borrelial target species[a]	5	Positive	Negative	Negative
Borrelia near neighbors[b]	7	Negative	Negative	Negative
Rickettsial target species[c]	5	Negative	Positive	Negative
Rickettsiales near neighbors[d]	6	Negative	Negative	Negative
Babesial target species[e]	6	Negative	Negative	Positive
Babesia near neighbors[f]	8	Negative	Negative	Negative
Tick DNA[g]	228	Negative	Negative	Negative
Canine DNA, blood	1121	Negative	Negative	Negative

[a] *Borrelia hermsii* GGI, *B. hermsii* GGII, *B. turicatae*, *B. parkeri*, and *B. burgdorferi*.
[b] *B. miyamotoi*, *B. coriaceae*, *B. anserina*, *B. crocidurae*, *B. recurrentis*, *B. garinii*, and *B. afzelii*.
[c] *Ehrlichia canis*, *E. chaffeensis*, *E. ewingii*, *Anaplasma phagocytophilum*, *and Rickettsia rickettsii*.
[d] *E. ruminantium*, *E. muris*, *A. marginale*, *A. central*, *A. ovis*, and *R. typhi*.
[e] *B. canis*, *B. gibsoni*, *B. caballi*, *B. odocoilei*, *B. divergens*, and *B. bigemina*.
[f] *Babesia conradae*, *B. microti*, *B. duncani*, *B. bovis*, *Theileria equi*, and *Cytauxzoon felis*.
[g] *Rhipicephalus sanguineus*, *Ixodes scapularis*

Inhibitory analysis

Through triplicate testing, quantification cycle (Cq) values derived from qPCR analysis were comparable for the detection of all species by singleplex testing and the detection of the same species in layerplex format. Further, there was no statistically significant inhibition ($p > 0.05$) between either assay conditions by paired t-test statistical analysis of mean Cq values (Figure 3-2, Appendix D 1-3). Results also indicated that the EIPC-K9 did not experience significant inhibition in the layerplex format when compared to the singleplex version (Appendix D 4).

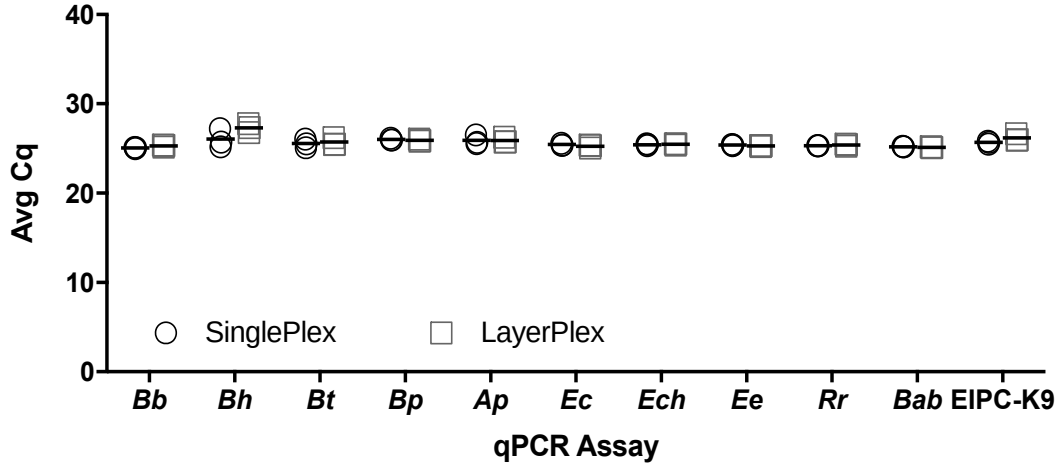

Figure 3-2. Comparison analysis of singleplex real-time PCR assays Cq values against combined layerplex real-time PCR assay Cq values. Pathogens assayed are as follows: *Borrelia burgdorferi* (Bb), *B. hermsii* (Bh), *B. turicatae* (Bt), *B. parkeri* (Bp), *Anaplasma phagocytophilum* (Ap), *Ehrlichia canis* (Ec), *E. chaffeensis* (Ech), *E. ewingii* (Ee), *Rickettsia rickettsii* (Rr), *Babesia* species (Bab), and endogenous internal positive control (EIPC-K9). Singleplex qPCR conditions contained only the primers and probes needed for respective testing. Layerplex qPCR conditions contained all primers and probes listed in Table 1. All assays (singleplex and layerplex) were tested in triplicate against the same respective genomic DNA for each species. A paired t-test was conducted to statistically analyze Cq values obtained from both assay conditions.

Layerplex qPCR performance evaluation using randomly collected animal diagnostic samples

A collection of 1,171 blood samples from domestic dog (*Canis lupus familiaris*), 211 brown dog ticks (*Rhipicephalus sanguineus*), 35 black-legged ticks (*Ixodes scapularis*), and 18 tissues (9 skin and 9 joint) from 9 mice (*Mus musculus*) infected with *Borrelia burgdorferi* B31 A3, were screened by layerplex qPCR for determining diagnostic sensitivity and specificity. Analysis revealed a total of 26, 37, and 5 positives from borrelial, rickettsial, and babesial layers, respectively. Positive samples at the layered level were then subjected to relevant singleplex analysis to determine species identity, with the exception of the 5 babesial layer positives due to the pan-*Babesia* spp. screening nature

of the assay in which conventional PCR alone was used for species identification. Pathogen species identified from the diagnostic sample set included *Ehrlichia canis* (19 from dogs, 18 from brown-dog ticks), *Borrelia turicatae* (8 from dogs), *B. burgdorferi* (9 joint and 9 skin from mice), and *Babesia gibsoni* (5 from dogs). All positive samples were confirmed through relevant conventional PCR and Sanger sequencing. Diagnostic analysis at a Cq value cutoff of 38 revealed sensitivity and specificity values of 100% (86.8-100%) and 99.8% (99.4-99.9%), 100% (90.5-100%) and 99.1% (98.4-99.5%), and 100% (47.8-100%) and 100% (99.7-100%) for borrelial, rickettsial, and babesial layers, respectively (Table 3-4). Singleplex analysis of relevant pathogen assays revealed similar results. EIPC-K9 detected 100% of the dog DNA screened in this study at a mean Cq value of 21.2, and all sample values were within the appropriate range (Modarelli et al., 2018a).

Table 3-4. Diagnostic test evaluation of layerplex assay from analyzed sample set.

	Borrelial	Rickettsial	Babesial
True Positives	26	37	5
False Positives	3	13	0
False Negatives	0	0	0
True Negatives	1396	1375	1420
Sensitivity	100% (86.8-100%)	100% (90.5-100%)	100% (47.8-100%)
Specificity	99.8% (99.4-99.9%)	99.1% (98.4-99.5%)	100% (99.7-100%)

Discussion

Early detection and pathogen identification is critical to limiting the impact of borreliosis, anaplasmosis, ehrlichiosis, rickettsiosis, and babesiosis on an infected canine patient. The ability to screen for all 5 infections simultaneously and rapidly using a single sample and test is highly desirable to aid in obtaining a diagnosis. The main benefit of the newly termed layerplex qPCR method, described herein, includes the ability to screen for

all 10 pathogen specific assays concurrently without a reduction in sensitivity or specificity compared to singleplex analysis. The method described herein also allows for an endogenous internal positive control (EIPC) to be utilized, despite already targeting numerous pathogens, due to the consolidation of probe labels. Though this study utilized an EIPC, an exogenous internal positive control (XIPC) could be substituted and probe labeled accordingly.

While the detection of a positive layer from qPCR testing would require additional conventional, singleplex and/or multiplex testing to reveal the specific pathogen species identity, an obtained negative result by the same method would not require additional testing and instead indicate the lack of pathogen presence in the screened sample. As treatment is similar for all pathogens screened within the respective layers, diagnosticians and veterinarians may find that additional singleplex testing is not necessary for appropriate patient treatment. Although treatment can be determined based on results at the layer level, it is strongly recommended that positive results be subsequently identified to the species level due to public health concern of reportable pathogens screened (e.g. Rocky Mountain spotted fever, Lyme disease, etc.).

It is noteworthy that most assays designed here were able to differentiate between species at the primer level (Appendix B). In other words, the oligonucleotide probes simply acted as a labeling dye that facilitated qPCR detection under multiplex/layerplex conditions. Therefore, SYBR® Green based reactions may also be utilized for sample analysis for all described assays in a singleplex approach. While comparable specificity and sensitivity can be achieved utilizing SYBR® Green formulation for the assays, the ability to screen a sample for all pathogens simultaneously will be limited. However, as

this study has indicated no primer inhibition when all assays are combined together, multiplexing may be accomplished with SYBR® Green due to potentially unique melting temperatures generated by each assay for each respective pathogen. Future studies aimed at utilizing the assays with a SYBR® Green reaction should conduct further validation analysis.

Oligonucleotides designed for qPCR detection of the aforementioned tick-borne disease have resulted in a unique look into the specificity of oligonucleotides under various mismatch conditions. Though the intention of this study was not to determine the exact number of mismatches needed to support efficient qPCR differentiation between species, data presented here does provide insightful evidence for future qPCR assays aiming to differentiate between genetically similar species. As depicted with *B. parkeri* (Appendix B 1C), for example, a minimum of 1-2 mismatches in a general primer location, and 1 in the 3' position of a primers annealing location, was sufficient in restricting primer annealing on a heterologous species, and therefore preventing the extension of DNA polymerase and subsequent formation of an undesired amplicon. Additionally, in the case of *Ehrlichia* species detection, analysis revealed that although the probe sequence used for the detection of all *Ehrlichia* species is identical, differentiation can be achieved at the primer level, due in part, to the presence of significant mismatches. Further, differentiation was achieved even when the probe and reverse primer sequence were identical, as is the case in *Ehrlichia chaffeensis* and *E. ewingii*, and *Borrelia turicatae* and *B. parkeri* (Appendix B 1E and F, C and D, respectively). Here, placing the forward primer over detected mismatches, and designing the probe to anneal on the species' sense strand only, achieved species differentiation. In this case, the mismatches of the forward primer prevent the DNA

polymerase from successfully annealing and cleaving the probe that would anneal onto heterologous species, and only provide detection for the appropriate species.

In specific situations, a number of assays described in this study utilized multiple forward primers. The utilization of more than one forward primer was necessary to anneal and subsequently detect all strain variants within the intended species. *Borrelia hermsii*, for example, has been described to contain two unique genomic groups (GG), which differ slightly genetically (Porcella et al., 2005). Therefore, the assay designed to detect the pathogen required two forward primers to compensate for the additional mismatches within the *flaB* gene of the two GG (Appendix B 1B). A similar technique was also required for efficient detection *of B. turicatae* (Appendix B 1D). In the case of the pan-*Babesia* assay, two forward primers were utilized in order to detect all canine specific species desired with one assay (Appendix B 1J). The pan-*Babesia* assay proved efficient in amplifying a number of additional species including the desired canine specific pathogens. Although there are mismatches present in the additional *Babesia* species detected by the assay, the mismatches are mostly situated on the 5' end of the forward primer and was not found to negatively affect primer binding activity. Consequently, the pan-*Babesia* assay allowed for a more thorough screening of a sample for a more complete *Babesia* species repertoire. Future studies should aim to define the limitations of the assay in respect to broad-spectrum *Babesia* species not covered in this study.

The goal of this study was to evaluate the layerplex methodology for targeting 11 targets (i.e. 10 tick-borne pathogens and an EIPC) in terms of performance (i.e. LOD, efficiency, and R^2), and specificity to a wide range of homologous and heterologous species reference controls. In that respect, performance of the layerplex qPCR was

comparable to other singleplex and duplex qPCR assays available for the detection of tick-borne pathogens (Annoscia et al., 2017, Courtney et al., 2004, Hojgaard et al., 2014, Kledmanee et al., 2009, Peleg et al., 2010, Primus et al., 2018, Rodriguez et al., 2015, Sirigireddy and Ganta, 2005). Efficiency and R^2 values for all assays in both singleplex and layerplex formats were within ideal ranges and were shown to be unaffected by the large collection of oligonucleotides present in the assay. In analytical sensitivity testing, the layerplex displayed no loss in sensitivity in any layer when compared to the respective singleplex qPCR assays. Further, no oligonucleotide-induced inhibition was observed when comparing the detection capabilities of the layerplex format to singleplex testing. As the layerplex assay depicted in this study revealed efficient detection of 11 targets labeled with 4 probes in a layerplex format, further studies are warranted to evaluate the potential of detecting more targets than the limited analysis presented here.

Though linear regression analysis revealed that a Cq value of 36 was an adequate positive sample cutoff (Appendix D), diagnostic sample analysis indicated a number of false negatives at that cutoff value. When the Cq cutoff value was increase to 38, sensitivity evaluations increased to 100%, and eliminated the occurrence of false negatives. Therefore, a Cq of 38 should be considered the cutoff value for diagnostic samples in order to detect all potentially weak positive samples. It is important to note that analyzing samples in terms of a Cq value of 38 increases sensitivity at the expense of specificity. Samples presetting Cq values near the cutoff value should be assessed in conjunction with additional diagnostic modalities (i.e. serological findings, clinical presentation, etc.). Further, due to the lack of identified positive samples for various TBD species (e.g. *Babesia canis, Borrelia turicatae, Ehrlichia chaffeensis*, etc.) current validation analysis

can only estimate the diagnostic specificity and sensitivity of these assays until further studies are conducted. However, the provided analytical and *in silico* analysis for each assay, accompanied with the diagnostic performance of the respective layered assays, should be used as a guideline until additional positive diagnostic samples are supplemented into additional analysis. Furthermore, though no coinfections were observed from the available diagnostic sample data set, the ability of the layerplex assay to support parallel detection through amplification of multiple probe dyes is supported by the linear regression analysis that depicted results for all layers labeled independently with unique probe dyes during concurrent testing.

Access to additional reference controls was limited, resulting in substantial reliance on *in silico* analysis of publicly available nucleotide sequences. It is important to note that additional *Rickettsia rickettsii* reference controls, and controls representing near-neighbors (i.e. *R. parkeri, R. akari,* etc.), were not available for evaluation. Additionally, as the *R. rickettsii* assay is targeting a hypothetical protein conserved in *R. rickettsii* strains only (hypothetical protein A1G_04230), available GenBank® sequences were also limited for *in silico* analysis. However, *in silico* sequence analysis of the *R. rickettsii* qPCR assay depicted conservation within all available *R. rickettsii* gene sequences, a lack of gene similarity in whole genome DNA analysis of other *Rickettsia* species, and the absence of amplification of the available near-neighbor *R. typhi* reference control (Appendix B 1I). Further studies should be conducted to further verify assay specificity in respect to additional *Rickettsia* species reference controls. *In silico* analysis limitations also extend to the *Anaplasma phagocytophilum* and *Borrelia turicatae* assays and their respective targeted *msp2* and *bipA* genes. As in the case of *R. rickettsii*, limited *msp2* gene sequences

are available due to pathogen specific conservation (Courtney et al., 2004). However, the *bipA* gene has been shown to be conserved in other tick-borne relapsing fever (TBRF) species, though a majority of these species do not have *bipA* sequences available in NCBI (Lopez et al., 2010). Nevertheless, despite limited *in silico* analysis of both *A. phagocytophilum* and *B. turicatae*, qPCR analysis against numerous close neighbor reference controls supports assay specificity. In respect to *in silico* analysis of the *Borrelia burgdorferi* assay, there are numerous mismatches in which the oligonucleotides are situated in comparison to gene sequences from various species within the *B. burgdorferi sensu lato* complex (BBSL) (Appendix B 1A). The BBSL group, at present date, contains approximately 20 identified spirochete species with public health concern (Becker et al., 2016). However, due to limited reference control availability it is not conclusive if the assay will not cross-amplify and subsequently detect these species during qPCR screening. Therefore, future studies should be conducted to verify the specificity of the assay to *B. burgdorferi sensu stricto* when screening samples with unknown BBSL infection status.

Despite these limitations, this study achieved the goal of simultaneous screening for 11 targets through layerplex methodology. Collectively, these findings provide support for additional studies to further validate the layerplex qPCR capabilities in terms of applying the methodology to different disease groups that require the detection of a broad spectrum of pathogens, as well as assessing the methodologies limits of detection in terms of targets labeled in a given reaction. In conclusion, this evaluation demonstrates the capacity of the layerplex qPCR assay to detect *Borrelia hermsii, B. turicatae, B. parkeri, B. burgdorferi, Ehrlichia canis, E. chaffeensis, E. ewingii, Anaplasma phagocytophilum,*

Rickettsia rickettsii, and *Babesia* species DNA simultaneously with high sensitivity and specificity in clinical domesticated dog and tick specimens.

CHAPTER IV

MOLECULAR PREVALENCE AND ECOREGION DISTRIBUTION OF TICK-BORNE PATHOGENS IN DOGS OF TEXAS

Introduction

Due to the increased resistance of ticks to acaricides (Coles and Dryden, 2014), ease of travel, and the continuous geographical expansion of ticks (Schurer et al., 2014), dogs (*canis lupus familiaris*) are at continuous risk for tick-borne diseases (TBD) in the United States (Chomel, 2011, Fritz, 2009). The groups consisting of borrelial (*Borrelia turicatae, B. hermsii, B. parkeri, B. burgdorferi*), rickettsial (*Ehrlichia canis, E. chaffeensis, E. ewingii, Anaplasma phagocytophilum, Rickettsia rickettsii*), and babesial (*Babesia gibsoni, B. canis*) pathogens have been documented as the most common causes of TBDs in dogs (Chomel, 2011, Esteve-Gasent et al., 2017, Sudhakara Reddy et al., 2016). Primary tick vectors responsible for transmitting these pathogens vary across disease groups and even at the pathogens' genus level, but are contained within the families of Ixodidae (hard ticks) and Argasidae (soft ticks) (Dantas-Torres et al., 2012). Wildlife are generally considered appropriate reservoir hosts for the majority of these ticks and vectored pathogens, though dogs and humans can also act as incidental hosts and manifest disease if exposed (Dantas-Torres et al., 2012, Lopez et al., 2016). Consequently, dogs are implicated as effective sentinels for human TBDs and may indicate geographical areas of increased zoonotic risk (Abdullah et al., 2018, Esteve-Gasent et al., 2017, Mead et al., 2011).

Few molecular prevalence studies concerning TBDs in dogs have been conducted in the U.S., including limited surveillance in dogs residing in Minnesota (Beall et al., 2008)

and Oklahoma (Little et al., 2010b), but none in Texas. Instead, the majority of TBD prevalence studies in the U.S. have been limited to molecular detection in humans (Harris et al., 2016, Heitman, 2016), or serological analyses in dogs (Beall et al., 2012, Bowman et al., 2009, Esteve-Gasent et al., 2017, Little et al., 2014, Little et al., 2010a, Little et al., 2010b, Qurollo et al., 2014). The consensus from these reports indicated an approximate TBD seroprevalence of 2% across Texas. In addition, over the last 5 years IDEXX laboratories have serologically documented 11,406 cases of ehrlichiosis, 5,040 of anaplasmosis, and 2,705 of Lyme disease in dogs from the state of Texas (http://www.dogsandticks.com, accessed July 2018). This information alone is impressive, but does not include any data on canine babesiosis, which has been recently reported in Texas dogs (Cannon et al., 2016). Therefore, although there is seroprevalence documentation of TBDs in Texas dogs, little is known about the prevalence of actively infected dogs.

The aim of this study was to expand epidemiological data of TBDs in Texas dogs by evaluating the molecular prevalence of their respective causative agents with an emphasis on ecoregion distribution in Texas. Molecular screening, in contrast to serological screening, may identify active infections and indicate specific ecoregions containing sentinels of disease. Ecologists commonly delineate Texas into 10 natural ecological regions, primarily based on unique plant communities as a result of differing climate, soil, and weather conditions (Figure 1-1) (Gould et al., 1960). This study may reveal a unique association of TBDs within subsequent ecosystems. To that end, 1,171 whole-blood dog samples were collected opportunistically from two Texas A&M

Veterinary Medical Diagnostic Laboratory (TVMDL) locations (Amarillo and College Station) and screened for the presence of tick-borne pathogens.

This study was designed in order to estimate the molecular prevalence of TBDs in domestic dogs of Texas. Conducting a molecular prevalence study of TBDs may provide updated rates of active exposure and indicate specific ecoregions that may contain sentinels of disease. To our knowledge, this is the first study if its kind in Texas and can provide baseline data for future research and public health surveillance programs.

Materials and methods

Study area and samples

Between June 2016 and February 2018, a total number of 1,171 EDTA whole-blood samples were collected from domesticated dogs submitted to the Texas A&M Veterinary Medical Diagnostic Laboratory (TVMDL). All blood samples were submitted initially to the TVMDL for complete blood count (CBC) analysis, and then transferred to the College of Veterinary Medicine & Biomedical Sciences at Texas A&M University after the 15-day legal hold period, in accordance with the Material Transfer Agreement between both institutions. No confidential information regarding the pet owners and/or veterinary clinic where the animals were evaluated was provided. No recruitment of animals for the study was performed, and the research team did no direct handling of animals.

Blood samples were collected from dogs of different ages, breed, sex, and health states, and originated from ten ecoregions of Texas: Blackland Prairie, Cross Timbers,

Edwards Plateau, Gulf Prairies, High Plains, Piney Woods, Post Oak Savanah, Rolling Plains, South Texas Plains, and Trans-Pecos (Gould et al., 1960). A total of 121 samples from each ecoregion, with the exception of 82 from the Trans-Pecos ecoregion due to limited availability, were collected in order to estimate true prevalence of disease. The sample set number was calculated assuming a TBD prevalence rate of 2% (seroprevalence) in Texas at a confidence interval of 95% (Beall et al., 2012, Bowman et al., 2009, Esteve-Gasent et al., 2017, Humphry et al., 2004, Little et al., 2014, Little et al., 2010a, Little et al., 2010b, Qurollo et al., 2014). Blood samples were collected opportunistically from two TVMDL clinical pathology departments located in College Station, TX (n = 960) and Amarillo, TX (n = 211). Figure 4-1 shows in grey the counties from which samples were collected and tested.

DNA extraction and real-time polymerase chain reactions (qPCR)

From each animal, an aliquot of EDTA whole-blood (50 μL) was DNA purified using the MagMAX™ Nucleic Acid Isolation Kit AMB1836 (Thermo Fisher Scientific, Waltham, MA) and the KingFisher™ Flex (Thermo Fisher Scientific) automated purification system following manufacturers recommendations adopted from a previous publication (Schroeder et al., 2013). To evaluate the success of DNA extraction, a canine specific endogenous internal positive control (EIPC-K9) targeting the *MT-ND5* gene was utilized in all qPCR reactions (Modarelli et al., 2018a).

qPCR analysis for all 11 targets of interest were screened simultaneously utilizing a qPCR layerplex methodology (Chapter 2. Provisional patent US 62/563, 780). In particular, the pathogens targeted with this assay include: *Borrelia burgdorferi sensu lato*,

B. turicatae, B hermsii (genomic groups I and II), *B parkeri, Anaplasma phagocytophilum, Ehrlichia canis, E. chaffeensis, E. ewingii, Rickettsia rickettsii* and *Babesia* spp. The layerplex qPCR was performed using an Applied Biosystems® 7500 Fast Real-Time PCR System (Thermo Fisher Scientific), following primer/probe concentrations and thermocycler conditions established in the patent pending disclosure. Samples with a quantification cycle (Cq) ≤ 38 were considered positive and confirmed through conventional PCR and Sanger sequencing.

DNA sequencing and sequence analysis

All positive and suspect results from layerplex qPCR analysis were compared with those obtained by conventional PCR. Conventional PCR protocols for the detection of the *16S rRNA* gene of *Ehrlichia* and *Anaplasma* species (Wen et al., 1997), the *16S rRNA-23S rRNA* intergenic spacer sequence (IGS) of *Borrelia* species (Bunikis et al., 2004), and the *18S rRNA* of *Babesia* species were utilized as described previously (Davitkov et al., 2015). Positive (genomic) controls and negative controls (water) were included in all PCR assays. All attained DNA amplicons were then Sanger sequenced in both directions to obtain a consensus sequence (Eurofins Scientific, Louisville, KY). Consensus sequences were then evaluated with CLC Main Workbench (CLCbio, Aarhus, Denmark) and compared with published sequences on the National Center for Biotechnology Information (NCBI) database using the Basic Local Alignment Search Tool (BLAST). All DNA extractions and PCR reactions were prepared and performed under veterinary diagnostic laboratory conditions (i.e. biosafety level 2, biosafety cabinets, good laboratory practices) to avoid potential cross-contamination among tested samples.

Results

Summary of study area and dog samples

The 1,171 canine whole blood samples originated from dogs residing in 55.9% (142/254) of the total counties in Texas, between June 2016 and February 2018. Due to the large geographic size and population dispersion within counties in Texas, the study area was separated into rural and urban counties per designations set by the Texas Department of State Health Services, which bases distinctions on population census reports (https://www.dshs.texas.gov/chs/hprc/counties.shtm, accessed July 2018). In that respect, samples originated from 36.4% (426/1171) rural counties, and 63.6% (745/1171) urban counties. Within this distinction, samples collected for this study accounted for 45.9% (79/172) and 76.8% (63/82) of all counties within either rural or urban settings, respectively. Sample coverage of each representative county within the 10 ecoregions of Texas ranged as follows: Piney Woods 68.0% (17/25), Gulf Parries 76.5% (13/17), Post Oak Savannah 89.3% (25/28), Blackland Prairies 73.7% (14/19), Cross Timbers 75.0% (21/28), South Texas Plains 48.0% (12/25), Edwards Plateau 51.9% (14/27), Rolling Plains 23.8% (10/42), High Plains 38.7% (12/31), and Trans-Pecos 33.3% (4/12). The average age of sampled dogs was 7.8 years (range 8 weeks - 20 years). The sex ratio of our sample set was 41.8% male, 52.3% female, and 5.9% unreported.

Of the samples tested, a total of 2.73% (32/1171) dogs across Texas had one or more tick-borne pathogen DNA detected by layerplex qPCR analysis and confirmed by subsequent conventional PCR and Sanger sequencing. Infections identified included 1.62% (19/1171) *Ehrlichia canis*, 0.17% (2/1171) *Anaplasma platys*, 0.68% (8/1171) *Borrelia*

turicatae, and 0.42% (5/1171) *Babesia gibsoni*. The two dogs infected with *A. platys* were also found to be coinfected with *E. canis*. Further, molecular prevalence rates of each tick-borne pathogen varied across each ecoregion as depicted in Table 4-1. Additional tick-borne pathogens screened in the sample set, including *Ehrlichia chaffeensis*, *E. ewingii*, *Rickettsia rickettsii*, *Anaplasma phagocytophilum*, *Borrelia burgdorferi*, *B. hermsii*, *B. parkeri*, and *Babesia canis*, were not detected.

Table 4-1. Molecular prevalence of tick-borne pathogens in domestic dogs across Texas ecoregions, ranging East to West.

Ecoregion	***Ehrlichia canis***	***Anaplasma platys***	***Borrelia turicatae***	***Babesia gibsoni***
Piney Woods	0.82% (1/121)	ND	ND	0.82% (1/121)
Gulf Parries	2.48% (3/121)	ND	ND	0.82% (1/121)
Post Oak Savannah	ND	ND	1.65% (2/121)	ND
Blackland Prairies	ND	ND	0.82% (1/121)	ND
Cross Timbers	1.65% (2/121)	0.82% (1/121)	1.65% (2/121)	1.65% (2/121)
South Texas Plains	2.48% (3/121)	ND	ND	0.82% (1/121)
Edwards Plateau	0.82% (1/121)	ND	0.82% (1/121)	ND
Rolling Plains	4.96% (6/121)	0.82% (1/121)	0.82% (1/121)	ND
High Plains	1.65% (2/121)	ND	0.82% (1/121)	ND
Trans-Pecos	1.22% (1/82)	ND	ND	ND
Total	1.62% (19/1171)	0.17% (2/1171)	0.68% (8/1171)	0.43% (5/1171)

ND, not detected

Rickettsial molecular findings

DNA from rickettsial pathogens were detected in a total of 21 (1.79%) rickettsial pathogens (19 *Ehrlichia canis* and 2 *Anaplasma platys*) across Texas. A higher molecular prevalence of *E. canis* infected dogs were detected in the Rolling plains ecoregion (4.96%), followed by a uniform prevalence of 0.82% - 2.48% across all other ecoregions except for the Post Oak Savannah and the Blackland Prairies, where *E. canis* DNA was not detected (Table 4-1, Figure 4-1). The mean age of dogs infected with *E. canis* was 6.3 years, (12 weeks - 12.5 years), and no predilection of breed or sex was found. In this study, molecular

detection was highest in September (n = 6), followed by February (n = 4), but were also detected in January, April, June, July, October, and December. Two dogs, aged 7 and 8, were found coinfected with *E. canis* and *A. platys*. Both dogs originated from different central ecoregions (Table 4-1, Figure 4-1) but were detected during the month of February. Moreover, 36.8% (including both coinfected dogs) and 63.2% of the dogs were detected in rural and urban counties, respectively. The CBC analysis revealed that 94.1% of the infected dogs were thrombocytopenic (platelets below reference interval of 200-500 K/µL), 52.9% were anemic (hematocrit below reference interval 32-50%), and 47.1% presented with both anemia and thrombocytopenia. When clinical history was available, the most common clinical signs and findings included lethargy (58%), inappetence (43%), and known exposure to ticks (43%). All *E. canis* and *A. platys* samples identified from Texas dogs were uploaded into GenBank® (Appendix E 1-2) and revealed 99 - 100% identity to *E. canis* and *A. platys* sequences already published. Of note, a single *E. canis* and *A. platys* coinfected dog was solely responsible for the 99% identity in both pathogen sequences, due to a single nucleotide polymorphism (SNP) present within each gene region in respect to published sequences. Additional sequence significance was not observed.

Borrelial molecular findings

A total of 8 (0.68%) *Borrelia turicatae* infections were detected at a molecular prevalence of 0.82 – 1.65% across 6 ecoregions (Table 4-1, Figure 4-1). Further depicted in Figure 4-1 were two clusters of counties in which infections were detected; one northern cluster maintaining a prevalence at 0.82%, and another located in central Texas ranging from 0.82 – 1.65%. The mean age of dogs infected with *B. turicatae* was 7.3 years, (2 - 10

years), and no predilection of breed or sex was indicated. Infections were detected in serial months ranging from February to August, with one to two detections per month. 37.5% and 62.5% of the infected dogs were detected in rural and urban counties, respectively. CBC analysis available for 6 of the dogs revealed that 100% were thrombocytopenic (platelets below reference interval of 200-500 K/µL), 16.7% anemic (hematocrit below reference interval 32-50%), and only one presented as both. Clinical history was not available for a majority of infected dogs, but spirochetemia was observed in 80% of the dogs by blood smear review. Sequence analysis of all 8 *B. turicatae* samples purified from Texas dogs indicated 99% identity with *B. turicatae* strain BTE5EL (CP015629) isolated from a Texas human (Christensen et al., 2017, Kingry et al., 2016). Various SNPs were observed in each sample, and a phylogenetic tree was generated (Figure 4-2) alongside two additional *B. turicatae* isolates from Texas (i.e. *Ornithodoros turicata*, CP000049; and human, CP015629). Interestingly, the phylogenetic tree revealed four distinct clusters, though no specific grouping pattern at the ecoregion level was noted. As depicted in Figure 3-2, one cluster contained only the tick isolate, two clusters contained seven of the dog samples across multiple county origins, and a final cluster comprised of one single dog sample alongside the human isolate. All *B. turicatae* sequences obtained from dogs were uploaded into GenBank® (Appendix E 3).

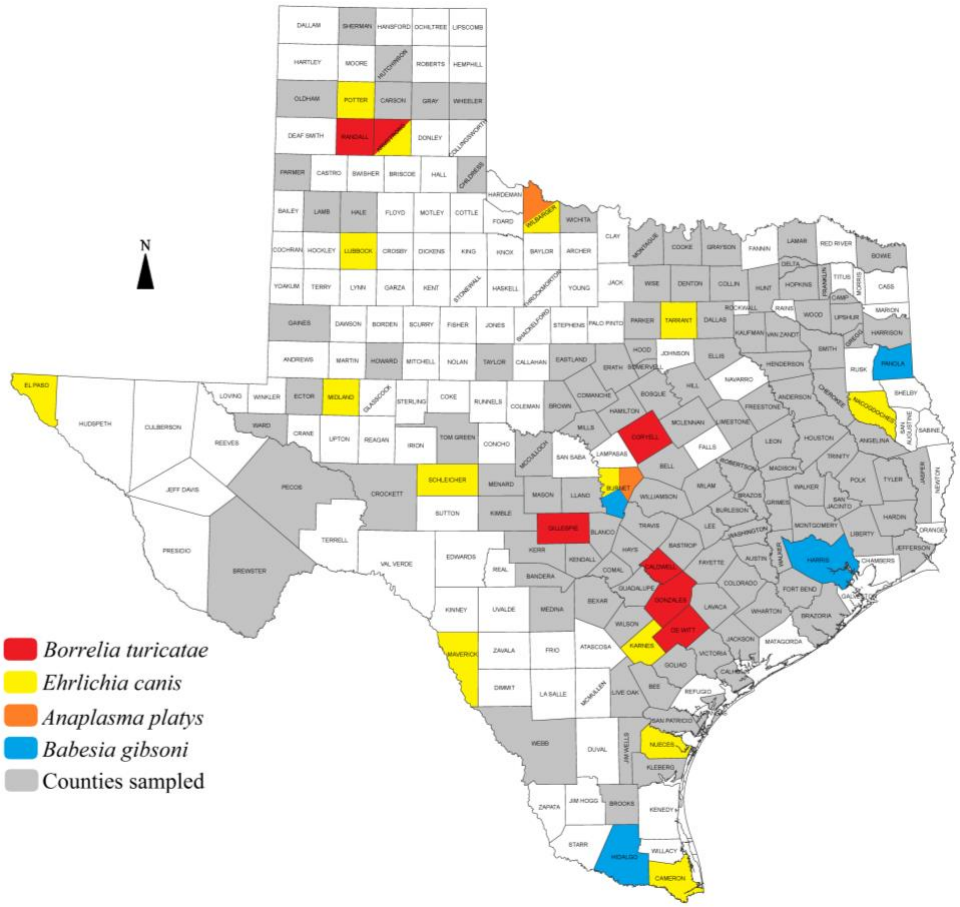

Figure 4-1. Geographic representation of study area and molecular prevalence of tick-borne pathogens in domestic dogs of Texas. Map adapted with permission from Texas Parks and Wildlife Department courtesy © 2011 (Wildlife, 2011).

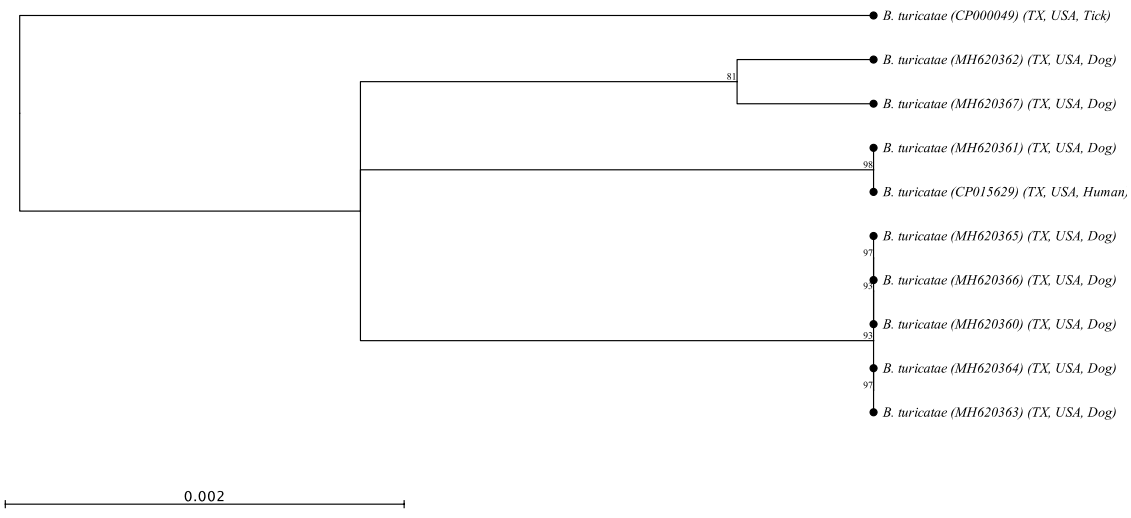

Figure 4-2. Phylogenetic tree of *16S-23S rRNA* intergenic spacer gene sequence alignments for *Borrelia turicatae.* Samples purified from dogs (this study), tick (*Ornithodoros turicata*), and a human in Texas.

Babesial molecular findings

A total of 5 (0.43%) *Babesia gibsoni* infections were detected at a molecular prevalence of 0.82 – 1.65% in 4 eastern ecoregions (Table 4-1, Figure 4-1). The mean age of dogs infected with *B. gibsoni* was 5.2 years, (1.5 - 10 years), and though no predilection of sex was found, 80% of the dogs were reported as pit bull-type dogs. Infections were distributed in January, February, March, and November. Moreover, 60% and 40% of the infected dogs were detected in rural and urban counties, respectively. The CBC analysis available for all of the dogs revealed that 100% were thrombocytopenic (platelets below reference interval of 200-500 K/µL), 80% anemic (hematocrit below reference interval 32-50%), and all but one presented as both. Although clinical history was not available for the infected dogs, small intraerythrocytic *Babesia* spp. parasites were observed in 80% of the dogs by blood smear review. All *B. gibsoni* samples purified from Texas dogs were

uploaded into GenBank® (Appendix E 4) and revealed 100% identity to *B. gibsoni* sequences published in GenBank®**.**

Discussion

TBDs of domestic dogs are caused by numerous pathogens belonging to multiple genera. Typical diseases found in Texas include borreliosis, ehrlichiosis, anaplasmosis, rickettsiosis, and babesiosis. While past TBDs prevalence investigations of dogs in Texas have focused on seroprevalence studies, and therefore potentially detecting past exposure and not active infections, this study aimed to characterize the molecular prevalence of active infection(s) in dogs by directly detecting the pathogen(s) in blood samples. To our knowledge, this is the first molecular prevalence study of tick-borne pathogens in domestic dogs in Texas, and the first molecular report of *A. platys* in Texas and coinfection of *E. canis* and *A. platys* in Texas dogs.

In the present study, the molecular prevalence of TBDs across Texas dogs ranged from 0.68% for borreliosis, 1.60% for ehrlichiosis, 0.17% for anaplasmosis, 0.00% for rickettsiosis, and 0.43% for babesiosis. As expected, these percentages are slightly lower than reported seroprevalence data for Texas as this data represents a current record of active infections by molecular analysis and not past or recent exposure detected by serological tools (e.g. antibody detection). When prevalence was analyzed by each ecoregion, a higher prevalence was found in specific regions that more closely resembles past seroprevalence data. The differences in prevalence among ecoregions may be attributed to the diverse topography, climate, and habitat features across Texas; characterized by west arid deserts, eastern swamps, southern subtropical, and a temperate

north. The state of Texas is also home to 91 mountain peaks with a majority located in far west Texas, contrasted by vast cave systems and canyons clustered in central and north Texas, respectively.

In respect to rickettsial infections, the highest prevalence was observed in the north-central Rolling Plains ecoregion at 5.78% (6 *E. canis* and 1 *A. platys* infections), followed by the South Texas Plains at 2.48% (3 *E. canis* infections). It is interesting to note that a majority of infections were detected in the Rolling Plains despite having the least sample coverage from representative counties when compared to coverage in other ecoregions. While these findings may potentially be inflated due to limited ecoregion coverage, the data also suggests that a higher prevalence may be determined if more samples from other counties within the ecoregion were available for collection. Future studies aimed at characterizing *E. canis* infections in Texas dogs should include collections in this ecoregion.

It is also worth noting that *E. canis* infections were detected in 80% of the ecoregions of Texas, indicating the pathogens ability to colonize dogs in numerous habitats. The ability for *E. canis* to be detected across Texas can be credited to its primary tick vector, *Rhipicephalus sanguineus* (brown dog tick), which is known as a hardy tick species found on dogs within either rural or urban settings, and can remain active in a variety of climates (Dantas-Torres et al., 2012). The brown dog tick is well known for its ability to dwell within homes and parasitize urban dogs, which is further supported by the 63.2% of *E. canis* infected dogs detected by this study residing within urban counties throughout most of the year. The brown dog tick has also been implicated as a primary vector for *A. platys*, supporting the potential for further coinfections in Texas dogs (Ramos

et al., 2014). It is important to note that while *A. platys* was detected in this study, the molecular layerplex assay utilized for screening samples does not detect any other *Anaplasma* species besides *A. phagocytophilum* (Chapter 2. Provisional patent US 62/563, 780). Both *A. platys* infections were incidentally detected through confirmation testing with conventional PCR analysis. Therefore, the potential for additional dogs to be actively infected with *A. platys* in Texas should be realized and further investigated.

In this study no other rickettsial pathogens (i.e. *Ehrlichia ewingii, E. chaffeensis, Anaplasma phagocytophilum*, and *Rickettsia rickettsii*) were detected despite past studies indicating serological evidence of exposure in the study area. Possible considerations for the discrepancies include inadequate sample size or coverage of ecoregions for molecular detection, previous exposure without active infection, and false positive serologic results. Another potential reason for prevalence discrepancies between studies may be due to increased cross reactivity or limited specificity featured by serological methods utilized for seroprevalence investigations for closely related species currently or previously circulating in infected dogs (Modarelli et al., In press).

Infections by the borrelial pathogen, *Borrelia turicatae,* were limited at a total molecular prevalence of 0.68% across Texas, and was the only borrelial pathogen detected. Within Texas, 60% of ecoregions indicated molecular exposure ranging from 0.68 – 1.65%, with a majority of detection occurring only in north or central Texas. Interestingly, data from this study indicated two clusters of counties where *B. turicatae* infections were found. The first cluster was identified in northwest Texas with two dog infections. This cluster resembled counties within the same ecoregions described previously in a case report of three spirochetemic dogs in north Texas diagnosed with TBRF due to infection

with *B. turicatae* (Whitney et al., 2007). Further, the county locations of the three case report dogs reside in the same two ecoregions that contain the northern cluster of *B. turicatae* infected dogs indicated in this study (i.e. High Plains, and Rolling Plains). The second cluster, located in central Texas, contained six infected dogs within five counties across four ecoregions (i.e. Post Oak Savannah, Blackland Prairies, Cross Timbers, Edwards Plateau). A second case report of five dogs also coincide with our findings by indicating infections with *B. turicatae* centered in the Post Oak Savanah, Cross Timbers, and the Edwards Plateau ecoregions (Piccione et al., 2016). Geographical clustering of samples may be explained by the ecology of its primary soft tick vector, *Ornithodoros turicata,* which has traditionally been associated with the cave system of central Texas, therefore corroborating the central cluster observed in this current study (Dworkin et al., 2008).

The northern cluster from this study was identified in the High Plains and Rolling Plains ecoregions, of which the topography does not typically include cave systems. However, both ecoregions contain vast canyons, cliffs, and tunnels, which leads us to suspect that this landscape, despite the lack of caves, may provide a competent habitat for *O. turicata* ticks to thrive and transmit *B. turicatae* to susceptible hosts. It is important to note, that a soft tick species (i.e. *Carios kelleyi*) ecologically similar to *O. turicata* has been collected from bats emerging from cave systems in Texas (Donaldson et al., 2016). Donaldson and colleagues suggest that bats may facilitate the dissemination of *O. turicata* ticks given the regular cave locality and opportunistic feeding nature of the ticks. Texas Parks and Wildlife report 12 major sites where bats roost in Texas, including 9 caves/bridges in central Texas ecoregions (i.e. Edwards Plateau, Blackland Prairies), 1

tunnel system in north Texas (i.e. Rolling Plains), and 2 bridges in east Texas (i.e. Gulf Prairies). Interestingly, bat roosting sites coincide with the two *B. turicatae* clustering locations identified in this study, specifically in the central Edwards Plateau and the northern Rolling Plains ecoregions. A similar association has been observed in respect to another TBRF species, *B. hermsii*, where it is hypothesized that infected migratory birds may contribute to the geographic distribution of the pathogen (Schwan et al., 2007). Therefore, the potential for bats to be implicated in the dispersion of *B. turicatae* should be further explored.

It is also predicted that *O. turicata* ticks are sensitive to specific environmental conditions that restrict its spread within additional U.S. states that span between the established locations of Texas and Florida (Donaldson et al., 2016). Briefly, this intrastate region has been described to feature elevated temperatures during the driest quarter of the year and low temperatures during the wettest quarter as compared to average readings across the country, which may impede the ticks ability to colonize the area (Lopez et al., 2016). Therefore, the same environmental variables may be viewed within the vastly different Texas ecoregions, resulting in the geographical clustering observed within this study and both case reports.

Nevertheless, it should be noted that the clustering may be due to sampling bias around both TVMDL facility locations. Sequence analysis of the *16S-23S rRNA* IGS gene region amplified from all 8 *B. turicatae* samples were aligned and evaluated for SNP groupings in order to identify potential evolutionary support for the two geographical cluster locations (Figure 4-2). While SNPs were observed across all samples of *B. turicatae*, and independent clusters were formed within the constructed phylogenetic tree,

no remarkable patterns among clusters were noted. Thus, there is no current evidence that the two groups are genetically distinct.

Of the three tick-borne relapsing fever species screened for in this study (i.e. *B. turicatae, B. parkeri, B. hermsii*) only *B. turicatae* was expected to be circulating in Texas dogs (Lopez et al., 2016). However, due to limited past prevalence studies of TBRF in Texas, and recent predictions of additional soft tick species migrating south towards Texas (i.e. *Ornithodoros hermsi, O. parkeri*), we included surveillance testing for the respective *B. hermsii* and *B. parkeri* pathogens in our analysis (Sage et al., 2017). Findings from this study support the conclusions of past investigations and emphasize, that currently, the only TBRF species that has been detected in Texas is *B. turicatae*. The lack of *B. burgdorferi sensu lato* detected infections may be due to utilizing blood as a sole sample type, as well as the use of single aliquot of blood (50 µL), and should not be viewed as supporting evidence for lack of Texas dog exposure to the pathogen (Primus et al., 2018).

In respect to babesial infections, only *Babesia gibsoni* was detected and indicated limited molecular prevalence from 0.82 – 1.65% across four eastern ecoregions (i.e. Cross Timbers, Gulf Prairies, Piney Woods, South Texas Plains). Molecular prevalence of *Babesia gibsoni* within Texas has been established in the past, though it was limited to a single analysis of dogs rescued from dog fighting rings, and no indication of specific prevalence within the state was available (Cannon et al., 2016). As expected, a breed specific association was observed in the present study with 80% of the *B. gibsoni* infections occurring in pit bull-type dogs. In addition to a breed specific genetic predisposition for *B. gibsoni* to infect pit bull-type dogs, these breeds are unfortunately more likely to encounter the infection through direct blood transmission from bites, or

unsterile ear/tail cropping/docking commonly associated with dog fighting rings (Cannon et al., 2016). Data from this study should serve as a reminder in conjunction with findings from Cannon et al. to properly screen susceptible dogs for potential infections and carrier states, and promptly administer appropriate treatment.

The layerplex qPCR assay utilized for this study detects pan-*Babesia* species, though only *B. canis vogeli* was expected to potentially indicate prevalence alongside *B. gibsoni* due to suggestions of a shared tick vector, the brown dog tick (Jongejan et al., 2018). However, it is important to note that it is currently unknown which babesiosis causing pathogens are most prevalent within Texas dogs. Additional *Babesia* species such as *B. conradae* are expected to re-emerge within the dog population, though, the geographic distribution of the pathogen is also unknown and the screening assay used in this study does not detect this specific species of *Babesia* (Di Cicco et al., 2012). Future studies aiming to characterize babesial infections within Texas dogs should include *B. conradae* in their analysis.

Limitations of the study include potential sampling bias due to dog samples originating only from two TVMDL locations in contrast to active sample collections within the study areas. Further, samples were randomly selected from an archived pool of opportunistically collected TVMDL cases, and were only available from counties with established TVMDL clients. Ecoregions sampled in this study are represented by counties containing submitting veterinarians, and in the case of more rural areas, may not accurately reflect the origin of the dog sample. Sample analysis from the Trans-Pecos ecoregion, consisting of 83.3% rural counties, was severely restricted due to limited submitted samples, resulting in an incomplete sample set. Finally, it is important to note that whole-

blood samples are not ideal for detecting *Borrelia burgdorferi* and *Rickettsia rickettsii* due to limited blood-borne circulation, and therefore findings from this investigation may differ from true prevalence of the pathogens in the area. However, studies have documented a low percentage of detection of the pathogens by PCR in dog and human blood samples (Kidd et al., 2008, Primus et al., 2018). In addition, this study based the 121 dogs desired per ecoregion sample size on prior seroprevalence investigations due to a lack of available molecular prevalence data. Findings presented here may not be representative of true prevalence of the study area, but should be used as a baseline for future investigations.

Despite these limitations, this study highlights the significance of molecular surveillance screening in order to characterize areas where active infections occur. Furthermore, it is important to note the zoonotic implication of *B. turicatae*, *E. canis*, and *A. platys* detected in this study (Christensen et al., 2017, Maggi et al., 2013, Ojeda-Chi et al., 2018). As Texas supports competent tick vectors for all pathogen species detected in this study (e.g. *Ornithodoros turicata* and *Rhipicephalus sanguineus*), and dogs may represent effective sentinels for human TBDs, the zoonotic transmission potential of the diseases should be considered in ecoregions indicating an increased molecular prevalence.

In conclusion, the present study provided an estimation of molecular prevalence of various TBDs in domestic dogs of Texas. Our findings indicate that dogs are experiencing clinical infections with several pathogens, many of which have zoonotic implications. Future studies aiming to further characterize TBDs in Texas should consult the ecoregion findings established in this preliminary report when designing new molecular surveillance investigations in order to provide a more accurate molecular prevalence study.

CHAPTER V

SUMMARY AND CONCLUSIONS

TBDs are common across the United States and can result in critical and chronic diseases in a variety of veterinary and human patients. In the U.S. alone, reports indicate that roughly 48,000 humans every year are infected with tick-borne pathogens; though recent studies estimate the true prevalence to be 10-fold higher. Domestic dogs that inhabit urban homes throughout the U.S. are analogously exposed to the same pathogens and have been implicated as sentinels for human disease. Due to the documented increasing emergence of TBDs it is important, now more than ever, to characterize active infections in dogs so that maps depicting high risk areas of disease can be updated. Consequently, these maps may aid public health agencies in developing preventative measures for the affected areas and veterinary/human populations. However, little is known about the active infection prevalence of tick-borne pathogens within dogs, mainly due to a lack of consolidated molecular tools that can screen for a variety of causative agents and facilitate surveillance investigations for the pathogens. Through this work, the goal of developing a highly comprehensive molecular tool that can be applied to veterinary diagnostics and prevalence investigations was evaluated.

To this end, the work detailed in this dissertation addressed three main aims to approach the fulfilment of a novel molecular tool for detecting numerous tick-borne pathogens threatening canine health. Initially, in chapter II a qPCR quality control mechanism, or EIPC, was developed and validated to facilitate the detection of canine specific mtDNA, which increases confidence in obtained qPCR results when paired with

an assay targeting multiple pathogens. While a fully validated and multiplex qPCR compatible canine specific EIPC has not been reported in the literature at present date, this study hypothesized that such a control could be developed and featured in a variety of multiplex qPCR assays with no added effect on sensitivity or specificity. As such, this study revealed the development of EIPC-K9 that monitors the DNA extraction and qPCR reaction process along with mitigating false-negative results. Additionally, preliminary data generated from testing EIPC-K9 with various biological samples sourced from dogs indicated the potential ability to discriminate between host sample types.

Upon validating a multiplex qPCR compatible EIPC, a similar design strategy was applied to developing qPCR assays for each tick-borne pathogen species of interest to canine health. Recent literature indicated that the most common bacterial tick-borne agents in the U.S. include *Borrelia hermsii, B. turicatae, B. parkeri, B. burgdorferi, Ehrlichia canis, E. chaffeensis, E. ewingii, Anaplasma phagocytophilum*, and *Rickettsia rickettsii*, and have been documented infecting both dogs and humans resulting in increased zoonotic threats. Further, the parasitic species *Babesia gibsoni* and *B. canis vogeli* have emerged as significant threats to canine health. Therefore, this study aimed to simultaneously detect and characterize all 11 causative agents for borreliosis, anaplasmosis, rickettsiosis, ehrlichiosis, and babesiosis using qPCR instruments readily accessible within veterinary diagnostic laboratories.

As discussed in Chapter III, although all pathogen specific assays, coupled with the EIPC, revealed high specificity and sensitivity to the intended targets, there remained an issue in respect to combining all assays into a single consolidated panel. Contemporary versions of qPCR instruments commonly utilized in veterinary diagnostic laboratories are

unable to differentiate between more than four to five unique fluorescent labels simultaneously. While current technology restricts the ability to insert additional fluorophores within the limited wavelength spectrum, the possibility to instead modify the process by manipulating available fluorescent signatures arose.

In Chapter III a new hypothesis was formed and evaluated regarding an approach to modify current multiplex strategies. The technique, termed in this dissertation as layerplexing, was briefly introduced in 2013 through work by Wernike et al. and involved incorporating multiple targets within the same wavelength signatures emitted by fluorescent probes. While the previous team utilized this technique for "layering" four targets under one probe, this study extrapolated that a similar approach could facilitate the detection of all 11 pathogen/EIPC targets simultaneously. Chapter III demonstrated the diagnostic potential of the layerplex technique in efficacious detection and identification of all targets of interest with no statistical interference in regards to sensitivity or specificity. Further, the fully validated molecular diagnostic tool has been translated into a provisional patent (US 62/563, 780) with the goal of commercialization. At this time, the patent pending diagnostic tool has been implemented into the TVMDL test catalogue (i.e. TickPath layerplex), which allows veterinarians or research teams the ability to utilize the tool in various states or countries. By ensuring that diagnosticians and research teams have access to a commercial kit that does not require further standardizations, consistent methodologies for the detection of these diseases can be established. Subsequently, this gives clients who depend on these diagnostic laboratories additional confidence in the results they receive.

Upon establishing the new layerplex molecular tool in a diagnostic setting, its ability to facilitate a molecular prevalence study was evaluated. Chapter IV describes the investigation of active infections concerning 11 common tick-borne pathogens in domestic dogs of Texas. The state of Texas was selected due to its diverse geographic ecology, transboundary relationship with Mexico, and mutualistic collaboration with two state veterinary diagnostic laboratories. As no prior molecular prevalence studies of Texas were available, our study extrapolated upon recent seroprevalence studies in order to determine an appropriate sample size for screening. To our knowledge, this is the first study of its kind in Texas and may provide baseline data for future research and public health surveillance programs. As such, a representative sample size of 1,171 dogs distributed across 10 natural ecological divisions of Texas was collected, and the molecular prevalence of borrelial, rickettsial, and babesial pathogens was determined.

The molecular prevalence of TBDs across Texas dogs ranged from 0.68% for borreliosis, 1.60% for ehrlichiosis, 0.17% for anaplasmosis, 0.00% for rickettsiosis, and 0.43% for babesiosis. While these findings are slightly lower than reported seroprevalence data for Texas, it is important to note that this data represents a current record of active infections by molecular analysis. When prevalence was analyzed by each ecoregion, a higher prevalence was found in specific regions that more closely resembled past seroprevalence data. The differences in prevalence among ecoregions may be attributed to the diverse topography, climate, and habitat features across Texas. This investigation also highlighted the first molecular detection of *Anaplasma platys* in Texas and hypothesized the contribution that bats may have in the dissemination of *Borrelia turicatae.*

Although the works presented here were successful in demonstrating the layerplex qPCR technique for determining the molecular prevalence of TBDs within dogs of an entire state, limitations of the study exist. For example, future studies are needed to expand upon presented validation analysis with emphasis on pathogens not presently detected in Texas dogs (e.g. *Borrelia parkeri, Ehrlichia chaffeensis, Rickettsia rickettsii*, etc.). In addition, the inherent nature of the layerplex technique requires testing to be conducted initially at the layer level for screening, then with subsequent singleplex or multiplex testing for specific species determination. This two-tier testing can aid in the rapid screening of large sample sets but may impede diagnostic applications if a species identification is desired. Further, when applying the layerplex tool to characterize the molecular prevalence of TBDs in Texas dogs, there was no precedent set to model a prevalence investigation from. Therefore, the findings presented here should be viewed as preliminary until future studies can be conducted to corroborate our analysis.

Despite these limitations, this study achieved the goal of simultaneous screening for 11 targets through layerplex methodology. Collectively, this dissertation provides support for additional studies to further validate the layerplex qPCR capabilities in terms of applying the methodology to different disease groups that require the detection of a broad spectrum of pathogens, as well as assessing the methodologies limits of detection in terms of targets labeled in a given reaction. Upon success with the layerplex technique, the next logical step includes evaluating the technique with more pathogen specific targets (e.g. *Anaplasma platys, Rickettsia parkeri*, etc.), or other susceptible animal models (e.g. cattle, horses, bats, etc.). Theoretically, additional targets may be layered into the reaction without resulting in adverse specificity or sensitivity restrictions. The addition of more targets may

facilitate a more complete understanding of all tick-borne pathogens implicated in causing disease in an area. Furthermore, a more comprehensive molecular screening tool may enable a more efficient method of collecting TBD data and provide a means for aggregating the data for long term analysis.

The CDC gathers and monitors all reportable disease data for humans in the U.S., including TBDs. Despite the zoonotic implications of TBDs in U.S. dogs, no disease data is collected by the CDC nor any other official government agency for veterinary patients except for pathogens deemed reportable (e.g. Rocky Mountain spotted fever). Consistent characterization of tick-borne pathogens in companion animals may indicate a rise or decline of prevalence over years of analysis that can then be correlated to contributing factors such as climate fluctuations and transboundary influences.

Taken together, this work demonstrated the capacity of the layerplex qPCR assay to detect 11 common tick-borne pathogens of interest to canine and human health simultaneously with high sensitivity and specificity in domesticated dog and tick specimens. The success found in these studies have potential to influence molecular diagnostic tool development and molecular prevalence investigations, and may one day contribute to a national surveillance system for companion animal diseases.

REFERENCES

Abdullah S, Helps C, Tasker S, Newbury H, Wall R. Prevalence and distribution of Borrelia and Babesia species in ticks feeding on dogs in the U.K. Med Vet Entomol 2018;32(1):14-22.

Allison RW, Little SE. Diagnosis of rickettsial diseases in dogs and cats. Vet Clin Pathol 2013;42(2):127-44.

Altschul SF, Gish W, Miller W, Myers EW, Lipman DJ. Basic local alignment search tool. J Mol Biol 1990;215(3):403-10.

Alvarez-Hernandez G. [Rocky Mountain spotted fever, a forgotten epidemic]. Salud Publica Mex 2010;52(1):1-3.

Annoscia G, Latrofa MS, Cantacessi C, Olivieri E, Manfredi MT, Dantas-Torres F, et al. A new PCR assay for the detection and differentiation of Babesia canis and Babesia vogeli. Ticks Tick Borne Dis 2017;8(6):862-5.

Babady NE, Sloan LM, Vetter EA, Patel R, Binnicker MJ. Percent positive rate of Lyme real-time polymerase chain reaction in blood, cerebrospinal fluid, synovial fluid, and tissue. Diagn Microbiol Infect Dis 2008;62(4):464-6.

Bastien P, Procop GW, Reischl U. Quantitative real-time PCR is not more sensitive than "conventional" PCR. J Clin Microbiol 2008;46(6):1897-900.

Beall MJ, Alleman AR, Breitschwerdt EB, Cohn LA, Couto CG, Dryden MW, et al. Seroprevalence of Ehrlichia canis, Ehrlichia chaffeensis and Ehrlichia ewingii in dogs in North America. Parasit Vectors 2012;5:29.

Beall MJ, Chandrashekar R, Eberts MD, Cyr KE, Diniz PP, Mainville C, et al. Serological and molecular prevalence of Borrelia burgdorferi, Anaplasma phagocytophilum, and Ehrlichia species in dogs from Minnesota. Vector Borne Zoonotic Dis 2008;8(4):455-64.

Becker NS, Margos G, Blum H, Krebs S, Graf A, Lane RS, et al. Recurrent evolution of host and vector association in bacteria of the Borrelia burgdorferi sensu lato species complex. BMC Genomics 2016;17(1):734.

Bilgic HB, Karagenc T, Simuunza M, Shiels B, Tait A, Eren H, et al. Development of a multiplex PCR assay for simultaneous detection of Theileria annulata, Babesia bovis and Anaplasma marginale in cattle. Exp Parasitol 2013;133(2):222-9.

Birkenheuer AJ, Correa MT, Levy MG, Breitschwerdt EB. Geographic distribution of babesiosis among dogs in the United States and association with dog bites: 150 cases (2000-2003). J Am Vet Med Assoc 2005;227(6):942-7.

Bischof R, Rogers DG. Serologic survey of select infectious diseases in coyotes and raccoons in Nebraska. J Wildl Dis 2005;41(4):787-91.

Bouza-Mora L, Dolz G, Solorzano-Morales A, Romero-Zuniga JJ, Salazar-Sanchez L, Labruna MB, et al. Novel genotype of Ehrlichia canis detected in samples of human blood bank donors in Costa Rica. Ticks Tick Borne Dis 2017;8(1):36-40.

Bowman D, Little SE, Lorentzen L, Shields J, Sullivan MP, Carlin EP. Prevalence and geographic distribution of Dirofilaria immitis, Borrelia burgdorferi, Ehrlichia canis, and Anaplasma phagocytophilum in dogs in the United States: results of a national clinic-based serologic survey. Vet Parasitol 2009;160(1-2):138-48.

Brzeski, Harrison, Waddell, Wolf, Rabon. Infectious disease and red wolf conservation: assessment of disease occurrence and associated risks. Journal of Mammalogy 2015;96(4):751–61.

Buller RS, Arens M, Hmiel SP, Paddock CD, Sumner JW, Rikhisa Y, et al. Ehrlichia ewingii, a newly recognized agent of human ehrlichiosis. N Engl J Med 1999;341(3):148-55.

Bunikis J, Tsao J, Garpmo U, Berglund J, Fish D, Barbour AG. Typing of Borrelia relapsing fever group strains. Emerg Infect Dis 2004;10(9):1661-4.

Cannon SH, Levy JK, Kirk SK, Crawford PC, Leutenegger CM, Shuster JJ, et al. Infectious diseases in dogs rescued during dogfighting investigations. Vet J 2016;211:64-9.

Carrade DD, Foley JE, Borjesson DL, Sykes JE. Canine granulocytic anaplasmosis: a review. J Vet Intern Med 2009;23(6):1129-41.

Centers for Disease C. National Notifiable Diseases Surveillance System, 2016 Annual Tables of Infectious Disease Data. Atlanta, GA CDC Division of Health Informatics and Surveillance 2017.

Chan K, Marras SA, Parveen N. Sensitive multiplex PCR assay to differentiate Lyme spirochetes and emerging pathogens Anaplasma phagocytophilum and Babesia microti. BMC Microbiol 2013;13:295.

Chapman AS, Bakken JS, Folk SM, Paddock CD, Bloch KC, Krusell A, et al. Diagnosis and management of tickborne rickettsial diseases: Rocky Mountain spotted fever, ehrlichioses, and anaplasmosis--United States: a practical guide for physicians and other health-care and public health professionals. MMWR Recomm Rep 2006;55(RR-4):1-27.

Chomel B. Tick-borne infections in dogs-an emerging infectious threat. Vet Parasitol 2011;179(4):294-301.

Christensen AM, Pietralczyk E, Lopez JE, Brooks C, Schriefer ME, Wozniak E, et al. Diagnosis and Management of Borrelia turicatae Infection in Febrile Soldier, Texas, USA. Emerg Infect Dis 2017;23(5):883-4.

Coburn J, Leong J, Chaconas G. Illuminating the roles of the Borrelia burgdorferi adhesins. Trends Microbiol 2013;21(8):372-9.

Coles TB, Dryden MW. Insecticide/acaricide resistance in fleas and ticks infesting dogs and cats. Parasit Vectors 2014;7:8.

Courtney JW, Kostelnik LM, Zeidner NS, Massung RF. Multiplex real-time PCR for detection of anaplasma phagocytophilum and Borrelia burgdorferi. J Clin Microbiol 2004;42(7):3164-8.

D'Haene B, Vandesompele J, Hellemans J. Accurate and objective copy number profiling using real-time quantitative PCR. Methods 2010;50(4):262-70.

Dahmani M, Davoust B, Benterki MS, Fenollar F, Raoult D, Mediannikov O. Development of a new PCR-based assay to detect Anaplasmataceae and the first report of Anaplasma phagocytophilum and Anaplasma platys in cattle from Algeria. Comp Immunol Microbiol Infect Dis 2015;39:39-45.

Dall'Agnol B, Souza UA, Weck B, Trigo TC, Jardim MMA, Costa FB, et al. Rickettsia parkeri in free-ranging wild canids from Brazilian Pampa. Transbound Emerg Dis 2018;65(2):e224-e30.

Dantas-Torres F. Canine vector-borne diseases in Brazil. Parasit Vectors 2008;1(1):25.

Dantas-Torres F, Chomel BB, Otranto D. Ticks and tick-borne diseases: a One Health perspective. Trends Parasitol 2012;28(10):437-46.

Davitkov D, Vucicevic M, Stevanovic J, Krstic V, Tomanovic S, Glavinic U, et al. Clinical babesiosis and molecular identification of Babesia canis and Babesia gibsoni infections in dogs from Serbia. Acta Vet Hung 2015;63(2):199-208.

De Tommasi AS, Baneth G, Breitschwerdt EB, Stanneck D, Dantas-Torres F, Otranto D, et al. Anaplasma platys in bone marrow megakaryocytes of young dogs. J Clin Microbiol 2014;52(6):2231-4.

Di Cicco MF, Downey ME, Beeler E, Marr H, Cyrog P, Kidd L, et al. Re-emergence of Babesia conradae and effective treatment of infected dogs with atovaquone and azithromycin. Vet Parasitol 2012;187(1-2):23-7.

Donaldson TG, Perez de Leon AA, Li AY, Castro-Arellano I, Wozniak E, Boyle WK, et al. Assessment of the Geographic Distribution of Ornithodoros turicata (Argasidae): Climate Variation and Host Diversity. PLoS Negl Trop Dis 2016;10(2):e0004383.

Drake TA, Hindler JA, Berlin OG, Bruckner DA. Rapid identification of Mycobacterium avium complex in culture using DNA probes. J Clin Microbiol 1987;25(8):1442-5.

Dunbar SA. Applications of Luminex xMAP technology for rapid, high-throughput multiplexed nucleic acid detection. Clin Chim Acta 2006;363(1-2):71-82.

Dworkin MS, Schwan TG, Anderson DE, Jr., Borchardt SM. Tick-borne relapsing fever. Infect Dis Clin North Am 2008;22(3):449-68, viii.

Elbir H, Henry M, Diatta G, Mediannikov O, Sokhna C, Tall A, et al. Multiplex real-time PCR diagnostic of relapsing fevers in Africa. PLoS Negl Trop Dis 2013;7(1):e2042.

Eremeeva ME, Weiner LM, Zambrano ML, Dasch GA, Hu R, Vilcins I, et al. Detection and characterization of a novel spotted fever group Rickettsia genotype in Haemaphysalis leporispalustris from California, USA. Ticks Tick Borne Dis 2018;9(4):814-8.

Esteve-Gasent MD, Snell CB, Adetunji SA, Piccione J. Serological detection of Tick-Borne Relapsing Fever in Texan domestic dogs. PLoS One 2017;12(12):e0189786.

Esteve-Gassent MD, Perez de Leon AA, Romero-Salas D, Feria-Arroyo TP, Patino R, Castro-Arellano I, et al. Pathogenic Landscape of Transboundary Zoonotic Diseases in the Mexico-US Border Along the Rio Grande. Front Public Health 2014;2:177.

Finotello F, Lavezzo E, Fontana P, Peruzzo D, Albiero A, Barzon L, et al. Comparative analysis of algorithms for whole-genome assembly of pyrosequencing data. Brief Bioinform 2012;13(3):269-80.

Frey KG, Bishop-Lilly KA. Next-Generation Sequencing for Pathogen Detection and Identification. Methods in Microbiology 2015;42:525-54.

Fritz CL. Emerging tick-borne diseases. Vet Clin North Am Small Anim Pract 2009;39(2):265-78.

Gal A, Harrus S, Arcoh I, Lavy E, Aizenberg I, Mekuzas-Yisaschar Y, et al. Coinfection with multiple tick-borne and intestinal parasites in a 6-week-old dog. Can Vet J 2007;48(6):619-22.

Gibson UE, Heid CA, Williams PM. A novel method for real time quantitative RT-PCR. Genome Res 1996;6(10):995-1001.

Gieg J, Rikihisa Y, Wellman M. Diagnosis of Ehrlichia ewingii infection by PCR in a puppy from Ohio. Vet Clin Pathol 2009;38(3):406-10.

Glas AS, Lijmer JG, Prins MH, Bonsel GJ, Bossuyt PM. The diagnostic odds ratio: a single indicator of test performance. J Clin Epidemiol 2003;56(11):1129-35.

Glenn TC. Field guide to next-generation DNA sequencers. Mol Ecol Resour 2011;11(5):759-69.

Goncalves-de-Albuquerque Sda C, Pessoa ESR, de Morais RC, Trajano-Silva LA, Regis-da-Silva CG, Brandao-Filho SP, et al. Tracking false-negative results in molecular diagnosis: proposal of a triplex-PCR based method for leishmaniasis diagnosis. J Venom Anim Toxins Incl Trop Dis 2014;20:16.

Gould FW, Hoffman GO, Rechenthin CA. Vegetational areas of Texas. Texas Agricultural Experiment Station, Texas A&M University 1960;Leaflet no. 492.

Harris RM, Couturier BA, Sample SC, Coulter KS, Casey KK, Schlaberg R. Expanded Geographic Distribution and Clinical Characteristics of Ehrlichia ewingii Infections, United States. Emerg Infect Dis 2016;22(5):862-5.

Harrus S, Waner T. Diagnosis of canine monocytotropic ehrlichiosis (Ehrlichia canis): an overview. Vet J 2011;187(3):292-6.

Harrus S, Waner T, Bark H, Jongejan F, Cornelissen AW. Recent advances in determining the pathogenesis of canine monocytic ehrlichiosis. J Clin Microbiol 1999;37(9):2745-9.

Heather JM, Chain B. The sequence of sequencers: The history of sequencing DNA. Genomics 2016;107(1):1-8.

Hegarty BC, Maggi RG, Koskinen P, Beall MJ, Eberts M, Chandrashekar R, et al. Ehrlichia muris infection in a dog from Minnesota. J Vet Intern Med 2012;26(5):1217-20.

Heitman K, et al. Increasing Incidence of Ehrlichiosis in the United States: A Summary of National Surveillance of Ehrlichia chaffeensis and Ehrlichia ewingii Infections in the United States, 2008-2012. Am J Trop Med Hyg 2016;94(1):52-60.

Higuchi R, Fockler C, Dollinger G, Watson R. Kinetic PCR analysis: real-time monitoring of DNA amplification reactions. Biotechnology (N Y) 1993;11(9):1026-30.

Hojgaard A, Lukacik G, Piesman J. Detection of Borrelia burgdorferi, Anaplasma phagocytophilum and Babesia microti, with two different multiplex PCR assays. Ticks Tick Borne Dis 2014;5(3):349-51.

Homer MJ, Bruinsma ES, Lodes MJ, Moro MH, Telford S, 3rd, Krause PJ, et al. A polymorphic multigene family encoding an immunodominant protein from Babesia microti. J Clin Microbiol 2000;38(1):362-8.

Huber D, Reil I, Duvnjak S, Jurkovic D, Lukacevic D, Pilat M, et al. Molecular detection of Anaplasma platys, Anaplasma phagocytophilum and Wolbachia sp. but not Ehrlichia canis in Croatian dogs. Parasitol Res 2017;116(11):3019-26.

Huhn GD, Badri S, Vibhakar S, Tverdek F, Crank C, Lubelchek R, et al. Early development of non-hodgkin lymphoma following initiation of newer class antiretroviral therapy among HIV-infected patients - implications for immune reconstitution. AIDS Res Ther 2010;7:44.

Humphry RW, Cameron A, Gunn GJ. A practical approach to calculate sample size for herd prevalence surveys. Prev Vet Med 2004;65(3-4):173-88.

IDEXX. The SNAP®4Dx® Plus Test provides sensitive and specific detection of tick-borne diseases; 2016. Available from: Available at: https://idexxcom-live-

b02da1e51e754c9cb292133b-9c56c33.aldryn-media.com/filer_public/34/32/34328f81-21ee-47aa-bd34-29084292e22d/snap-4dx-plus-sensitivity-specificity.pdf. [Accessed March 8 2018].

Inokuma H, Raoult D, Brouqui P. Detection of Ehrlichia platys DNA in brown dog ticks (Rhipicephalus sanguineus) in Okinawa Island, Japan. J Clin Microbiol 2000;38(11):4219-21.

Ivacic L, Reed KD, Mitchell PD, Ghebranious N. A LightCycler TaqMan assay for detection of Borrelia burgdorferi sensu lato in clinical samples. Diagn Microbiol Infect Dis 2007;57(2):137-43.

Jefferies R, Ryan UM, Jardine J, Broughton DK, Robertson ID, Irwin PJ. Blood, Bull Terriers and Babesiosis: further evidence for direct transmission of Babesia gibsoni in dogs. Aust Vet J 2007;85(11):459-63.

Johnson BJ. Laboratory Diagnostic Testing for
Borrelia burgdorferi Infection. In: Halperin J, editor. Lyme Disease: An Evidence-based Approach. CAB International: CDC; 2011. p. 73-88.

Johnson TL, Fischer RJ, Raffel SJ, Schwan TG. Host associations and genomic diversity of Borrelia hermsii in an endemic focus of tick-borne relapsing fever in western North America. Parasit Vectors 2016;9(1):575.

Jongejan F, Su BL, Yang HJ, Berger L, Bevers J, Liu PC, et al. Molecular evidence for the transovarial passage of Babesia gibsoni in Haemaphysalis hystricis (Acari: Ixodidae) ticks from Taiwan: a novel vector for canine babesiosis. Parasit Vectors 2018;11(1):134.

Kamani J, Baneth G, Mumcuoglu KY, Waziri NE, Eyal O, Guthmann Y, et al. Molecular detection and characterization of tick-borne pathogens in dogs and ticks from Nigeria. PLoS Negl Trop Dis 2013;7(3):e2108.

Kato CY, Chung IH, Robinson LK, Austin AL, Dasch GA, Massung RF. Assessment of real-time PCR assay for detection of Rickettsia spp. and Rickettsia rickettsii in banked clinical samples. J Clin Microbiol 2013;51(1):314-7.

Kelly AL, Raffel SJ, Fischer RJ, Bellinghausen M, Stevenson C, Schwan TG. First isolation of the relapsing fever spirochete, Borrelia hermsii, from a domestic dog. Ticks Tick Borne Dis 2014;5(2):95-9.

Kidd L, Maggi R, Diniz PP, Hegarty B, Tucker M, Breitschwerdt E. Evaluation of conventional and real-time PCR assays for detection and differentiation of Spotted Fever Group Rickettsia in dog blood. Vet Microbiol 2008;129(3-4):294-303.

Kledmanee K, Suwanpakdee S, Krajangwong S, Chatsiriwech J, Suksai P, Suwannachat P, et al. Development of multiplex polymerase chain reaction for detection of Ehrlichia canis, Babesia spp and Hepatozoon canis in canine blood. Southeast Asian J Trop Med Public Health 2009;40(1):35-9.

Koh FX, Panchadcharam C, Tay ST. Vector-Borne Diseases in Stray Dogs in Peninsular Malaysia and Molecular Detection of Anaplasma and Ehrlichia spp. from Rhipicephalus sanguineus (Acari: Ixodidae) Ticks. J Med Entomol 2016;53(1):183-7.

Komnenou AA, Mylonakis ME, Kouti V, Tendoma L, Leontides L, Skountzou E, et al. Ocular manifestations of natural canine monocytic ehrlichiosis (Ehrlichia canis): a retrospective study of 90 cases. Vet Ophthalmol 2007;10(3):137-42.

Kordick SK, Breitschwerdt EB, Hegarty BC, Southwick KL, Colitz CM, Hancock SI, et al. Coinfection with multiple tick-borne pathogens in a Walker Hound kennel in North Carolina. J Clin Microbiol 1999;37(8):2631-8.

Kubelova M, Sedlak K, Panev A, Siroky P. Conflicting results of serological, PCR and microscopic methods clarify the various risk levels of canine babesiosis in Slovakia: a complex approach to Babesia canis diagnostics. Vet Parasitol 2013;191(3-4):353-7.

Kuehn BM. CDC estimates 300,000 US cases of Lyme disease annually. JAMA 2013;310(11):1110.

Labruna MB, Ogrzewalska M, Soares JF, Martins TF, Soares HS, Moraes-Filho J, et al. Experimental infection of Amblyomma aureolatum ticks with Rickettsia rickettsii. Emerg Infect Dis 2011;17(5):829-34.

Lauring AS, Andino R. Quasispecies theory and the behavior of RNA viruses. PLoS Pathog 2010;6(7):e1001005.

Lawyer FC, Stoffel S, Saiki RK, Chang SY, Landre PA, Abramson RD, et al. High-level expression, purification, and enzymatic characterization of full-length Thermus aquaticus DNA polymerase and a truncated form deficient in 5' to 3' exonuclease activity. PCR Methods Appl 1993;2(4):275-87.

Lewis JS, Fakile O, Foss E, Legarza G, Leskys A, Lowe K, et al. Direct DNA probe assay for Neisseria gonorrhoeae in pharyngeal and rectal specimens. J Clin Microbiol 1993;31(10):2783-5.

Lin Q, Rikihisa Y, Felek S, Wang X, Massung RF, Woldehiwet Z. Anaplasma phagocytophilum has a functional msp2 gene that is distinct from p44. Infect Immun 2004;72(7):3883-9.

Little SE. Ehrlichiosis and anaplasmosis in dogs and cats. Vet Clin North Am Small Anim Pract 2010;40(6):1121-40.

Little SE, Beall MJ, Bowman DD, Chandrashekar R, Stamaris J. Canine infection with Dirofilaria immitis, Borrelia burgdorferi, Anaplasma spp., and Ehrlichia spp. in the United States, 2010-2012. Parasit Vectors 2014;7:257.

Little SE, Heise SR, Blagburn BL, Callister SM, Mead PS. Lyme borreliosis in dogs and humans in the USA. Trends Parasitol 2010a;26(4):213-8.

Little SE, O'Connor TP, Hempstead J, Saucier J, Reichard MV, Meinkoth K, et al. Ehrlichia ewingii infection and exposure rates in dogs from the southcentral United States. Vet Parasitol 2010b;172(3-4):355-60.

Littman MP, Gerber B, Goldstein RE, Labato MA, Lappin MR, Moore GE. ACVIM consensus update on Lyme borreliosis in dogs and cats. J Vet Intern Med 2018;32(3):887-903.

Lohmeyer KH, May MA, Thomas DB, Perez de Leon AA. Implication of Nilgai Antelope (Artiodactyla: Bovidae) in Reinfestations of Rhipicephalus (Boophilus) microplus (Acari: Ixodidae) in South Texas: A Review and Update. J Med Entomol 2018;55(3):515-22.

Long SW, Pound JM, Yu XJ. Ehrlichia prevalence in Amblyomma americanum, Central Texas. Emerg Infect Dis 2004;10(7):1342-3.

Lopez JE, Krishnavahjala A, Garcia MN, Bermudez S. Tick-borne relapsing fever spirochetes in the Americas. Veterinary Sciences 2016;3(3):16.

Lopez JE, Schrumpf ME, Nagarajan V, Raffel SJ, McCoy BN, Schwan TG. A novel surface antigen of relapsing fever spirochetes can discriminate between relapsing fever and Lyme borreliosis. Clinical and Vaccine Immunology 2010;17(4):564-71.

Lopez JE, Vinet-Oliphant H, Wilder HK, Brooks CP, Grasperge BJ, Morgan TW, et al. Real-time monitoring of disease progression in rhesus macaques infected with Borrelia turicatae by tick bite. J Infect Dis 2014;210(10):1639-48.

Lopez JE, Wilder HK, Boyle W, Drumheller LB, Thornton JA, Willeford B, et al. Sequence analysis and serological responses against Borrelia turicatae BipA, a putative species-specific antigen. PLoS Negl Trop Dis 2013;7(9):e2454.

Maeda K, Markowitz N, Hawley RC, Ristic M, Cox D, McDade JE. Human infection with Ehrlichia canis, a leukocytic rickettsia. N Engl J Med 1987;316(14):853-6.

Maggi RG, Birkenheuer AJ, Hegarty BC, Bradley JM, Levy MG, Breitschwerdt EB. Comparison of serological and molecular panels for diagnosis of vector-borne diseases in dogs. Parasit Vectors 2014;7:127.

Maggi RG, Mascarelli PE, Havenga LN, Naidoo V, Breitschwerdt EB. Co-infection with Anaplasma platys, Bartonella henselae and Candidatus Mycoplasma haematoparvum in a veterinarian. Parasit Vectors 2013;6:103.

Mead P, Goel R, Kugeler K. Canine serology as adjunct to human Lyme disease surveillance. Emerg Infect Dis 2011;17(9):1710-2.

Medlin JS, Cohen JI, Beck DL. Vector potential and population dynamics for Amblyomma inornatum. Ticks Tick Borne Dis 2015;6(4):463-72.

Michelet L, Delannoy S, Devillers E, Umhang G, Aspan A, Juremalm M, et al. High-throughput screening of tick-borne pathogens in Europe. Front Cell Infect Microbiol 2014;4:103.

Mikel P, Vasickova P, Kralik P. Methods for Preparation of MS2 Phage-Like Particles and Their Utilization as Process Control Viruses in RT-PCR and qRT-PCR Detection of RNA Viruses From Food Matrices and Clinical Specimens. Food Environ Virol 2015.

Modarelli JJ, Borst MM, Piccione J, Esteve-Gasent MD. Molecular identification of Ehrlichia ewingii in a polyarthritic Texas dog. Vet Clin Pathol In press.

Modarelli JJ, Ferro PJ, Esteve-Gasent MD. Development and application of a canine endogenous internal positive control for use in real-time PCR assays. J Vet Diagn Invest 2018a:1040638718795206.

Modarelli JJ, Piccione J, Ferro PJ, Esteve-Gasent MD. Novel real-time PCR assays for genomic group identification of tick-borne relapsing fever species Borrelia hermsii. Diagn Microbiol Infect Dis 2018b.

Mullis K, Faloona F, Scharf S, Saiki R, Horn G, Erlich H. Specific enzymatic amplification of DNA in vitro: the polymerase chain reaction. Cold Spring Harb Symp Quant Biol 1986;51 Pt 1:263-73.

Mullis KB. The unusual origin of the polymerase chain reaction. Sci Am 1990;262(4):56-61, 4-5.

Mullis KB, Faloona FA. Specific synthesis of DNA in vitro via a polymerase-catalyzed chain reaction. Methods Enzymol 1987;155:335-50.

Musial CE, Tice LS, Stockman L, Roberts GD. Identification of mycobacteria from culture by using the Gen-Probe Rapid Diagnostic System for Mycobacterium avium complex and Mycobacterium tuberculosis complex. J Clin Microbiol 1988;26(10):2120-3.

Mylonakis ME, Koutinas AF, Breitschwerdt EB, Hegarty BC, Billinis CD, Leontides LS, et al. Chronic canine ehrlichiosis (Ehrlichia canis): a retrospective study of 19 natural cases. J Am Anim Hosp Assoc 2004;40(3):174-84.

Nair AD, Cheng C, Ganta CK, Sanderson MW, Alleman AR, Munderloh UG, et al. Comparative Experimental Infection Study in Dogs with Ehrlichia canis, E. chaffeensis, Anaplasma platys and A. phagocytophilum. PLoS One 2016;11(2):e0148239.

Navarro E, Serrano-Heras G, Castano MJ, Solera J. Real-time PCR detection chemistry. Clin Chim Acta 2015;439:231-50.

Neer TM, Breitschwerdt EB, Greene RT, Lappin MR. Consensus statement on ehrlichial disease of small animals from the infectious disease study group of the ACVIM. American College of Veterinary Internal Medicine. J Vet Intern Med 2002;16(3):309-15.

Ojeda-Chi MM, Rodriguez-Vivas RI, Esteve-Gasent MD, Perez de Leon AA, Modarelli JJ, Villegas-Perez SL. Ticks infesting dogs in rural communities of Yucatan, Mexico and molecular diagnosis of rickettsial infection. Transbound Emerg Dis 2018.

Otranto D, Testini G, Dantas-Torres F, Latrofa MS, Diniz PP, de Caprariis D, et al. Diagnosis of canine vector-borne diseases in young dogs: a longitudinal study. J Clin Microbiol 2010;48(9):3316-24.

Paras KL, Little SE, Reichard MV, Reiskind MH. Detection of Dirofilaria immitis and Ehrlichia species in coyotes (Canis latrans), from rural Oklahoma and Texas. Vector Borne Zoonotic Dis 2012;12(7):619-21.

Pareek CS, Smoczynski R, Tretyn A. Sequencing technologies and genome sequencing. J Appl Genet 2011;52(4):413-35.

Peleg O, Baneth G, Eyal O, Inbar J, Harrus S. Multiplex real-time qPCR for the detection of Ehrlichia canis and Babesia canis vogeli. Vet Parasitol 2010;173(3-4):292-9.

Perez M, Bodor M, Zhang C, Xiong Q, Rikihisa Y. Human infection with Ehrlichia canis accompanied by clinical signs in Venezuela. Ann N Y Acad Sci 2006;1078:110-7.

Piccione J, Levine GJ, Duff CA, Kuhlman GM, Scott KD, Esteve-Gassent MD. Tick-Borne Relapsing Fever in Dogs. J Vet Intern Med 2016;30(4):1222-8.

Policastro PF, Raffel SJ, Schwan TG. Borrelia hermsii acquisition order in superinfected ticks determines transmission efficiency. Infect Immun 2013;81(8):2899-908.

Porcella SF, Raffel SJ, Anderson DE, Jr., Gilk SD, Bono JL, Schrumpf ME, et al. Variable tick protein in two genomic groups of the relapsing fever spirochete Borrelia hermsii in western North America. Infect Immun 2005;73(10):6647-58.

Portnoi D, Sertour N, Ferquel E, Garnier M, Baranton G, Postic D. A single-run, real-time PCR for detection and identification of Borrelia burgdorferi sensu lato species, based on the hbb gene sequence. FEMS Microbiol Lett 2006;259(1):35-40.

Primus S, Akoolo L, Schlachter S, Gedroic K, Rojtman AD, Parveen N. Efficient detection of symptomatic and asymptomatic patient samples for Babesia microti and Borrelia burgdorferi infection by multiplex qPCR. PLoS One 2018;13(5):e0196748.

Qurollo BA, Chandrashekar R, Hegarty BC, Beall MJ, Stillman BA, Liu J, et al. A serological survey of tick-borne pathogens in dogs in North America and the Caribbean as assessed by Anaplasma phagocytophilum, A. platys, Ehrlichia canis, E. chaffeensis, E. ewingii, and Borrelia burgdorferi species-specific peptides. Infect Ecol Epidemiol 2014;4.

Radford AD, Chapman D, Dixon L, Chantrey J, Darby AC, Hall N. Application of next-generation sequencing technologies in virology. J Gen Virol 2012;93(Pt 9):1853-68.

Ramos RA, Latrofa MS, Giannelli A, Lacasella V, Campbell BE, Dantas-Torres F, et al. Detection of Anaplasma platys in dogs and Rhipicephalus sanguineus group ticks by a quantitative real-time PCR. Vet Parasitol 2014;205(1-2):285-8.

Raoult D, Parola P. Rocky Mountain spotted fever in the USA: a benign disease or a common diagnostic error? Lancet Infect Dis 2008;8(10):587-9.

Renvoise A, Merhej V, Georgiades K, Raoult D. Intracellular Rickettsiales: Insights into manipulators of eukaryotic cells. Trends Mol Med 2011;17(10):573-83.

Rikihisa Y. Molecular Pathogenesis of Ehrlichia chaffeensis Infection. Annu Rev Microbiol 2015;69:283-304.

Rodgers SJ, Morton RJ, Baldwin CA. A serological survey of Ehrlichia canis, Ehrlichia equi, Rickettsia rickettsii, and Borrelia burgdorferi in dogs in Oklahoma. J Vet Diagn Invest 1989;1(2):154-9.

Rodriguez I, Burri C, Noda AA, Douet V, Gern L. Multiplex PCR for molecular screening of Borrelia burgdorferi sensu lato, Anaplasma spp. and Babesia spp. Ann Agric Environ Med 2015;22(4):642-6.

Rosenberg R, Lindsey NP, Fischer M, Gregory CJ, Hinckley AF, Mead PS, et al. Vital Signs: Trends in Reported Vectorborne Disease Cases - United States and Territories, 2004-2016. MMWR Morb Mortal Wkly Rep 2018;67(17):496-501.

Rozej-Bielicka W, Masny A, Golab E. High-resolution melting PCR assay, applicable for diagnostics and screening studies, allowing detection and differentiation of several Babesia spp. infecting humans and animals. Parasitol Res 2017;116(10):2671-81.

Sage KM, Johnson TL, Teglas MB, Nieto NC, Schwan TG. Ecological niche modeling and distribution of Ornithodoros hermsi associated with tick-borne relapsing fever in western North America. PLoS Negl Trop Dis 2017;11(10):e0006047.

Saiki RK, Gelfand DH, Stoffel S, Scharf SJ, Higuchi R, Horn GT, et al. Primer-directed enzymatic amplification of DNA with a thermostable DNA polymerase. Science 1988;239(4839):487-91.

Saiki RK, Scharf S, Faloona F, Mullis KB, Horn GT, Erlich HA, et al. Enzymatic amplification of beta-globin genomic sequences and restriction site analysis for diagnosis of sickle cell anemia. Science 1985;230(4732):1350-4.

Sanger F, Air GM, Barrell BG, Brown NL, Coulson AR, Fiddes CA, et al. Nucleotide sequence of bacteriophage phi X174 DNA. Nature 1977a;265(5596):687-95.

Sanger F, Brownlee GG, Barrell BG. A two-dimensional fractionation procedure for radioactive nucleotides. J Mol Biol 1965;13(2):373-98.

Sanger F, Nicklen S, Coulson AR. DNA sequencing with chain-terminating inhibitors. Proc Natl Acad Sci U S A 1977b;74(12):5463-7.

Sanogo YO, Davoust B, Inokuma H, Camicas JL, Parola P, Brouqui P. First evidence of Anaplasma platys in Rhipicephalus sanguineus (Acari: Ixodida) collected from dogs in Africa. Onderstepoort J Vet Res 2003;70(3):205-12.

Sarkar M, Troese MJ, Kearns SA, Yang T, Reneer DV, Carlyon JA. Anaplasma phagocytophilum MSP2(P44)-18 predominates and is modified into multiple isoforms in human myeloid cells. Infect Immun 2008;76(5):2090-8.

Schroeder ME, Johnson DJ, Ostlund EN, Meier J, Bounpheng MA, Clavijo A. Development and performance evaluation of a streamlined method for nucleic acid purification, denaturation, and multiplex detection of Bluetongue virus and Epizootic hemorrhagic disease virus. J Vet Diagn Invest 2013;25(6):709-19.

Schurer JM, Ndao M, Quewezance H, Elmore SA, Jenkins EJ. People, pets, and parasites: one health surveillance in southeastern Saskatchewan. Am J Trop Med Hyg 2014;90(6):1184-90.

Schuster FL. Cultivation of Babesia and Babesia-like blood parasites: agents of an emerging zoonotic disease. Clin Microbiol Rev 2002;15(3):365-73.

Schwan TG, Raffel SJ, Schrumpf ME, Porcella SF. Diversity and distribution of Borrelia hermsii. Emerg Infect Dis 2007;13(3):436-42.

Schwan TG, Schrumpf ME, Hinnebusch BJ, Anderson D, Konkel ME. GlpQ: an antigen for serological discrimination between relapsing fever and Lyme borreliosis. Journal of clinical microbiology 1996;34(10):2483-92.

Scott JD, Foley JE, Clark KL, Anderson JF, Durden LA, Manord JM, et al. Established Population of Blacklegged Ticks with High Infection Prevalence for the Lyme Disease Bacterium, Borrelia burgdorferi Sensu Lato, on Corkscrew Island, Kenora District, Ontario. Int J Med Sci 2016;13(11):881-91.

Shock BC, Moncayo A, Cohen S, Mitchell EA, Williamson PC, Lopez G, et al. Diversity of piroplasms detected in blood-fed and questing ticks from several states in the United States. Ticks Tick Borne Dis 2014;5(4):373-80.

Sirigireddy KR, Ganta RR. Multiplex detection of Ehrlichia and Anaplasma species pathogens in peripheral blood by real-time reverse transcriptase-polymerase chain reaction. J Mol Diagn 2005;7(2):308-16.

Skotarczak B. Why are there several species of Borrelia burgdorferi sensu lato detected in dogs and humans? Infect Genet Evol 2014;23:182-8.

Small CM, Ajithdoss DK, Rodrigues Hoffmann A, Mwangi W, Esteve-Gassent MD. Immunization with a Borrelia burgdorferi BB0172-derived peptide protects mice against lyme disease. PLoS One 2014;9(2):e88245.

Snowden J, Simonsen KA. Ehrlichiosis. StatPearls. Treasure Island (FL); 2018.

Solano-Gallego L, Baneth G. Babesiosis in dogs and cats--expanding parasitological and clinical spectra. Vet Parasitol 2011;181(1):48-60.

Stanek G, Wormser GP, Gray J, Strle F. Lyme borreliosis. Lancet 2012;379(9814):461-73.

Starkey LA, West MD, Barrett AW, Saucier JM, O'Connor TP, Paras KL, et al. Prevalence of antibodies to spotted fever group Rickettsia spp. and Ehrlichia spp. in coyotes (Canis latrans) in Oklahoma and Texas, USA. J Wildl Dis 2013;49(3):670-3.

Sudhakara Reddy B, Sivajothi S, Varaprasad Reddy LS, Solmon Raju KG. Clinical and laboratory findings of Babesia infection in dogs. J Parasit Dis 2016;40(2):268-72.

Talagrand-Reboul E, Boyer PH, Bergstrom S, Vial L, Boulanger N. Relapsing Fevers: Neglected Tick-Borne Diseases. Front Cell Infect Microbiol 2018;8:98.

Teal AE, Habura A, Ennis J, Keithly JS, Madison-Antenucci S. A new real-time PCR assay for improved detection of the parasite Babesia microti. J Clin Microbiol 2012;50(3):903-8.

Technologies B. SPECTRAL OVERLAY TOOL FOR MULTIPLEXED QPCR; 2018. Available from: https://www.biosearchtech.com/qpcr-multiplex-spectral-overlay-tool. 2018].

Thomson K, Yaaran T, Belshaw A, Curson L, Tisi L, Maurice S, et al. A new TaqMan method for the reliable diagnosis of Ehrlichia spp. in canine whole blood. Parasit Vectors 2018;11(1):350.

Tinoco-Gracia L, Lomeli MR, Hori-Oshima S, Stephenson N, Foley J. Molecular Confirmation of Rocky Mountain Spotted Fever Epidemic Agent in Mexicali, Mexico. Emerg Infect Dis 2018;24(9):1723-5.

Tomassone L, Portillo A, Novakova M, de Sousa R, Oteo JA. Neglected aspects of tick-borne rickettsioses. Parasit Vectors 2018;11(1):263.

Tritt A, Eisen JA, Facciotti MT, Darling AE. An integrated pipeline for de novo assembly of microbial genomes. PLoS One 2012;7(9):e42304.

Trout Fryxell RT, Steelman CD, Szalanski AL, Billingsley PM, Williamson PC. Molecular Detection of Rickettsia Species Within Ticks (Acari: Ixodidae) Collected from Arkansas United States. J Med Entomol 2015;52(3):500-8.

Uchiyama T, Kishi M, Ogawa M. Restriction of the growth of a nonpathogenic spotted fever group rickettsia. FEMS Immunol Med Microbiol 2012;64(1):42-7.

van Rijn SJ, Riemers FM, van den Heuvel D, Wolfswinkel J, Hofland L, Meij BP, et al. Expression stability of reference genes for quantitative RT-PCR of healthy and diseased pituitary tissue samples varies between humans, mice, and dogs. Mol Neurobiol 2014;49(2):893-9.

Vojdani A, Hebroni F, Raphael Y, Erde J, Raxlen B. Novel Diagnosis of Lyme Disease: Potential for CAM Intervention. Evid Based Complement Alternat Med 2009;6(3):283-95.

Waner T, Harrus S, Bark H, Bogin E, Avidar Y, Keysary A. Characterization of the subclinical phase of canine ehrlichiosis in experimentally infected beagle dogs. Vet Parasitol 1997;69(3-4):307-17.

Wang HY, Wu SQ, Jiang L, Xiao RH, Li T, Mei L, et al. Establishment and optimization of a liquid bead array for the simultaneous detection of ten insect-borne pathogens. Parasit Vectors 2018;11(1):442.

Wen B, Rikihisa Y, Mott JM, Greene R, Kim HY, Zhi N, et al. Comparison of nested PCR with immunofluorescent-antibody assay for detection of Ehrlichia canis infection in dogs treated with doxycycline. J Clin Microbiol 1997;35(7):1852-5.

Wernike K, Hoffmann B, Beer M. Single-tube multiplexed molecular detection of endemic porcine viruses in combination with background screening for transboundary diseases. J Clin Microbiol 2013;51(3):938-44.

Whitney MS, Schwan TG, Sultemeier KB, McDonald PS, Brillhart MN. Spirochetemia caused by Borrelia turicatae infection in 3 dogs in Texas. Vet Clin Pathol 2007;36(2):212-6.

Wildlife TPa. Gould Ecoregions of Texas; 2011. Available from: https://tpwd.texas.gov/publications/pwdpubs/media/pwd_mp_e0100_1070ac_34.pdf. 2018].

Wodecka B. flaB gene as a molecular marker for distinct identification of Borrelia species in environmental samples by the PCR-restriction fragment length polymorphism method. Appl Environ Microbiol 2011;77(19):7088-92.

Woldehiwet Z. The natural history of Anaplasma phagocytophilum. Vet Parasitol 2010;167(2-4):108-22.

Wormser GP, Dattwyler RJ, Shapiro ED, Halperin JJ, Steere AC, Klempner MS, et al. The clinical assessment, treatment, and prevention of lyme disease, human granulocytic anaplasmosis, and babesiosis: clinical practice guidelines by the Infectious Diseases Society of America. Clin Infect Dis 2006;43(9):1089-134.

Yabsley MJ. Natural history of Ehrlichia chaffeensis: vertebrate hosts and tick vectors from the United States and evidence for endemic transmission in other countries. Vet Parasitol 2010;167(2-4):136-48.

Ybanez AP, Perez ZO, Gabotero SR, Yandug RT, Kotaro M, Inokuma H. First molecular detection of Ehrlichia canis and Anaplasma platys in ticks from dogs in Cebu, Philippines. Ticks Tick Borne Dis 2012;3(5-6):288-93.

Yeagley TJ, Reichard MV, Hempstead JE, Allen KE, Parsons LM, White MA, et al. Detection of Babesia gibsoni and the canine small Babesia 'Spanish isolate' in blood samples obtained from dogs confiscated from dogfighting operations. J Am Vet Med Assoc 2009;235(5):535-9.

Zavala-Castro JE, Zavala-Velazquez JE, del Rosario Garcia M, Leon JJ, Dzul-Rosado KR. A dog naturally infected with Rickettsia akari in Yucatan, Mexico. Vector Borne Zoonotic Dis 2009;9(3):345-7.

APPENDIX A

1. GenBank® accession codes for the *16S rRNA* gene sequences of *Ehrlichia*, *Anaplasma,* and *Rickettsia* species. Sequences utilized for *in silico* analysis in Appendix B are emphasized in bold.

Rickettsial Species	Isolate/Strain	GenBank
E. canis	NA	U26740
E. canis	GR78	EF011111
E. canis	GR21	EF011110
E. canis	Kiwi	HQ844983
E. canis	TWN1	EU106856
E. canis	Kagoshima	AF536827
E. canis	NA	KM879929
E. canis	171	KC479023
E. canis	105	KC479022
E. canis	MSIA	JF429693
E. canis	B	JX893523
E. canis	A	JX893522
E. canis	NGR	JN982339
E. canis	NGR	JN982336
E. canis	NGR	JN622141
E. canis	TWN4	EU143637
E. canis	Nero	EU439944
E. canis	TWN	GU810149
E. canis	TWN3	EU143636
E. canis	TWN2	EU123923
E. canis	DT	HQ290362
E. canis	NA	EF139458
E. canis	TWN17	EU139493
E. canis	Kutahya	AY621071
E. canis	TWN18	EU178797
E. canis	NA	DQ915970
E. canis	NA	AY394465
E. canis	VDE	AF373613
E. canis	VHE	AF373612
E. canis	Gxht67	AF156786
E. canis	Gdt3	AF156785
E. canis	b2-15	KY594915
E. canis	WHBMXZ-124	KX987326
E. canis	M66	KX180945
E. canis	NA	KR920044
E. canis	**Oklahoma**	**NR_118741**
E. canis	S3b	KJ659037
E. canis	TrKysEcan3	KJ513197
E. canis	TrKysEcan2	KJ513196
E. canis	TrKysEcan1	KJ513194
E. canis	CMM-19-2002	AB723711
E. canis	CMM-19-2006	AB723712
E. canis	W-137J	AB723710
E. canis	E-60	AB723709
E. canis	W-134	AB723708
E. canis	E-89J	AB723707
E. canis	Bareilly	JX861392
E. canis	Brazil-CO2	EF195135
E. canis	Brazil-CO1	EF195134
E. canis	Hd48	GQ395381
E. canis	NA	M73221
E. canis	NA	M73226
E. canis	Hd22	GQ395378
E. canis	Hd38-1	GQ395380
E. canis	ECAN_Bkk_07	EU263991
E. canis	NA	AF162860
E. canis	Jake	CP000107
E. canis	YZ-1	CP025749
E. chaffeensis	X1	KX505292
E. chaffeensis	Arkansas	NR_074500
E. chaffeensis	NA	AF147752
E. chaffeensis	NA	U23503
E. chaffeensis	Arkansas	NR_037059
E. chaffeensis	NA	AF000721
E. chaffeensis	**Arkansas**	**AF416764**
E. chaffeensis	NA	U60476
E. chaffeensis	NA	U86665
E. chaffeensis	NA	U86664
E. chaffeensis	NA	M73222
E. chaffeensis	West Paces	CP007480
E. chaffeensis	Wakulla	CP007479
E. chaffeensis	Saint Vincent	CP007478
E. chaffeensis	Osceola	CP007477
E. chaffeensis	Liberty	CP007476
E. chaffeensis	Jax	CP007475
E. chaffeensis	Heartland	CP007473
E. chaffeensis	Arkansas	CP000236
E. ewingii	Stillwater	NR_044747
E. ewingii	**Stillwater**	**M73227**
E. ewingii	95E9-TS	U96436
E. ewingii	95E7-Mk	U96435
E. muris	AS145	NR_025962
E. muris	AS145	NR_121714
E. muris	T-388	KU315171
E. muris	Est1709	KU535865
E. muris	WI22	HQ660491
E. muris	Ip16	AY587608
E. muris	NA	AB013009
E. muris	NA	AB196302
E. muris	Kh-1550	GU358692
E. muris	NA	AB013008
E. muris	Nov-Ip205	GU358691
E. muris	m12	AB275137
E. muris	NA	U15527
E. muris	**AS145**	**CP006917**
E. ruminantium	Welgevonden	NR_074513
E. ruminantium	AaFT299	KJ942239
E. ruminantium	AaFT77	KJ942221
E. ruminantium	Aa2FT306	KJ942213
E. ruminantium	SBF4	KF786044
E. ruminantium	SBF1	KF786042
E. ruminantium	Welgevonden	NR_074155
E. ruminantium	MB9_04	DQ640395
E. ruminantium	MB9_03	DQ640394
E. ruminantium	Hmr4	DQ640390
E. ruminantium	Sheep	DQ640389
E. ruminantium	Umbanein	DQ647616
E. ruminantium	c-4	DQ482922
E. ruminantium	c-3	DQ482921
E. ruminantium	c-2	DQ482920
E. ruminantium	c-1	DQ482919
E. ruminantium	c-3	DQ482918
E. ruminantium	c-2	DQ482917
E. ruminantium	c-1	DQ482916
E. ruminantium	c-1	DQ482915
E. ruminantium	NA	U03777
E. ruminantium	NA	X62432
E. ruminantium	**Welgevonden**	**CR925678**
E. ruminantium	Gardel	CR925677
E. ruminantium	Welgevonden	CR767821
E. ruminantium	Vista	AF318022
E. ruminantium	Henrique	AF318021
E. ruminantium	ribosomal	AF069758
E. ruminantium	rRNA	U03776
E. ruminantium	NA	X61659

E. ruminantium	S22	HQ908081
E. ruminantium	Kiswani	DQ647615
A. phagocytophilum	6952	KY486261
A. phagocytophilum	6097	KY486259
A. phagocytophilum	6403	KY486258
A. phagocytophilum	6403	KY462831
A. phagocytophilum	CPLA-HS	MG050134
A. phagocytophilum	DKRH-HS	MG050133
A. phagocytophilum	ItalyIRH004711	KY319198
A. phagocytophilum	Italy149-12B	KY319197
A. phagocytophilum	ItalyIRH012411	KY319196
A. phagocytophilum	ItalyIRH01221	KY319195
A. phagocytophilum	ItalyIRH004811	KY319194
A. phagocytophilum	ItalyH3th-28	KY319193
A. phagocytophilum	JXARSA-32	KU585968
A. phagocytophilum	JXARSA-2	KU585967
A. phagocytophilum	JXARSA-15	KU585966
A. phagocytophilum	HunChun17	KX279357
A. phagocytophilum	RB3	KY458571
A. phagocytophilum	RS10556	KY458570
A. phagocytophilum	Y_G14 16S	KU705164
A. phagocytophilum	Y_C35 16S	KU705163
A. phagocytophilum	Y_C34 16S	KU705162
A. phagocytophilum	Y_A04 16S	KU705161
A. phagocytophilum	I_BwReh33	KU705160
A. phagocytophilum	X_BwReh32	KU705159
A. phagocytophilum	16S-25	KU705130
A. phagocytophilum	W_BwRo6 1	KU705129
A. phagocytophilum	S_BwRo5 1	KU705128
A. phagocytophilum	W_BwRo4 1	KU705127
A. phagocytophilum	16S-30	KU705126
A. phagocytophilum	W_BwRo2 1	KU705125
A. phagocytophilum	Norway variant2, co	CP015376
A. phagocytophilum	ApGDrom1	KF002508
A. phagocytophilum	AAIK4	KR611719
A. phagocytophilum	AAIK3	KR611718
A. phagocytophilum	AAIK2	KR611717
A. phagocytophilum	AAIK1	KR611716
A. phagocytophilum	14DRS	KR092129
A. phagocytophilum	tick-EU329	KM215231
A. phagocytophilum	tick-EU322	KM215230
A. phagocytophilum	d-3216	KM215224
A. phagocytophilum	Aa2FT11	KJ942185
A. phagocytophilum	Aa2FT06	KJ942183
A. phagocytophilum	gw1	KF805344
A. phagocytophilum	Dog2	CP006618
A. phagocytophilum	JMe	CP006617
A. phagocytophilum	HZ2	CP006616
A. phagocytophilum	sheep19	KF293698
A. phagocytophilum	sheep28	KF293697
A. phagocytophilum	sheep29	KF293676
A. phagocytophilum	sheep54	KF293675
A. phagocytophilum	sheep52	KF293673
A. phagocytophilum	sheep50	KF293671
A. phagocytophilum	sheep49	KF293670
A. phagocytophilum	sheep48	KF293669
A. phagocytophilum	Rus30-10	HQ629911
A. phagocytophilum	Bel6-22-07	HQ629915
A. phagocytophilum	BelBmi37	HQ629914
A. phagocytophilum	Rus29-12	HQ629912
A. phagocytophilum	HB-SZ-HGA-S02	HQ171975
A. phagocytophilum	ZJ01/2008	HM439430
A. phagocytophilum	Sv-Ip854	HM366579
A. phagocytophilum	h997	HM138366
A. phagocytophilum	KWDAP5	GU556625
A. phagocytophilum	HLAP327	GU064899
A. phagocytophilum	KWDAP2	GU556622
A. phagocytophilum	KWDAP1	GU556621
A. phagocytophilum	sheep_5010_EM	GU236611
A. phagocytophilum	GC19	GU111744
A. phagocytophilum	roe_deer_137_05	GU236574
A. phagocytophilum	roe_deer_16	GU236554
A. phagocytophilum	YN-XD-HGA-S131	GQ500084
A. phagocytophilum	YN-XD-HGA-S103	GQ500080
A. phagocytophilum	YN-XD-HGA-S102	GQ500079
A. phagocytophilum	ZJ-TT-HGA-O37	GQ500060
A. phagocytophilum	ZJ-TT-HGA-O35	GQ500058
A. phagocytophilum	ZJ-TT-HGA-O23	GQ500047
A. phagocytophilum	BJ-MY-HGA-S13	GQ499986
A. phagocytophilum	BJ-MY-HGA-S2	GQ499977
A. phagocytophilum	BJ-MY-HGA-S1	GQ499956
A. phagocytophilum	AH-MG-HGA-S36	GQ499928
A. phagocytophilum	China-C-Aa	GQ412337
A. phagocytophilum	PoTiA2dt	EU098007
A. phagocytophilum	PoTiA1dt	EU098006
A. phagocytophilum	PoAnA1dt	EF693890
A. phagocytophilum	EHR02	EF217398
A. phagocytophilum	EHR1	EF217397
A. phagocytophilum	AH-HGA-9	EF473210
A. phagocytophilum	**HZ**	**CP000235**
A. phagocytophilum	M20	DQ361024
A. phagocytophilum	DBMGH	AY886761
A. phagocytophilum	474	AF481852
A. phagocytophilum	470	AF481850
A. phagocytophilum	AP-CBHL	AF470699
A. phagocytophilum	16S	AF384214
A. phagocytophilum	16S	AF384212
A. phagocytophilum	Jilin-1	DQ342324
A. phagocytophilum	BV-1	AY082656
A. phagocytophilum	TXCTR3	DQ088128
A. phagocytophilum	WA-variant	AY741095
A. phagocytophilum	h-1148	KM215222
A. platys	**Okinawa**	**AF536828**
A. platys	D35	KX792089
A. platys	4	KT982643
A. platys	QQQ	KX447505
A. platys	RRR	KX447502
A. platys	Rodo-p1-66	JX976181
A. platys	A.pl.#87	JQ396431
A. platys	Gigio	EU439943
A. platys	NA	EF139459
A. platys	YY36	MF289478
A. platys	YY33	MF289477
A. platys	b3-7	KY594914
A. platys	dog-72	LC269822
A. platys	dog-99	LC269821
A. platys	dog-166	LC269820
A. platys	WHBMXZ-126	KX987336
A. platys	ZJARSA-8	KU586183
A. platys	WHARSA-7	KU586175
A. platys	WHANSL-27-1	KU586172
A. platys	WHANSA-24-2	KU586168
A. platys	WHAEAP-26	KU586165
A. platys	WHAEAL-17-2	KU586163
A. platys	JXARSA-29	KU586161
A. platys	JXANSA-19	KU586159
A. platys	WHANSE-2	KU586124
A. platys	WHARSP-17	KU586058
A. platys	WHARSL-30	KU586051
A. platys	WHARSA-47-1	KU586031
A. platys	WHARSA-14	KU586028
A. platys	WHANSA-8	KU586006
A. platys	WHANSA-7-4	KU586001
A. platys	WHANSA-6-3	KU585997
A. platys	WHANSA-45-1	KU585989

A. platys	WHANSA-40	KU585988
A. platys	M48A	KX180946
A. platys	P30	KX180944
A. platys	NA	KY114935
A. platys	3ax1	KJ659045
A. platys	2ax1	KJ659044
A. platys	NA	AY530806
A. platys	Okinawa	AY077619
A. platys	NA	AF303467
A. platys	NA	AF399917
A. platys	NA	AF287153
A. platys	NA	AF286699
A. platys	NA	AF156784
A. platys	NA	M82801
A. marginale	BAGHS-B47	MG018436
A. marginale	Wayanad 17	MG728098
A. marginale	TVM 3	MG709131
A. marginale	Thrissur 8	MG709056
A. marginale	Thrissur 6	MG709054
A. marginale	Thrissur 5	MG709053
A. marginale	WHANSA-6-2	KU586171
A. marginale	WHAEAP-33	KU586166
A. marginale	JXANSA-2	KU586160
A. marginale	WHANSE-2-1	KU586125
A. marginale	ZJCUTA-30	KU586074
A. marginale	ZJCUTA-2	KU586073
A. marginale	ZJCUTA-10	KU586072
A. marginale	WHCUTA-25	KU586066
A. marginale	WHARSP-30-2	KU586062
A. marginale	WHARSP-19	KU586059
A. marginale	WHARSL-38-1	KU586056
A. marginale	WHARSA-47-2	KU586032
A. marginale	WHANSL-8-1	KU586022
A. marginale	WHANSL-27-2	KU586017
A. marginale	WHANSL-11-1	KU586012
A. marginale	WHANSA-92	KU586011
A. marginale	WHANSA-8-2	KU586005
A. marginale	WHANSA-60-2	KU585998
A. marginale	WHANSA-53-2	KU585995
A. marginale	WHANSA-48	KU585992
A. marginale	WHANSA-45-2	KU585990
A. marginale	JXANSA-8	KU585964
A. marginale	JXANSA-34	KU585963
A. marginale	JXANSA-24	KU585960
A. marginale	Uganda MT27	KU686794
A. marginale	Uganda MT28	KU686793
A. marginale	Uganda MT34	KU686792
A. marginale	Uganda MT30	KU686791
A. marginale	Uganda MT29	KU686790
A. marginale	Uganda MT31	KU686789
A. marginale	Uganda MT38	KU686788
A. marginale	Uganda KT7	KU686787
A. marginale	Uganda MT32	KU686786
A. marginale	Uganda MT37	KU686782
A. marginale	Uganda MT35	KU686781
A. marginale	Uganda MT33	KU686780
A. marginale	Uganda KT9	KU686779
A. marginale	Uganda MT42	KU686778
A. marginale	Uganda KT10	KU686777
A. marginale	Uganda KT6	KU686776
A. marginale	Uganda MT39	KU686775
A. marginale	Uganda MT36	KU686774
A. marginale	AM-SAR2011	KP877314
A. marginale	**Zaria**	**KJ095114**
A. marginale	NA	AB916498
A. marginale	NA	LC007100
A. marginale	NA	AB916499
A. marginale	Sivas SS101	KJ183086
A. marginale	Sivas SS84	KJ183083
A. marginale	NA	CP006847
A. marginale	NA	CP006846
A. marginale	C6A	JQ839012
A. marginale	C7D	JQ839011
A. marginale	5C	JQ839009
A. marginale	4C	JQ839008
A. marginale	ZJ02/2009	HM439433
A. marginale	K1	GU129918
A. marginale	NA	FJ155998
A. marginale	NA	CP001079
A. marginale	Ishigaki-2007	FJ226454
A. marginale	TG26	DQ000617
A. marginale	IG42	DQ000616
A. marginale	GP4	DQ000615
A. marginale	BS19	DQ000614
A. marginale	BS16	DQ000613
A. marginale	NA	AY048816
A. marginale	Hongan buffalo	DQ341369
A. marginale	16S	AJ633048
A. marginale	Zimbabwe	AF414878
A. marginale	Uruguay	AF414877
A. marginale	non-tailed	AF414875
A. marginale	F12	AF414874
A. marginale	Veld	AF414873
A. marginale	Eland	AF414872
A. marginale	South Africa	AF414871
A. marginale	NA	AF311303
A. marginale	South Idaho	AF309868
A. marginale	Virginia	AF309866
A. marginale	NA	CP000030
A. marginale	58	M60313
A. marginale	WHARSL-28	KU586048
A. marginale	ZJCUTA-6	KU586076
A. marginale	ZJCUTA-5	KU586075
A. marginale	WHARSA-30	KU586030
A. marginale	WHANSL-41	KU586021
A. marginale	WHCUTA-8	KU586067
A. marginale	WHANSL-24-1	KU586015
A. marginale	WHAEAL-17-1	KU585973
A. marginale	WHANSA-36	KU585984
A. marginale	CPY31	KM009068
A. marginale	AMSP4-MDK2	KX989511
A. marginale	AMSP4-MDK1	KX989510
A. marginale	HiP_5AM	KY305599
A. marginale	KNP_582AM	KY305598
A. ovis	BAGHS-B47	MG018436
A. ovis	Wayanad 17	MG728098
A. ovis	TVM 3	MG709131
A. ovis	Thrissur 8	MG709056
A. ovis	Thrissur 6	MG709054
A. ovis	Thrissur 5	MG709053
A. ovis	WHANSA-6-2	KU586171
A. ovis	WHAEAP-33	KU586166
A. ovis	JXANSA-2	KU586160
A. ovis	WHANSE-2-1	KU586125
A. ovis	ZJCUTA-30	KU586074
A. ovis	ZJCUTA-2	KU586073
A. ovis	ZJCUTA-10	KU586072
A. ovis	WHCUTA-25	KU586066
A. ovis	WHARSP-30-2	KU586062
A. ovis	WHARSP-19	KU586059
A. ovis	WHARSL-38-1	KU586056
A. ovis	WHARSA-47-2	KU586032
A. ovis	WHANSL-8-1	KU586022
A. ovis	WHANSL-27-2	KU586017
A. ovis	WHANSL-11-1	KU586012
A. ovis	WHANSA-92	KU586011
A. ovis	WHANSA-8-2	KU586005
A. ovis	WHANSA-60-2	KU585998
A. ovis	WHANSA-53-2	KU585995
A. ovis	WHANSA-48	KU585992

A. ovis	WHANSA-45-2	KU585990
A. ovis	JXANSA-8	KU585964
A. ovis	JXANSA-34	KU585963
A. ovis	JXANSA-24	KU585960
A. ovis	Uganda MT27	KU686794
A. ovis	Uganda MT28	KU686793
A. ovis	Uganda MT34	KU686792
A. ovis	Uganda MT30	KU686791
A. ovis	Uganda MT29	KU686790
A. ovis	Uganda MT31	KU686789
A. ovis	Uganda MT38	KU686788
A. ovis	Uganda KT7	KU686787
A. ovis	Uganda MT32	KU686786
A. ovis	Uganda MT37	KU686782
A. ovis	Uganda MT35	KU686781
A. ovis	Uganda MT33	KU686780
A. ovis	Uganda KT9	KU686779
A. ovis	Uganda MT42	KU686778
A. ovis	Uganda KT10	KU686777
A. ovis	Uganda KT6	KU686776
A. ovis	Uganda MT39	KU686775
A. ovis	Uganda MT36	KU686774
A. ovis	AM-SAR2011	KP877314
A. ovis	Zaria	KJ095114
A. ovis	NA	AB916498
A. ovis	NA	LC007100
A. ovis	NA	AB916499
A. ovis	Sivas SS101	KJ183086
A. ovis	Sivas SS84	KJ183083
A. ovis	NA	CP006847
A. ovis	NA	CP006846
A. ovis	C6A	JQ839012
A. ovis	C7D	JQ839011
A. ovis	5C	JQ839009
A. ovis	4C	JQ839008
A. ovis	ZJ02/2009	HM439433
A. ovis	**K1**	**GU129918**
A. ovis	NA	FJ155998
A. ovis	NA	CP001079
A. ovis	Ishigaki-2007	FJ226454
A. ovis	TG26	DQ000617
A. ovis	IG42	DQ000616
A. ovis	GP4	DQ000615
A. ovis	BS19	DQ000614
A. ovis	BS16	DQ000613
A. ovis	NA	AY048816
A. ovis	Hongan buffalo	DQ341369
A. ovis	16S	AJ633048
A. ovis	Zimbabwe	AF414878
A. ovis	Uruguay	AF414877
A. ovis	non-tailed	AF414875
A. ovis	F12	AF414874
A. ovis	Veld	AF414873
A. ovis	Eland	AF414872
A. ovis	South Africa	AF414871
A. ovis	NA	AF311303
A. ovis	South Idaho	AF309868
A. ovis	Virginia	AF309866
A. ovis	NA	CP000030
A. ovis	58	M60313
A. ovis	WHARSL-28	KU586048
A. ovis	ZJCUTA-6	KU586076
A. ovis	ZJCUTA-5	KU586075
A. ovis	WHARSA-30	KU586030
A. ovis	WHANSL-41	KU586021
A. ovis	WHCUTA-8	KU586067
A. ovis	WHANSL-24-1	KU586015
A. ovis	WHAEAL-17-1	KU585973
A. ovis	WHANSA-36	KU585984
A. ovis	CPY31	KM009068

A. ovis	AMSP4-MDK2	KX989511
A. ovis	AMSP4-MDK1	KX989510
A. ovis	HiP_5AM	KY305599
A. ovis	KNP_582AM	KY305598
A. centrale	NA	AF283007
A. centrale	16	EF520690
A. centrale	14	EF520689
A. centrale	8	EF520688
A. centrale	1	EF520687
A. centrale	CC	EF520686
A. centrale	**South Africa**	**AF414869**
A. centrale	Vaccine	AF414868
A. centrale	NA	AB211164
A. centrale	LP17	MF289482
A. centrale	LP10	MF289481
A. centrale	JJ5	MF289480
A. centrale	ZJ68	KP062966
A. centrale	ZJ64	KP062965
A. centrale	ZJ62	KP062964
A. centrale	Uganda KT5	KU686784
A. centrale	Uganda KT8	KU686783
A. centrale	C4B	JQ839010
A. centrale	HIP/A8/e	KC189842
A. centrale	HIP/A8/d	KC189841
A. centrale	HIP/A8/c	KC189840
A. centrale	NA	AB588977
A. centrale	HLAC222	GU064903
A. centrale	NA	AF318944
A. centrale	Israel	AF309869
A. bovis	Y258	KY425447
A. bovis	Y257	KY425445
A. bovis	Y201	KY425441
A. bovis	Y197	KY425439
A. bovis	Y196	KY425435
A. bovis	Y111	KY425433
A. bovis	Y102	KY425431
A. bovis	Y85	KY425429
A. bovis	Y83	KY425426
A. bovis	Y59	KY425423
A. bovis	Y11	KY425420
A. bovis	**Zhongxian**	**FJ169957**
A. bovis	SG176_HL	EU181143
A. bovis	SG175_HL	EU181142
A. bovis	Tottori-97	HM131218
A. bovis	Hiroshima-Z27	HM131217
A. bovis	ribosomal	AY144729
A. bovis	FL17	MF289479
A. bovis	Shandong JN2	KY242455
A. bovis	WHHLHP-119	KX987337
A. bovis	WHARSL-38-2	KU586176
A. bovis	WHARSA-40-2	KU586174
A. bovis	WHANSA-6-1	KU586170
A. bovis	WHANSA-24-1	KU586167
A. bovis	WHANSL-8	KU586023
A. bovis	20/China/2013	KP314253
A. bovis	19/China/2013	KP314252
A. bovis	18/China/2013	KP314251
A. bovis	17/China/2013	KP314250
A. bovis	15/China/2013	KP314249
A. bovis	14/China/2013	KP314248
A. bovis	13/China/2013	KP314247
A. bovis	12/China/2013	KP314246
A. bovis	11/China/2013	KP314245
A. bovis	10/China/2013	KP314244
A. bovis	9/China/2013	KP314243
A. bovis	8/China/2013	KP314242
A. bovis	6/China/2013	KP314240
A. bovis	4/China/2013	KP314239
A. bovis	1/China/2013	KP314236
A. bovis	ZJ98	KP062959

A. bovis	ZJ69	KP062958
A. bovis	ZJ66	KP062957
A. bovis	ZJ54	KP062956
A. bovis	ZJ46	KP062955
A. bovis	ZJ15	KP062954
A. bovis	ZJ12	KP062953
A. bovis	TYM19	LC012818
A. bovis	TYM14	LC012817
A. bovis	KUM7	LC012813
A. bovis	KUM5	LC012812
A. bovis	KOC4	LC012811
A. bovis	115	KM114613
A. bovis	85	KM114612
A. bovis	88	KM114611
A. bovis	sika35	LC060988
A. bovis	CMS-34_20111224	AB983439
A. bovis	CFT-27_20111223	AB983438
A. bovis	3ay	KJ659043
A. bovis	3ax	KJ659042
A. bovis	2ay	KJ659041
A. bovis	2ax	KJ659040
A. bovis	CFT-27-2010	AB723716
A. bovis	CFT-27-2009	AB723715
A. bovis	CFT-24-2010	AB723714
A. bovis	CFT-24-2009	AB723713
A. bovis	Am-vole57	JX092098
A. bovis	China-chipmunk25	JX092096
A. bovis	Kh-Hc215	JX092094
A. bovis	Am-Hc60	JX092092
A. bovis	Ab38B	AB588969
A. bovis	Ab59B	AB588965
A. bovis	raccoon513	GU937023
A. bovis	raccoon510	GU937022
A. bovis	raccoon501	GU937021
A. bovis	raccoon499	GU937020
A. bovis	raccoon493	GU937019
A. bovis	raccoon490	GU937018
A. bovis	raccoon464	GU937017
A. bovis	raccoon462	GU937016
A. bovis	raccoon458	GU937015
A. bovis	raccoon453	GU937014
A. bovis	raccoon439	GU937013
A. bovis	raccoon426	GU937012
A. bovis	raccoon109	GU937011
A. bovis	Yu12	JN558829
A. bovis	R7	JN558828
A. bovis	G55	JN558825
A. bovis	G49	JN558824
A. bovis	G21	JN558823
A. bovis	G1	JN558822
A. bovis	B7	JN558819
A. bovis	YX4	JN558817
A. bovis	G41	HQ913646
A. bovis	ES1090	HQ913645
A. bovis	ES1019	HQ913644
A. bovis	HLAB352	GU064902
A. bovis	HLAB187	GU064901
A. bovis	AB-KGHL	AF470698
A. bovis	NA	U03775
R. typhi	**Wilmington**	**L36221**
R. typhi	NA	M20499
R. typhi	Wilmington	U12463
R. rickettsii	NA	M21293
R. rickettsii	**R**	**L36217**
R. rickettsii	1995H02	DQ150694
R. rickettsii	1995H01	DQ150691
R. rickettsii	1994C02	DQ150688
R. rickettsii	1991C03	DQ150685
R. rickettsii	1989C01	DQ150682
R. rickettsii	NA	U11021

2. GenBank® accession codes for the *18S rRNA* gene sequences of *Babesia* and *Theileria* species. Sequences utilized for *in silico* analysis in Appendix B are emphasized in bold.

***Babesia* Species**	**Isolate/Strain**	**GenBank**
B. canis vogeli	NA	HM590440
B. canis vogeli	NA	AY072925
B. canis vogeli	TWN2	HQ148664
B. canis vogeli	TWN1	HQ148663
B. canis vogeli	2B-158459	KY290979
B. canis vogeli	192704	KY290978
B. canis vogeli	105796	KY290977
B. canis vogeli	59239	KY290976
B. canis vogeli	dog 102	KT323936
B. canis vogeli	cat 100	KT323935
B. canis vogeli	dog 94	KT323934
B. canis vogeli	dog 86	KT323933
B. canis vogeli	cat 73	KT323932
B. canis vogeli	Belem Bv02	KT333456
B. canis vogeli	Dog#149	JX871891
B. canis vogeli	Dog#44	JX304683
B. canis vogeli	Dog#31	JX304682
B. canis vogeli	Dog#26	JX304681
B. canis vogeli	Dog#23	JX304680
B. canis vogeli	Dog#22	JX304679
B. canis vogeli	Dog#19	JX304677
B. canis vogeli	Guangxi	KJ939326
B. canis vogeli	SK-011	JX112785
B. canis vogeli	RO/FMVB/B/9	HQ662635
B. canis vogeli	NA	JF825145
B. canis vogeli	dog	AY150061
B. canis vogeli	NA	EU084681
B. canis vogeli	**Venezuela**	**DQ297390**
B. canis vogeli	Spain 1	DQ439545
B. canis vogeli	USA	AY371198
B. canis vogeli	Egypt	AY371197
B. canis vogeli	Brazil	AY371196
B. canis vogeli	Brazil	AY371195
B. canis vogeli	Brazil	AY371194
B. canis canis	Dog-1	KT008057
B. canis canis	BccTR2	KF499115
B. canis canis	2	EU622793
B. canis canis	1	EU622792
B. canis canis	NA	AY072926
B. canis canis	Bd6-2	AY962187
B. canis canis	Bd6-1	AY962186
B. canis canis	NA	AY649326
B. canis canis	**D5**	**AY527063**
B. canis canis	43 ldrf	DQ869308
B. canis canis	dog	DQ869307
B. canis canis	Dog#5	KC593879
B. canis canis	Dog#1	KC593878
B. canis canis	Dog#1	KC593877
B. canis canis	204A/13b	KP216422
B. canis canis	RO/FMVB/B/7	HQ662634
B. canis canis	BCC2	FJ209025
B. canis canis	BBC1	FJ209024
B. canis canis	NA	EU152128
B. canis canis	NA	AY321119
B. canis rossi	**Dog-76**	**DQ111764**
B. canis rossi	Dog-74	DQ111763
B. canis rossi	Dog-69	DQ111762

B. canis rossi	Dog-55	DQ111761
B. canis rossi	Dog-44	DQ111760
B. canis rossi	RLB1501/cl3	KY463434
B. canis rossi	RLB1535/cl1	KY463433
B. canis rossi	RLB1501/cl2	KY463432
B. canis rossi	RLB1501/cl1	KY463431
B. canis rossi	RLB1535/cl2	KY463430
B. canis rossi	RLB1535/cl3	KY463429
B. canis rossi	N4	AB935166
B. canis rossi	N3	AB935165
B. canis rossi	N2	AB935164
B. canis rossi	N1	AB935163
B. canis rossi	RLB67	JQ613105
B. canis rossi	RLB42	JQ613104
B. canis rossi	Dog#127, #135	AB303075
B. canis rossi	Dog#25, #354, #398	AB303074
B. canis rossi	Dog#23	AB303073
B. canis rossi	Dog#8	AB303072
B. canis rossi	Dog#2	AB303071
B. canis rossi	NA	KC453992
B. gibsoni	1-1665	KC461261
B. gibsoni	Yamaguchi dog-5672	AY077720
B. gibsoni	CMVL-06/2013/Chopin	KP901253
B. gibsoni	Assam 2	KF928958
B. gibsoni	Ludhiana 3	KF511956
B. gibsoni	Ludhiana 2	KF511955
B. gibsoni	Kolkata 2	KF171474
B. gibsoni	Kolkata 3	KF171473
B. gibsoni	**Siliguri**	**KF171471**
B. gibsoni	Dehradoon	KF171470
B. gibsoni	Kolkata	KJ142323
B. gibsoni	CMVL-05/2013/Kiki	KF878947
B. gibsoni	CMVL-01/2013/Mahesh	KF878943
B. gibsoni	218/Assam	KF112075
B. gibsoni	178/Assam	KF112074
B. gibsoni	TWN5	FJ769388
B. gibsoni	TWN4	FJ769387
B. gibsoni	TWN3	FJ769386
B. gibsoni	Bab/Asm-QM/11/Ind	KF606876
B. gibsoni	Bab/Asm-41/11/Ind	KF606867
B. gibsoni	Johor 314	KU500921
B. gibsoni	Pahang7	KU500920
B. gibsoni	Johor 282	KU500919
B. gibsoni	Sarawak 40	KU500918
B. gibsoni	Sarawak 18	KU500917
B. gibsoni	Selangor 53	KU500916
B. gibsoni	Sabah24	KU500915
B. gibsoni	WH123	KP666168
B. gibsoni	WH121	KP666167
B. gibsoni	WH120	KP666166
B. gibsoni	WH114	KP666165
B. gibsoni	WH110	KP666164
B. gibsoni	WH91	KP666163
B. gibsoni	WH87	KP666162
B. gibsoni	WH82	KP666161
B. gibsoni	WH71	KP666160
B. gibsoni	WH61	KP666159
B. gibsoni	WH58	KP666158
B. gibsoni	WH56	KP666157
B. gibsoni	WH54	KP666156
B. gibsoni	WH35	KP666155
B. gibsoni	BD37	LC008285
B. gibsoni	BD05	LC008284
B. gibsoni	BD02	LC006968

B. gibsoni	Punjab	KC954653
B. gibsoni	Kolkata-1	KC811803
B. gibsoni	Assam	KC811802
B. gibsoni	Bareilly-1	KC811801
B. gibsoni	TWN5	JQ710685
B. gibsoni	KOR07-20	EU430494
B. gibsoni	KOR06-104	EU430493
B. gibsoni	KOR06-102	EU430492
B. gibsoni	KOR0685	EU430491
B. gibsoni	KOR0675	EU430490
B. gibsoni	KOR0674	EU430489
B. gibsoni	KOR0656	EU430488
B. gibsoni	KOR0654-4	EU430487
B. gibsoni	KOR0644-2	EU430486
B. gibsoni	KOR0501-10	EU430481
B. gibsoni	NRCPD	AB478326
B. gibsoni	Aomori	AB118032
B. gibsoni	TWN1	EF587269
B. gibsoni	TWN2	EF587268
B. gibsoni	CMVL-01/2014	KY563118
B. gibsoni	CMVL Apr-13	KY524481
B. gibsoni	G135	LC169085
B. gibsoni	G112	LC169084
B. gibsoni	G111	LC169083
B. gibsoni	MB_P3	LC168621
B. gibsoni	MB_D2	LC168620
B. gibsoni	YGC17	LC012809
B. gibsoni	YGC15	LC012808
B. gibsoni	YGC14	LC012807
B. gibsoni	YGC11	LC012806
B. gibsoni	YGC10	LC012805
B. gibsoni	YGC8	LC012804
B. gibsoni	YGC7	LC012803
B. gibsoni	TKS20	LC012802
B. gibsoni	TKS5	LC012801
B. gibsoni	OSK7	LC012800
B. gibsoni	OSK3	LC012799
B. gibsoni	NGS6	LC012798
B. gibsoni	KUM4	LC012797
B. gibsoni	KUM3	LC012796
B. gibsoni	KUM2	LC012795
B. gibsoni	KGW18	LC012794
B. gibsoni	KGS4	LC012793
B. gibsoni	KGS1	LC012792
B. gibsoni	HNXY-2/2013	KJ715178
B. gibsoni	Nanjing1081	HG328237
B. gibsoni	Nanjing0010	HG328236
B. gibsoni	Nanjing0009	HG328235
B. gibsoni	SK-013	JX112784
B. gibsoni	Pig/J78	JX962780
B. gibsoni	Aydin	JN562745
B. gibsoni	11HS	EU084680
B. gibsoni	NA	EU084679
B. gibsoni	NA	EU084678
B. gibsoni	WM-1	EU084677
B. gibsoni	Okinawa dog-15	AY077718
B. bigemina	**Swiss_6**	**KM046917**
B. bigemina	JRHC-1	JX974332
B. bigemina	Umiam	KF112076
B. bigemina	Hs5	HQ688689
B. bigemina	Hs4	HQ688688
B. bigemina	Hs3	HQ688687
B. bigemina	Hs2	HQ688686
B. bigemina	Hs1	HQ688685
B. bigemina	Bab/Umi-H2/Ind	KF606866
B. bigemina	Bab/Umi-Hi/12/Ind	KF606865
B. bigemina	Bab/Umi-C2/12/Ind	KF606864
B. bigemina	Bab/Umi-T2/10/Ind	KF606863
B. bigemina	RG	JQ437264
B. bigemina	Bond	JQ437261

B. bigemina	ZJK17	KP710228
B. bigemina	TS103	KP710227
B. bigemina	CZ52	KP710226
B. bigemina	TJ09	KP710225
B. bigemina	SJZ26	KP710224
B. bigemina	MT26	KU206297
B. bigemina	MT25	KU206296
B. bigemina	KT4	KU206295
B. bigemina	MT24	KU206294
B. bigemina	MT23	KU206293
B. bigemina	MT22	KU206292
B. bigemina	MT21	KU206291
B. bigemina	TB5	KX115425
B. bigemina	Trkene3yumurta	KP745624
B. bigemina	Trkoz10	KP745623
B. bigemina	NA	JQ723014
B. bigemina	biLushi	JX495402
B. bigemina	PISJD34	JX104106
B. bigemina	563	HQ840960
B. bigemina	493	HQ840959
B. bigemina	B_bi19	EF458206
B. bigemina	B_bi18	EF458205
B. bigemina	B_bi17	EF458204
B. bigemina	B_bi16	EF458203
B. bigemina	B_bi14	EF458202
B. bigemina	B_bi12	EF458201
B. bigemina	B_bi11	EF458200
B. bigemina	B_bi10	EF458199
B. bigemina	B_bi09	EF458198
B. bigemina	B_bi08	EF458197
B. bigemina	B_bi07	EF458196
B. bigemina	B_bi06	EF458195
B. bigemina	B_bi05	EF458194
B. bigemina	B_bi04	EF458193
B. bigemina	B_bi03	EF458192
B. bigemina	B_bi02	EF458191
B. bigemina	B_bi01	EF458190
B. bigemina	BRC02	FJ426361
B. bigemina	Israel	EF612434
B. bigemina	Spain_1	DQ785311
B. microti	**US-Bm5**	**LC314658**
B. microti	US-Bm4	LC314657
B. microti	US-Bm3	LC314656
B. microti	US-Bm2	LC314655
B. microti	US-Bm1	LC314654
B. microti	IpSG13-18-1	LC127372
B. microti	IpSG13-16-3	LC127371
B. microti	IpSG13-10-2	LC127370
B. microti	IpSG13-1-2	LC127369
B. microti	Omsk-Tr17	KU955532
B. microti	Omsk-vole215_2015	KU955531
B. microti	Omsk-vole205_2015	KU955530
B. microti	Omsk-vole190_2015	KU955529
B. microti	Omsk-vole118_2013	KU955528
B. microti	Omsk-chipmunk2_2014	KU955527
B. microti	Omsk-vole130_2013	KU955526
B. microti	Omsk-vole92_2013	KU955525
B. microti	Omsk-vole57_2013	KU955524
B. microti	Omsk-vole45_2013	KU955523
B. microti	Omsk-vole24_2013	KU955522
B. microti	BmSSR218-3	LC005772
B. microti	BmSSR218-2	LC005771
B. microti	BmSSR218-1	LC005770
B. microti	BmSSR209-3	LC005769
B. microti	BmSSR209-1	LC005768
B. microti	BmSSR206-3	LC005767
B. microti	BmSSR206-2	LC005766
B. microti	BmSSR206-1	LC005765
B. microti	BmSSR190-5	LC005764
B. microti	BmSSR190-4	LC005763
B. microti	BmSSR190-3	LC005762
B. microti	BmSSR170-3	LC005761
B. microti	BmSSR170-2	LC005760
B. microti	BmSSR170-1	LC005759
B. microti	BmSSR168-3	LC005758
B. microti	BmSSR168-1	LC005757
B. microti	BmSSR167-9	LC005756
B. microti	BmSSR167-3	LC005755
B. microti	BmSSR167-1	LC005754
B. microti	BmSSR161-2	LC005753
B. microti	BmSSR159-1	LC005752
B. microti	TC-2012-C1	KF410827
B. microti	TC-2012-B99	KF410826
B. microti	TC-2012-B87	KF410825
B. microti	TC-2012-B1	KF410824
B. microti	Omsk-vole110	KC581934
B. microti	Yunnan-2	KC147723
B. microti	Yunnan-1	KC147722
B. microti	Ubl-104	AY943958
B. microti	Sbl-11	AY943957
B. microti	Gray	AY693840
B. microti	AF41002	AY918952
B. microti	AF2143	AY918951
B. microti	SN87-1	AY144702
B. microti	P8803	AY144701
B. microti	Rula	AY144700
B. microti	MT006	AY144699
B. microti	S837	AY144698
B. microti	Naushon	AY144697
B. microti	Nantucket	AY144696
B. microti	Pl2845Ips	AY144695
B. microti	Spooner	AY144694
B. microti	Russia	AY144693
B. microti	C5D182	AY144692
B. microti	VHSC1	AY144691
B. microti	GLS027Cg	AY144690
B. microti	400	AY144687
B. microti	NA	AB219802
B. microti	MM-1	EU168705
B. microti	Jena/Germany	EF413181
B. microti	NA	AB197940
B. microti	NA	AY094354
B. microti	Bm3	KX008036
B. microti	Bm2	KX008035
B. microti	Bm1	KX008034
B. microti	HLJ605	KU204798
B. microti	HLJ552	KU204797
B. microti	HLJ479	KU204796
B. microti	HLJ429	KU204795
B. microti	HLJ97	KU204794
B. microti	HLJ44	KU204793
B. microti	4IV	KT844560
B. microti	3IV	KT844559
B. microti	2IV	KT844558
B. microti	1IV	KT844557
B. microti	5BA	KT844556
B. microti	4BA	KT844555
B. microti	3BA	KT844554
B. microti	2BA	KT844553
B. microti	NA	KT867773
B. microti	NA	KT318132
B. microti	Irk-Ip332	KJ486556
B. microti	CNMM-2	AB736270
B. microti	CNMM-1	AB731747

B. microti	Yunnan-3	KC147724
B. microti	Rat/6	JX962781
B. microti	Fox/J28	JX962779
B. microti	hlj72	JQ993429
B. microti	449-L	JQ609304
B. microti	JM1	AB576641
B. microti	Nov-Ip307	GU057383
B. microti	NA	AY789075
B. microti	Kh-1026	GU057386
B. microti	Kh-Ip67	GU057384
		XR_00245
B. microti	RI	9986
B. caballi	**B1_CABRBEQ179**	**EU642513**
B. caballi	A_CABEQ30	EU642512
B. caballi	B1_CABRBEQ164	EU888904
B. caballi	CABEQ51_B1	EU888901
B. caballi	CABEQ50_B1	EU888900
B. caballi	B2_CABRBEQ115	EU642514
B. caballi	NA	KJ549665
B. caballi	EqP-117	JX049130
B. caballi	NA	MF384422
B. caballi	Jaboticabal	KY952238
B. caballi	142	KY952236
B. caballi	157	KY952235
B. caballi	151	KY952234
B. caballi	143	KY952233
B. caballi	Bacab5	KX375825
B. caballi	Bacab1	KX375824
B. caballi	U244	AB734409
B. caballi	A134	AB734408
B. caballi	A135	AB734407
B. caballi	A139	AB734406
B. caballi	A195	AB734405
B. caballi	A161	AB734404
B. caballi	A188	AB734403
B. caballi	A142	AB734402
B. caballi	U237	AB734401
B. caballi	U243	AB734400
B. caballi	U244	AB734399
B. caballi	U232	AB734398
B. caballi	U231	AB734397
B. caballi	T23	AB734396
B. caballi	U240	AB734395
B. caballi	A214	AB734394
B. caballi	A158	AB734393
B. caballi	A123	AB734392
B. caballi	T103	AB734391
B. caballi	T90	AB734390
B. caballi	T64	AB734389
B. caballi	T48	AB734388
B. caballi	T16	AB734387
B. caballi	T4	AB734386
B. caballi	NA	FJ209026
B. caballi	NA	AY309955
B. caballi	EB1	AY534883
B. caballi	NA	Z15104
B. divergens	NA	AY144688
B. divergens	**Spanish_2**	**MG944238**
B. divergens	IpSG14-2-2	LC279018
B. divergens	IPSG13-13-1	AB975389
B. divergens	Trbrt35	KP745627
B. divergens	IpSG10	KC493555
B. divergens	C139	FJ944826
B. divergens	1802A	FJ944825
B. divergens	Bob2	FJ944824
B. divergens	CF2000	FJ944823
B. divergens	Rouen 87	FJ944822
B. divergens	B2	EU182595
B. divergens	B1	EU182594
B. divergens	HLJ216	KU377437
B. divergens	HLJ216	KU204799
B. divergens	R105	KM657258
B. divergens	Spanish	KF533077
B. divergens	Aug-43	AB861507
B. divergens	Aug-40	AB861506
B. divergens	18-Aug	AB861505
B. divergens	4-Aug	AB861504
B. divergens	Aug-38	AB857846
B. divergens	Jul-33	AB857845
B. divergens	25-Aug	KC465974
B. divergens	12-Jul	KC465977
B. divergens	Aug-41	KC465976
B. divergens	20-Jul	KC465975
B. divergens	Aug-51	KC465973
B. divergens	RD54	JQ929916
B. divergens	CVD7	GQ304525
B. divergens	CVD2	GQ304524
B. divergens	Nov-Ip316	GU057385
B. divergens	NA	AY789076
B. divergens	BAB105	AY046576
B. divergens	B_di09	EF458228
B. divergens	B_di10	EF458229
B. divergens	B_di08	EF458227
B. divergens	B_di07	EF458226
B. divergens	B_di06	EF458225
B. divergens	B_di05	EF458224
B. divergens	B_di04	EF458223
B. divergens	B_di03	EF458222
B. divergens	B_di02	EF458221
B. divergens	B_di01	EF458220
B. divergens	B_di11	EF458219
B. divergens	NA	AY572456
B. divergens	NA	AJ439713
B. divergens	NA	U16370
B. divergens	NA	Z48751
B. bovis	**BRC01**	**FJ426364**
B. bovis	Bareilly	KF928959
B. bovis	BBOV2	L19077
B. bovis	BBOV3	L19078
B. bovis	USDA	HQ264112
B. bovis	USDA	HQ264111
B. bovis	H8	HQ264110
B. bovis	NR8	HQ264106
B. bovis	NR8	HQ264105
B. bovis	USDA	GU906886
B. bovis	Merida	GU906885
B. bovis	Merida	GU906884
B. bovis	Merida	GU906883
B. bovis	H81	JQ437262
B. bovis	8284	JQ437260
B. bovis	ZJK15	KP710223
B. bovis	TS35	KP710222
B. bovis	Trbrt36	KP745628
B. bovis	NA	JQ723013
B. bovis	boLushi	JX495403
B. bovis	cow	AY150059
B. bovis	B_bo18	EF458218
B. bovis	B_bo17	EF458217
B. bovis	B_bo16	EF458216
B. bovis	B_bo10	EF458215
B. bovis	B_bo09	EF458214
B. bovis	B_bo08	EF458213
B. bovis	B_bo07	EF458212
B. bovis	B_bo05	EF458211
B. bovis	B_bo03	EF458210
B. bovis	B_bo01	EF458209
B. bovis	B_bo19	EF458208
B. conradae	**NA**	**AF158702**
B. vulpes	**1061L**	**KJ871352**
B. vulpes	910L	KJ871351

B. vulpes	03/00349	KT223483
B. duncani	**BAB1615**	**HQ289870**
B. duncani	Bdu	KX008042
B. duncani	Bdi	KX008037
B. duncani	BAB2	HQ285838
Theileria		
(Babesia) equip	**RJ20**	**KJ573374**
Theileria		
(*Babesia*) *equi*	RJ19	KJ573373
Theileria		
(*Babesia*) *equi*	RJ15	KJ573372
Theileria		
(*Babesia*) *equi*	RJ4	KJ573371
Theileria		
(*Babesia*) *equi*	RJ2	KJ573370
Theileria		
(*Babesia*) *equi*	B_LFEQ164	EU642511
Theileria		
(*Babesia*) *equi*	B_LFEQ47	EU642510
Theileria		
(*Babesia*) *equi*	B_RBEQ105	EU642509
Theileria		
(*Babesia*) *equi*	A1_RBEQ178	EU642508
Theileria		
(*Babesia*) *equi*	A2_RBEQ101	EU642507
Theileria		
(*Babesia*) *equi*	LFEQ23_A	EU888906
Theileria		
(*Babesia*) *equi*	LFEQ178_C	EU888905
Theileria		
(*Babesia*) *equi*	LFEQ189_C	EU888903
Theileria		
(*Babesia*) *equi*	RBEQ63_A	EU888902
Theileria		
(*Babesia*) *equi*	TE/18s/GUJ	KP995259
Theileria		
(*Babesia*) *equi*	Te0022_CA	JX177673
Theileria		
(*Babesia*) *equi*	Te0001_FL	JX177672
Theileria		
(*Babesia*) *equi*	Te0002_TX	JX177671
Theileria		
(*Babesia*) *equi*	Te0004_TX	JX177670
Theileria		
(*Babesia*) *equi*	Ho233	JQ390047
Theileria		
(*Babesia*) *equi*	NA	KF559357
Theileria		
(*Babesia*) *equi*	203-7	JQ657703
Theileria		
(*Babesia*) *equi*	KNU	HM229408
Theileria		
(*Babesia*) *equi*	KNU	HM229407
Theileria		
(*Babesia*) *equi*	ET1	AY534882
Theileria		
(*Babesia*) *equi*	H16	KY111762
Theileria		
(*Babesia*) *equi*	H12	KY111761
Theileria		
(*Babesia*) *equi*	H01	KY111760
Theileria		
(*Babesia*) *equi*	RJ18	KX722525
Theileria		
(*Babesia*) *equi*	RJ3	KX722524
Theileria		
(*Babesia*) *equi*	RJ17	KX722523
Theileria		
(*Babesia*) *equi*	RJ16	KX722522
Theileria		
(*Babesia*) *equi*	RJ14	KX722521
Theileria		
(*Babesia*) *equi*	RJ13	KX722520
Theileria		
(*Babesia*) *equi*	RJ12	KX722519
Theileria		
(*Babesia*) *equi*	RJ11	KX722518
Theileria		
(*Babesia*) *equi*	RJ10	KX722517
Theileria		
(*Babesia*) *equi*	RJ9	KX722516
Theileria		
(*Babesia*) *equi*	RJ8	KX722515
Theileria		
(*Babesia*) *equi*	RJ7	KX722514
Theileria		
(*Babesia*) *equi*	RJ6	KX722513
Theileria		
(*Babesia*) *equi*	RJ5	KX722512
Theileria		
(*Babesia*) *equi*	RJ1	KX722511
Theileria		
(*Babesia*) *equi*	A11N	KX227641
Theileria		
(*Babesia*) *equi*	156N	KX227640
Theileria		
(*Babesia*) *equi*	347C	KX227639
Theileria		
(*Babesia*) *equi*	B1	KX227638
Theileria		
(*Babesia*) *equi*	3011C	KX227637
Theileria		
(*Babesia*) *equi*	U4S	KX227636
Theileria		
(*Babesia*) *equi*	U2S	KX227635
Theileria		
(*Babesia*) *equi*	T1N	KX227634
Theileria		
(*Babesia*) *equi*	PA20	KX227633
Theileria		
(*Babesia*) *equi*	PA13	KX227632
Theileria		
(*Babesia*) *equi*	PA46	KX227631
Theileria		
(*Babesia*) *equi*	O5S	KX227630
Theileria		
(*Babesia*) *equi*	O2S	KX227629
Theileria		
(*Babesia*) *equi*	G6	KX227628
Theileria		
(*Babesia*) *equi*	F14C	KX227627
Theileria		
(*Babesia*) *equi*	E37C	KX227626
Theileria		
(*Babesia*) *equi*	5512N	KX227625
Theileria		
(*Babesia*) *equi*	177S	KX227624
Theileria		
(*Babesia*) *equi*	101J	KX227623
Theileria		
(*Babesia*) *equi*	PA21	KX227622
Theileria		
(*Babesia*) *equi*	20J	KX227621
Theileria		
(*Babesia*) *equi*	9C	KX227620
Theileria		
(*Babesia*) *equi*	459N	KX227619
Theileria		
(*Babesia*) *equi*	Ho-79	KU672386

Theileria (*Babesia*) *equi*	Swiss-5	KM046922
Theileria (*Babesia*) *equi*	Swiss-4	KM046921
Theileria (*Babesia*) *equi*	Swiss-3	KM046920
Theileria (*Babesia*) *equi*	Swiss-2	KM046919
Theileria (*Babesia*) *equi*	Swiss-1	KM046918
Theileria (*Babesia*) *equi*	JJ42	KM819520
Theileria (*Babesia*) *equi*	El Obied46	AB515315
Theileria (*Babesia*) *equi*	Kosti5	AB515314
Theileria (*Babesia*) *equi*	Omdurman2	AB515313
Theileria (*Babesia*) *equi*	Khartoum North15	AB515312
Theileria (*Babesia*) *equi*	Atbara13	AB515311
Theileria (*Babesia*) *equi*	Atbara8	AB515310
Theileria (*Babesia*) *equi*	Atbara5	AB515309
Theileria (*Babesia*) *equi*	Atbara2	AB515308
Theileria (*Babesia*) *equi*	Atbara1	AB515307
Theileria (*Babesia*) *equi*	T42	AB733379
Theileria (*Babesia*) *equi*	T10	AB733378
Theileria (*Babesia*) *equi*	U225	AB733377
Theileria (*Babesia*) *equi*	T95	AB733376
Theileria (*Babesia*) *equi*	A200	AB733375
Theileria (*Babesia*) *equi*	T8	AB733374
Theileria (*Babesia*) *equi*	A129	AB733373
Theileria (*Babesia*) *equi*	A128	AB733372
Theileria (*Babesia*) *equi*	dog	AY150064
Theileria (*Babesia*) *equi*	Spain-2	AY150063
Theileria (*Babesia*) *equi*	Spain-1	AY150062
Theileria (*Babesia*) *equi*	Spain-3	DQ287951
Theileria (*Babesia*) *equi*	NA	Z15105
Cytauxzoon felis	NA	L19080
Cytauxzoon felis	**309**	**KU306948**
Cytauxzoon felis	307	KU306947
Cytauxzoon felis	303	KU306946
Cytauxzoon felis	53aug	KU306945
Cytauxzoon felis	26-Aug	KU306944
Cytauxzoon felis	20-Aug	KU306943
Cytauxzoon felis	18-Aug	KU306942
Cytauxzoon felis	13-Aug	KU306941
Cytauxzoon felis	7-Oct	KU306940
Cytauxzoon felis	NA	AF399930
Cytauxzoon felis	NA	GU903911

3. GenBank® accession codes for the *bipA* gene sequences of *Borrelia* species. Sequences utilized for *in silico* analysis in Appendix B are emphasized in bold.

***Borrelia* Species**	**Isolate/Strain**	**GenBank**
B. turicatae	**FCB-1**	**C845531**
B. turicatae	NA	GU270942
B. turicatae	91E135	HM008710
B. turicatae	95PE570	KC845528
B. turicatae	TCB-2	KC845530
B. turicatae	95PE1807	KC845527
B. turicatae	BTE5EL	CP015630
B. turicatae	**TCB-1**	**KC845529**
B. parkeri	**HR1**	**CP007036**
B. hermsii	SWA	GQ869822
B. hermsii	SIS	GQ869821
B. hermsii	RUM	GQ869820
B. hermsii	REN	GQ869819
B. hermsii	RAL	GQ869818
B. hermsii	OKA-3	GQ869817
B. hermsii	OKA-2	GQ869816
B. hermsii	OKA-1	GQ869815
B. hermsii	MTW-4	GQ869814
B. hermsii	MTW-3	GQ869813
B. hermsii	MTW-2	GQ869812
B. hermsii	MIL	GQ869811
B. hermsii	MCN	GQ869810
B. hermsii	MAT	GQ869809
B. hermsii	Man	GQ869808
B. hermsii	LAK-5	GQ869807
B. hermsii	LAK-4	GQ869806
B. hermsii	LAK-3	GQ869805
B. hermsii	LAK-2	GQ869804
B. hermsii	LAK-1	GQ869803
B. hermsii	HS1	GQ869802
B. hermsii	HAN	GQ869801
B. hermsii	HAL	GQ869800
B. hermsii	GMC	GQ869799
B. hermsii	GAR	GQ869798
B. hermsii	FRS	GQ869797
B. hermsii	FRO	GQ869796
B. hermsii	FRE	GQ869795
B. hermsii	EST	GQ869794
B. hermsii	CON	GQ869792
B. hermsii	CMC	GQ869791
B. hermsii	CAR	GQ869790
B. hermsii	BYM	GQ869789
B. hermsii	BRO	GQ869788
B. hermsii	BAK	GQ869787
B. hermsii	ALL	GQ869786
B. hermsii	**YOR**	**GQ869824**
B. hermsii	**DAH**	**GQ869793**
B. hermsii	DAH	FJ446703
B. hermsii	WAD	GQ869823

4. GenBank® accession codes for the *flaB* gene sequences of *Borrelia* species. Sequences utilized for *in silico* analysis in Appendix B are emphasized in bold.

***Borrelia* Species**	**Isolate/Strain**	**GenBank**
B. turicatae	FCB	AY934630
B. turicatae	**TCB-2**	**AY934629**
B. turicatae	TCB-1	AY934628
B. turicatae	PE1-926	AY934627
B. turicatae	99PE-1807	AY934626
B. turicatae	95PE-570	AY934625
B. turicatae	91E135	AY934624
B. turicatae	91E135	AY604979
B. turicatae	91E135	NC_008710
B. parkeri	CA221	AY934623
B. parkeri	CA220	AY934622
B. parkeri	CA219	AY934621
B. parkeri	CA218	AY934620
B. parkeri	CA216	AY934619
B. parkeri	RML	AY604980
B. parkeri	HR1	CP007022
B. parkeri	**SLO**	**NZ_CP005851**
B. miyamotoi	HoHe	KT932823
B. miyamotoi	ARH554	KT452933
B. miyamotoi	ARH624	KT452932
B. miyamotoi	ARH615	KT452930
B. miyamotoi	ARH657	KT452931
B. miyamotoi	CT13-2396	CP017126
B. miyamotoi	ARH656	KT452934
B. miyamotoi	Izh-16	CP024351
B. miyamotoi	Izh-4	CP024390
B. miyamotoi	Yekat-6	CP024316
B. miyamotoi	Izh-5	CP024205
B. miyamotoi	Izh-14	CP024371
B. miyamotoi	Yekat-1	CP024333
B. miyamotoi	**FR64b**	**CP004217**
B. miyamotoi	CA17-2241	CP021872
B. miyamotoi	13T392	KU749379
B. miyamotoi	15H532	KU749378
B. coriaceae	NA	DQ320140
B. coriaceae	**Co53**	**NZ_CP005745**
B. anserina	5AY_H01_8-125ans_E_G03	KY438930
B. anserina	Es	CP013704
B. anserina	PL	DQ849626
B. anserina	**BA2**	**CP005829**
B. crocidurae	DOS-27	JX292911
B. crocidurae	DOU-1b	JX292912
B. crocidurae	DOU-686	JX292913
B. crocidurae	DOU-690	JX292914
B. crocidurae	DOU	JX292915
B. crocidurae	DOS-2	JX292916
B. crocidurae	DOS-3	JX292917
B. crocidurae	DOS-6	JX292919
B. crocidurae	DOS-5	JX292918
B. crocidurae	DOS-7	JX292920
B. crocidurae	DOS-13	JX292921
B. crocidurae	DOS-16	JX292922
B. crocidurae	Achema	GU357619
B. crocidurae	**DOS-56**	**JX292925**
B. crocidurae	KOS-46	JX292924
B. crocidurae	KOS-39	JX292923
B. crocidurae	Achema	CP003426
B. recurrentis	**A1**	**DQ346814**
B. recurrentis	107	AY604982
B. recurrentis	A2	DQ346815
B. recurrentis	A3	DQ346816
B. recurrentis	A4	DQ346817
B. recurrentis	A6	DQ346819
B. recurrentis	A5	DQ346818
B. recurrentis	A18	DQ346831
B. recurrentis	A17	DQ346830
B. recurrentis	A16	DQ346829
B. recurrentis	A15	DQ346828
B. recurrentis	A14	DQ346827
B. recurrentis	A13	DQ346826
B. recurrentis	A12	DQ346825
B. recurrentis	A11	DQ346824
B. recurrentis	A10	DQ346823
B. recurrentis	A9	DQ346822
B. recurrentis	A8	DQ346821
B. recurrentis	A7	DQ346820
B. recurrentis	A1	CP000993
B. burgdorferi	DG1-04	DQ016625
B. burgdorferi	GL56-07	HM345910
B. burgdorferi	D69-04	DQ016620
B. burgdorferi	T90-5-02	HM345911
B. burgdorferi	Bb_V2	MF150052
B. burgdorferi	Bb_V3	MF150053
B. burgdorferi	Bb_V6	MF150055
B. burgdorferi	Bb_V5	MF150054
B. burgdorferi	Bb_V7	MF150056
B. burgdorferi	Tr293	AB091813
B. burgdorferi	NA	AB189460
B. burgdorferi	CA8	GQ247741
B. burgdorferi	B331	CP017201
B. burgdorferi	Pabe	CP019916
B. burgdorferi	Pali	CP019844
B. burgdorferi	B31-5A1	CP009656
B. burgdorferi	CA382	CP005925
B. burgdorferi	N40	CP002228
B. burgdorferi	JD1	CP002312
B. burgdorferi	ZS7	CP001205
B. burgdorferi	**B31**	**AE000783**
B. afzelii	A1_Aag_Waw	KY626318
B. afzelii	A1_Afl_Waw	KY626319
B. afzelii	B1_Aag_Waw	KY626320
B. afzelii	B2_Aag_Waw	KY626321
B. afzelii	B3_Aag_Waw	KY626322
B. afzelii	B4_Aag_Waw	KY626323
B. afzelii	B5_Aag_Waw	KY626324
B. afzelii	B6_Afl_Waw	KY626325
B. afzelii	Ba_V1a	MF150047
B. afzelii	Ba_V1b	MF150048
B. afzelii	Ba_V2cc	MF150049
B. afzelii	Ba_v2ct	MF150050
B. afzelii	Ba_V2tc	MF150051
B. afzelii	NA	AB236667
B. afzelii	Tr38	AB091806
B. afzelii	Tr96	AB091808
B. afzelii	NA	AB189459
B. afzelii	DB19N7-04	GQ918147
B. afzelii	41-M-11	KF894063
B. afzelii	9W10-04	FJ874924
B. afzelii	Mr11	AB178334
B. afzelii	Mp6	AB178335
B. afzelii	29-MD-11	KF894069
B. afzelii	21-O-12	KF894067
B. afzelii	25-M-11	KF894068
B. afzelii	14-MD-12	KF894066
B. afzelii	9-S-11	KF894065
B. afzelii	80-M-11	KF894064
B. afzelii	CFC8E	AB178780
B. afzelii	Mp4	AB178779
B. afzelii	51-S-12	KF894070
B. afzelii	OS17-07	HM345909

B. afzelii	ST19-05	HM345908
B. afzelii	ZL109-07	HM345907
B. afzelii	**BO23**	**CP018262**
B. afzelii	K78	CP009058
B. afzelii	Tom3107	CP009212
B. afzelii	HLJ01	CP003882
B. afzelii	Pko	CP002933
B. afzelii	Pko	CP000395
B. garinii	D106-04	DQ016621
B. garinii	D7-04	DQ016622
B. garinii	DB1F7-04	DQ650331
B. garinii	DB18N6-04	DQ650333
B. garinii	T32-5-05	DQ650336
B. garinii	PB35-99	HM345897
B. garinii	DB74-01	HM345898
B. garinii	T40-10-02	HM345902
B. garinii	T53-9-02	HM345901
B. garinii	ZL148-07	HM345900
B. garinii	DB60-01	HM345899
B. garinii	RP54-05	HM345906
B. garinii	ST12-05	HM345905
B. garinii	T44-4-02	HM345904
B. garinii	T41-2-02	HM345903
B. garinii	Bg_vA	MF150057
B. garinii	Bg_vAa	MF150058
B. garinii	Bg_vC	MF150062
B. garinii	Bg_vBb	MF150061
B. garinii	Bg_vBa	MF150060
B. garinii	Bg_vB	MF150059
B. garinii	Bg_vDf	MF150069
B. garinii	Bg_vDe	MF150068
B. garinii	Bg_vDd	MF150067
B. garinii	Bg_vDc	MF150066
B. garinii	Bg_vDb	MF150065
B. garinii	Bg_vDa	MF150064
B. garinii	Bg_vCa	MF150063
B. garinii	Bg_vEa	MF150070
B. garinii	Bg_vEb	MF150071
B. garinii	Bg_vEc	MF150072
B. garinii	Bg_vEd	MF150073
B. garinii	Bg_vEf	MF150074
B. garinii	Tr77	AB091807
B. garinii	Tr309	AB091814
B. garinii	Mr8	AB178325
B. garinii	Mr3	AB178326
B. garinii	Mr10	AB178327
B. garinii	Nr267	AB178328
B. garinii	Mp5	AB178329
B. garinii	Mr12	AB178330
B. garinii	23-M-11	KF894053
B. garinii	39-M-11	KF894052
B. garinii	Mp7	AB178332
B. garinii	61-M-11	KF894058
B. garinii	56-M-11	KF894057
B. garinii	67-S-12	KF894056
B. garinii	66-S-12	KF894055
B. garinii	60-S-12	KF894054
B. garinii	77-M-11	KF894061
B. garinii	58-M-11	KF894060
B. garinii	55-M-11	KF894059
B. garinii	Nsk-10-06	EU979630
B. garinii	**SZ**	**CP007564**
B. hermsii GGI	LAK-4	DQ855533
B. hermsii GGI	ELD	DQ855531
B. hermsii GGI	HS1	EF583449
B. hermsii GGI	HS1	GU357620
B. hermsii GGI	WAD	AY597794
B. hermsii GGI	MAN	AY597793
B. hermsii GGI	ALL	AY597791

B. hermsii GGI	GAR	AY597790
B. hermsii GGI	FR0	AY597789
B. hermsii GGI	SIS	AY597788
B. hermsii GGI	RAL	AY597787
B. hermsii GGI	BAK	AY597786
B. hermsii GGI	BYM	AY597785
B. hermsii GGI	CAR	AY597784
B. hermsii GGI	SWA	AY597783
B. hermsii GGI	FRE	AY597782
B. hermsii GGI	C0N	AY597781
B. hermsii GGI	HAL	AY597780
B. hermsii GGI	BR0	AY597779
***B. hermsii* GGI**	**DAH**	**AY597777**
B. hermsii GGI	HS1	CP014349
B. hermsii GGI	MIT-24	KX171817
B. hermsii GGI	YBT-21	KX171812
B. hermsii GGI	YBT-12	KX171807
B. hermsii GGI	YBT-7	KX171805
B. hermsii GGI	YBS-1171	KX171804
B. hermsii GGI	WHT-8	KX171798
B. hermsii GGI	DM-31	KX171797
B. hermsii GGI	WHS-90	KX171796
B. hermsii GGI	LAK-6	KX171792
B. hermsii GGI	WAR	KC883464
B. hermsii GGI	CC1	JF737019
B. hermsii GGI	EST	AY597792
B. hermsii GGI	OWL	GQ175063
B. hermsii GGI	YB-Th-60	GQ175059
B. hermsii GGI	HCT-4	KJ995789
B. hermsii GGI	COR	KJ995774
B. hermsii GGI	DAH 2E7	CP014808
B. hermsii GGII	LAK-5	DQ855534
B. hermsii GGII	LAK-3	DQ855532
B. hermsii GGII	REN	AY597805
B. hermsii GGII	OKA-3	AY597804
B. hermsii GGII	OKA-2	AY597803
B. hermsii GGII	OKA-1	AY597802
B. hermsii GGII	HAN	AY597801
B. hermsii GGII	SIL	AY597800
B. hermsii GGII	LAK-2	AY597799
B. hermsii GGII	LAK-1	AY597798
B. hermsii GGII	RUM	AY597797
B. hermsii GGII	GMC	AY597796
B. hermsii GGII	CMC	AY597795
***B. hermsii* GGII**	**YOR**	**AY597806**
B. hermsii GGII	MAT	DQ855535
B. hermsii GGII	MIL	AY597778
B. hermsii GGII	YBS-60	KX171799
B. hermsii GGII	MIT-27	KX171816
B. hermsii GGII	MIT-26	KX171815
B. hermsii GGII	MIS-491	KX171814
B. hermsii GGII	MIS-1014	KX171813
B. hermsii GGII	YBT-20	KX171811
B. hermsii GGII	YBT-18	KX171810
B. hermsii GGII	YBT-17	KX171809
B. hermsii GGII	YBT-13	KX171808
B. hermsii GGII	YBT-10	KX171806
B. hermsii GGII	YBS-1143	KX171803
B. hermsii GGII	YBS-479	KX171802
B. hermsii GGII	YBS-266	KX171801
B. hermsii GGII	YBS-70	KX171800
B. hermsii GGII	WHS-88	KX171795
B. hermsii GGII	WHS-81	KX171794
B. hermsii GGII	WHS-40	KX171793
B. hermsii GGII	WCB-1	KC883463
B. hermsii GGII	LP0	EF595741
B. hermsii GGII	MTW-2	EU194843
B. hermsii GGII	MTW-1	EU194839
B. hermsii GGII	COT-7	KJ995784

5. GenBank® accession codes for the *msp2* gene sequences of *Anaplasma phagocytophilum*. Sequences utilized for *in silico* analysis in Appendix B are emphasized in bold.

***Anaplasma* Species**	**Isolate/Strain**	**GenBank**
A. phagocytophilum	**HZ**	**CP000235**
A. phagocytophilum	AP-V1	AY780258
A. phagocytophilum	LL	AY568558
A. phagocytophilum	MRK	AY568557
A. phagocytophilum	NY-31	AY541007
A. phagocytophilum	NY-36	AY541006
A. phagocytophilum	NY-37	AY541005
A. phagocytophilum	OS	AY541004
A. phagocytophilum	Trustom	AY541003
A. phagocytophilum	AVK-HLPA1	AY541002
A. phagocytophilum	Gaillard	AY541001
A. phagocytophilum	MN-2	AY541000
A. phagocytophilum	MN-9	AY540999
A. phagocytophilum	S1025/09	JF893912
A. phagocytophilum	S2630/07	JF893911
A. phagocytophilum	S2614/07	JF893910
A. phagocytophilum	S1829/04	JF893909
A. phagocytophilum	S1741/07	JF893908
A. phagocytophilum	S1729/08	JF893907
A. phagocytophilum	S1523/07	JF893906
A. phagocytophilum	S1379/06	JF893905
A. phagocytophilum	S1220/08	JF893904
A. phagocytophilum	S1201/05	JF893903
A. phagocytophilum	S1085/09	JF893902
A. phagocytophilum	S1074/09	JF893901
A. phagocytophilum	S1071/08	JF893900
A. phagocytophilum	S654/04	JF893899
A. phagocytophilum	Cc20	FJ812387
A. phagocytophilum	Ce9	FJ812384
A. phagocytophilum	NY18	AY164513
A. phagocytophilum	6497	JN656334
A. phagocytophilum	9774	JN656332
A. phagocytophilum	630300	JN656333
A. phagocytophilum	8776	JN656331
A. phagocytophilum	232	JN656330
A. phagocytophilum	15526	JN656329
A. phagocytophilum	6385	JN656328
A. phagocytophilum	S2872/07	JN656327
A. phagocytophilum	2838	JN656326
A. phagocytophilum	S1710/05	JN656325
A. phagocytophilum	8340	JN656324
A. phagocytophilum	14524	JN656323
A. phagocytophilum	50	JN656319
A. phagocytophilum	6380	JN656318
A. phagocytophilum	633200	JN656317
A. phagocytophilum	KD	JN656316
A. phagocytophilum	4	JN656315
A. phagocytophilum	67	JN656314
A. phagocytophilum	1219	JN656313
A. phagocytophilum	614	JN656312
A. phagocytophilum	14908	JN656310
A. phagocytophilum	20684	JN656311
A. phagocytophilum	3547	JN656309
A. phagocytophilum	754	JN656308
A. phagocytophilum	7444	JN656307
A. phagocytophilum	8074	JN656306
A. phagocytophilum	29W	JN656304
A. phagocytophilum	20489	JN656305
A. phagocytophilum	S2070/03	JN656303
A. phagocytophilum	152595	JN656302
A. phagocytophilum	680200	JN656301
A. phagocytophilum	44	JN656300
A. phagocytophilum	19555	JN656299
A. phagocytophilum	9698	JN656298
A. phagocytophilum	14888	JN656297
A. phagocytophilum	R1592	JN244019
A. phagocytophilum	ovine 5	AY706393
A. phagocytophilum	Elsa	AY706392
A. phagocytophilum	JM	CP006617
A. phagocytophilum	HZ2	CP006616

APPENDIX B

1. Singleplex *in silico* specificity analysis depicted by oligonucleotide alignments for the forward primer, reverse primer, and probe sequences of (A) *B. burgdorferi*, (B) *B. hermsii*, (C) *B. parkeri*, (D) *B. turicatae*, (E) *E. ewingii*, (F) *E. chaffeensis*, (G) *E. canis*, (H) *A. phagocytophilum*, (I) *R. rickettsii*, and (J) pan-*Babesia* assays in 5' to 3' orientation. Assays were evaluated for analytical specificity against representative closely related species as indicated in S5-S10. Respective primers and probes used for analysis are highlighted in grey. The sequences for other species are only shown when they differ from respective species sequences. A dot indicates identity with the respective species sequence. Dashes in (A)-(C), (E)-(G) and (J) refer to an in/del, dashes in (D), (H) and (I) refer to absence of gene sequences. The second column indicates specificity in qualitative results (positive or negative). An asterisk represents hypothetical analysis based on NCBI BLAST analysis due to lack of available reference strains.

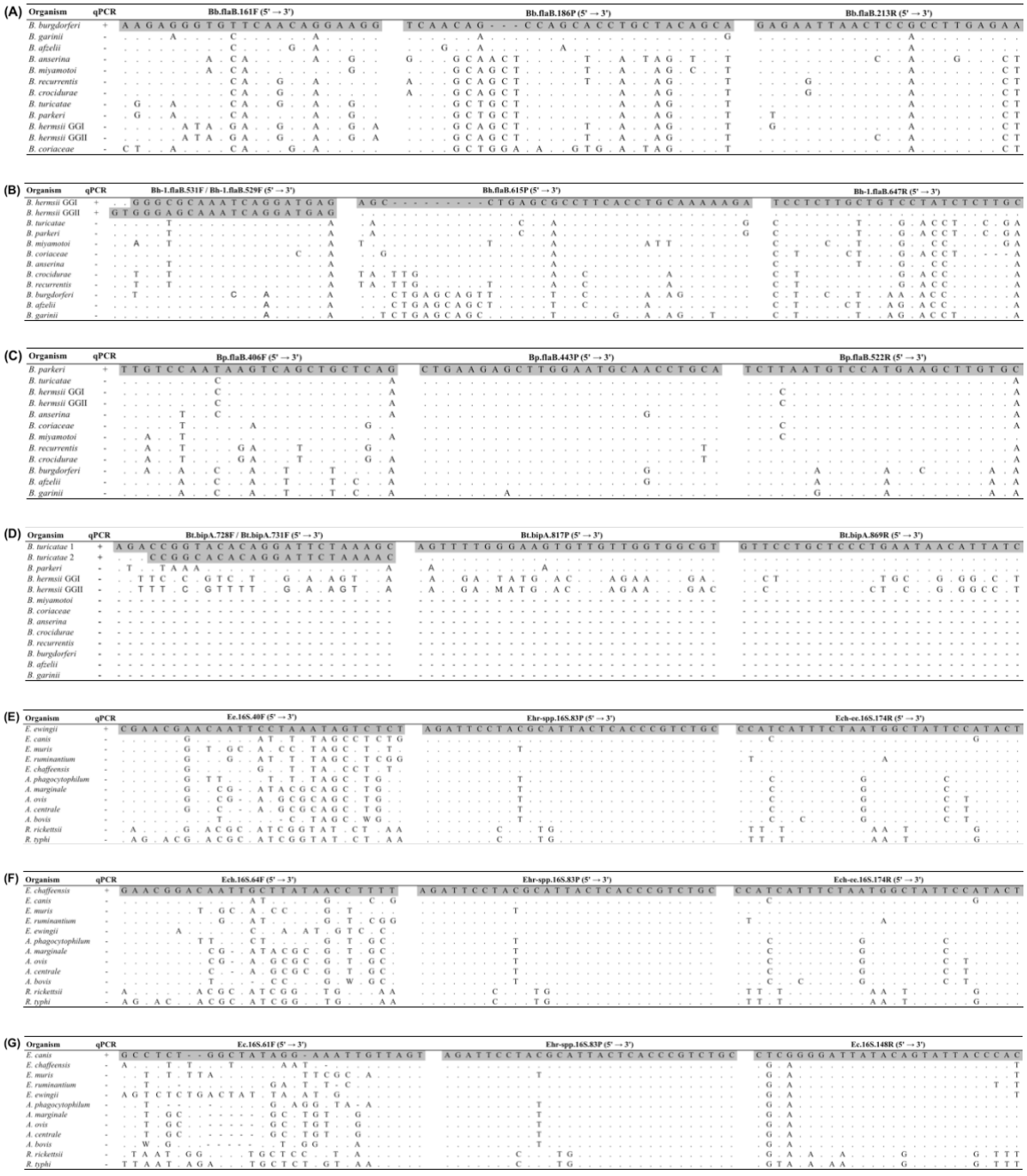

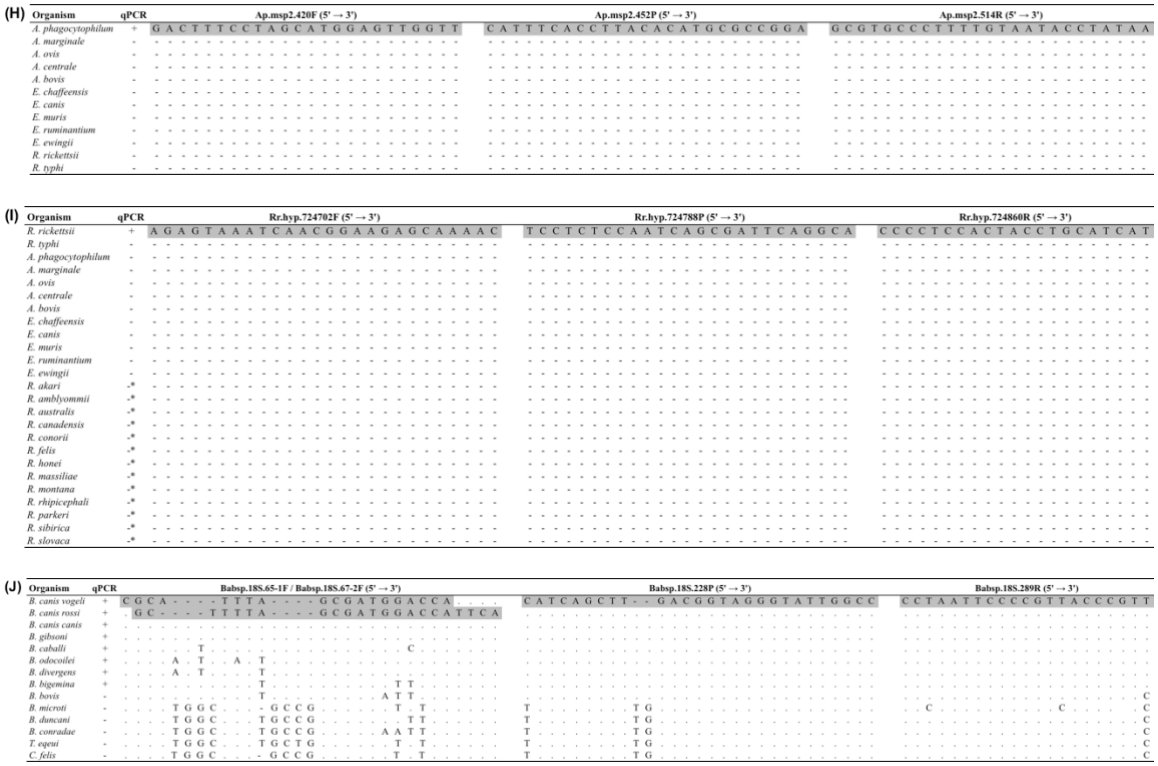
(H)
Organism
qPCR
Ap.msp2.420F (5' → 3')
Ap.msp2.452P (5' → 3')
Ap.msp2.514R (5' → 3')
A. phagocytophilum + G A C T T T C C T A G C A T G G A G T T G G T T C A T T T C A C C T T A C A C A T G C G C C G G A G C G T G C C C T T T T G T A A T A C C T A T A A
A. marginale -
A. ovis -
A. centrale -
A. bovis -
E. chaffeensis -
E. canis -
E. muris -
E. ruminantium -
E. ewingii -
R. rickettsii -
R. typhi -
(I)
Organism
qPCR
Rr.hyp.724702F (5' → 3')
Rr.hyp.724788P (5' → 3')
Rr.hyp.724860R (5' → 3')
R. rickettsii + A G A G T A A A T C A A C G G A A G A G C A A A A C T C C T C T C C A A T C A G C G A T T C A G G C A C C C C T C C A C T A C C T G C A T C A T
R. typhi -
A. phagocytophilum -
A. marginale -
A. ovis -
A. centrale -
A. bovis -
E. chaffeensis -
E. canis -
E. muris -
E. ruminantium -
E. ewingii -
R. akari -*
R. amblyommii -*
R. australis -*
R. canadensis -*
R. conorii -*
R. felis -*
R. honei -*
R. massiliae -*
R. montana -*
R. rhipicephali -*
R. parkeri -*
R. sibirica -*
R. slovaca -*
(J)
Organism
qPCR
Babsp.18S.65-1F / Babsp.18S.67-2F (5' → 3')
Babsp.18S.228P (5' → 3')
Babsp.18S.289R (5' → 3')
B. canis vogeli + C G C A - - - - T T T A - - - - G C G A T G G A C C A C A T C A G C T T - - G A C G G T A G G G T A T T G G C C C C T A A T T C C C C G T T A C C C G T T
B. canis rossi + G C - - - - T T T A - - - - G C G A T G G A C C A T T C A
B. canis canis +
B. gibsoni +
B. caballi +
B. odocoilei +
B. divergens +
B. bigemina +
B. bovis -
B. microti -
B. duncani -
B. conradae -
T. equi -
C. felis -

1. Continued

APPENDIX C

1. Limit of detection analysis of the *Borrelia* species assays. Quantification cycle (Cq) values reported in mean from duplicate testing. Plasmid DNA concentrations not tested are represented by NA.

Fold	Plasmid DNA (ng/µl)	Target Copy #	*B. hermsii* Cq	*B. burgdorferi* Cq	*B. parkeri* Cq	*B. turicatae* Cq
1	75.91	1.27E+11	NA	NA	NA	NA
1.00E-06	7.59E-05	127200	21.3	21.3	22.4	21.4
1.00E-07	7.59E-06	12720	24.6	24.6	25.8	24.9
1.00E-08	7.59E-07	1272	27.8	27.8	29.0	28.1
1.00E-09	7.59E-08	127	30.9	30.9	32.4	31.5
1.00E-10	7.59E-09	13	33.9	35.3	36.3	35.0
5.00E-11	3.80E-09	6	36.1	36.0	36.5	36.7
2.50E-11	1.90E-09	3	36.8	36.4	37.7	35.6

2. Limit of detection analysis of the *Ehrlichia, Anaplasma, and Rickettsia* species assays. Quantification cycle (Cq) values reported in mean from duplicate testing. Plasmid DNA concentrations not tested are represented by NA.

Fold	Plasmid DNA (ng/µl)	Target Copy #	*E. canis* Cq	*E. chaffeensis* Cq	*E. ewingii* Cq	*A. phagocytophilum* Cq	*R. rickettsii* Cq
1	75.91	1.27E+11	NA	NA	NA	NA	NA
1.00E-06	7.59E-05	127,200	22.1	23.6	23.2	21.8	22.1
1.00E-07	7.59E-06	12,720	25.4	27.1	26.6	25.2	25.5
1.00E-08	7.59E-07	1,272	28.5	30.3	30.1	28.3	28.8
1.00E-09	7.59E-08	127	31.9	34.0	33.7	31.9	32.2
2.50E-10	1.90E-08	32	34.8	36.5	35.8	34.7	33.7
1.25E-10	9.49E-09	16	35.1	36.7	37.1	34.8	35.9

3. Limit of detection analysis of the *Babesia* species assays. Quantification cycle (Cq) values reported in mean from duplicate testing. Plasmid DNA concentrations not tested are represented by NA.

Fold	Plasmid DNA (ng/µl)	Target Copy #	*Babesia* spp. Cq
1	75.91	1.27E+11	NA
1.00E-06	7.59E-05	127,200	21.8
1.00E-07	7.59E-06	12,720	24.6
1.00E-08	7.59E-07	1,272	28.0
1.00E-09	7.59E-08	127	32.0
2.50E-10	1.90E-08	32	34.2
1.25E-10	9.49E-09	16	35.6

4. Limit of detection analysis of the Borrelial, Rickettsial, and Babesial layers evaluated in layerplex format. Quantification cycle (Cq) values reported in mean from duplicate testing. Plasmid DNA concentrations not tested are represented by NA.

Fold	Plasmid DNA (ng/µl)	Target Copy #	Borrelial Cq	Rickettsial Cq	Babesial Cq
1	75.91	1.27E+11	NA	NA	NA
1.00E-06	7.59E-05	127,200	23.2	23.0	22.1
1.00E-07	7.59E-06	12,720	26.0	25.7	24.8
1.00E-08	7.59E-07	1,272	29.1	29.0	28.1
1.00E-09	7.59E-08	127	32.8	32.5	31.5
2.50E-10	1.90E-08	32	34.6	34.4	33.5
1.25E-10	9.49E-09	16	35.5	35.4	34.4

APPENDIX D

1. Paired t-test statistical analysis of *Borrelia* species with singleplex (SP) and Layerplex (LP) qPCR testing. Mean values reported as quantification cycles (Cq) from triplicate testing.

	B. hermsii		*B. turicatae*		*B. parkeri*		*B. burgdorferi*	
	SP	LP	SP	LP	SP	LP	SP	LP
Mean	26.040	27.306	23.550	25.713	26.018	25.912	25.061	25.297
Variance	1.133	0.254	0.245	0.191	0.014	0.014	0.003	0.014
Observations	3	3	3	3	3	3	3	3
P(T≤) two-tail	0.068		0.723		0.423		0.125	

2. Paired t-test statistical analysis of *Ehrlichia, Anaplasma, and Rickettsia* species with singleplex (SP) and layerplex (LP) qPCR testing. Mean values reported as quantification cycles (Cq) from triplicate testing.

	E. canis		*E. chaffeensis*		*E. ewingii*		*A. phagocytophilum*		*R. rickettsii*	
	SP	LP	SP	LP	SP	LP	SP	LP	SP	LP
Mean	25.434	25.253	25.429	25.475	25.387	25.280	25.906	25.894	25.302	25.394
Variance	0.017	0.032	0.011	0.005	0.005	0.003	0.280	0.091	0.001	0.017
Observations	3	3	3	3	3	3	3	3	3	3
P(T≤) two-tail	0.252		0.207		0.146		0.941		0.272	

3. Paired t-test statistical analysis of *Babesia* species with singleplex (SP) and layerplex (LP) qPCR testing. Mean values reported as quantification cycles (Cq) from triplicate testing.

	Babesia spp.	
	SP	LP
Mean	25.196	25.126
Variance	0.001	0.001
Observations	3	3
P(T≤) two-tail	0.135	

4. Paired t-test statistical analysis of the canine specific endogenous internal positive control (EIPC-K9) with singleplex (SP) and layerplex (LP) qPCR testing. Mean values reported as quantification cycles (Cq) from triplicate testing.

	EIPC-K9	
	SP	LP
Mean	25.673	25.175
Variance	0.026	0.166
Observations	3	3
P(T≤) two-tail	0.093	

APPENDIX E

1. GenBank® accession codes for the *16S rRNA* gene sequences of *Anaplasma*.

GenBank®	Sample	County
MH620179	23-33TX	Wilbarger
MH620180	22-07TX	Burnet

2. GenBank® accession codes for the *16S rRNA* gene sequences of *Ehrlichia canis*.

GenBank®	Sample	County
MH620182	18-75TX	Potter
MH620183	19-12TX	Potter
MH620184	23-72TX	Armstrong
MH620185	25-20TX	Wilbarger
MH620186	25-47TX	Armstrong
MH620187	21-77TX	Tarrant
MH620188	18-58TX	Nueces
MH620189	24-55TX	Nueces
MH620190	24-68TX	Nueces
MH620191	22-07TX	Burnet
MH620192	22-58TX	Midland
MH620193	25-55TX	Nacogdoches
MH620194	26-10TX	Schleicher
MH620195	18-43TX	El Paso
MH620196	22-16TX	Maverick
MH620197	25-74TX	Cameron
MH620198	21-36TX	Karnes
MH620199	23-33TX	Wilbarger
MH620200	25-24TX	Lubbock

3. GenBank® accession codes for the *16S rRNA-23S rRNA* IGS sequences of *Borrelia turicatae*.

GenBank®	Sample	County
MH620360	23-25TX	Randall
MH620361	05-07TX	Coryell
MH620362	14-46TX	Gillespie
MH620363	09-77TX	Coryell
MH620364	22-43TX	Armstrong
MH620365	24-24TX	DeWitt
MH620366	24-25TX	Caldwell
MH620367	25-25TX	Gonzales

4. GenBank® accession codes for the *18S rRNA* gene sequences of *Babesia gibsoni*.

GenBank®	Sample	County
MH620201	04-49TX	Burnet
MH620202	04-50TX	Burnet
MH620203	20-58TX	Harris
MH620204	27-23TX	Panola
MH620205	27-32TX	Hidalgo